

A CLIMATE PERSPECTIVE OF OBSERVED AND MODELED SURFACE-BASED
TEMPERATURE INVERSIONS IN ALASKA

By

Stefanie M. Bourne

RECOMMENDED: _____

Advisory Committee Chair

Chair, Department of Atmospheric Sciences

APPROVED: _____

Dean, College of Natural Science and Mathematics

Dean of the Graduate School

Date

A CLIMATE PERSPECTIVE OF OBSERVED AND MODELED SURFACE-BASED
TEMPERATURE INVERSIONS IN ALASKA

A
THESIS

Presented to the Faculty
of the University of Alaska Fairbanks

in Partial Fulfillment of the Requirements
for the Degree of

MASTER OF SCIENCE

By

Stefanie M. Bourne, B.S.

Fairbanks, Alaska

August 2008

Abstract

Alaska surface-based temperature inversion parameters (inversion depth, temperature difference, strength and frequency) were calculated using radiosonde observations for Fairbanks, McGrath, Anchorage, and Barrow. Trends and variability were examined for 1957-2008. At all sites, surface temperatures show increasing trends, while inversion depth and temperature difference are decreasing. Inversion strength shows increasing trends in Interior Alaska, but decreasing trends along the coast. Inversion parameters display similar interannual variability for all sites and show statistically significant correlation to large-scale climate variability.

Alaska surface-based inversions were evaluated in a hierarchy of model simulations. The global model is not able to capture key inversion characteristics. However, dynamically downscaled regional models can better simulate variability of inversion parameters, but the means display biases which are easily correctable. Inversions, evaluated in a downscaled A1B future scenario, show a general warming of the entire air column and an overall decrease in inversion depth and temperature difference.

Table of Contents

	Page
Signature Page.....	i
Title Page.....	ii
Abstract.....	iii
Table of Contents.....	iv
List of Figures.....	vi
List of Tables.....	viii
List of Appendices.....	ix
Acknowledgements.....	x
Chapter 1. Background and Justification	1
1.1 Introduction to Inversion Characteristics.....	1
1.2 Inversions in the Alaskan Interior.....	2
1.3 The Need for Simulating the Earth’s System	7
1.4 Downscaling Options and Successes	8
1.5 Goals of this Research.....	10
Chapter 2. Methods, Data, and Modeling Tools	11
2.1 Data Sources and Selection.....	11
2.1.2 Inversion Detection Algorithm.....	12
2.2 Global and Regional Climate Models	14
Chapter 3. Variability and Trends of Observed Surface-based Temperature	
Inversions in Alaska	18
3.1 Data Analysis.....	18
3.1.1 Inversion Climatology	19
3.1.2 Surface Temperature.....	26
3.1.3 Inversion Depth	31
3.1.4 Inversion Temperature Difference.....	35
3.1.5 Inversion Strength.....	39

	Page
3.2 Connections to Large-scale Climate Variability.....	44
Chapter 4. 20th Century Model Simulations and Future Scenarios.....	53
4.1 Introduction to Modeling Schemes.....	53
4.2 MM5 Downscaled from NCEP Reanalysis.....	57
4.3 Downscaled from Model.....	72
4.3.1 CCSM3 20 th Century Simulation.....	72
4.3.2. 20 th Century Downscaled Simulation.....	73
4.3.2 MM5 Downscaled from CCSM3-A1B.....	82
Chapter 5. Conclusion.....	91
References.....	95
Appendices.....	101

List of Figures

	Page
Figure 1.1. Extreme inversion events in Fairbanks, AK.....	4
Figure 1.2. Alaska radiosonde observation (RAOB) stations.....	6
Figure 2.1. Modeling hierarchy diagram.....	15
Figure 3.1. Inversion profile possibilities.....	18
Figure 3.2. Monthly average vertical temperature profiles in Fairbanks, AK.....	20
Figure 3.3. Seasonal variation of inversion parameters in Fairbanks, AK.....	21
Figure 3.4. Wintertime inversion frequency in Fairbanks, AK.....	22
Figure 3.5. Average vertical profile variability in December.....	24
Figure 3.6. Monthly averaged vertical temperature profiles at Alaska stations in December.....	25
Figure 3.7. Relationship between inversion depth and temperature difference.....	26
Figure 3.8. Wintertime surface temperatures in Alaska.....	29
Figure 3.9. Wintertime surface temperature anomalies in Alaska.....	30
Figure 3.10. Wintertime inversion depth in Alaska.....	32
Figure 3.11. Wintertime inversion depth anomalies in Alaska.....	34
Figure 3.12. Wintertime inversion temperature difference in Alaska.....	37
Figure 3.13. Wintertime inversion temperature difference anomalies in Alaska.....	38
Figure 3.14. Wintertime inversion strength in Alaska.....	40
Figure 3.15. Wintertime inversion strength anomalies in Alaska.....	43
Figure 3.16. PDO connections to inversion parameters.....	46
Figure 3.17. Inversion parameters correlated to wintertime PDO index.....	47
Figure 3.18. NAO connections to inversion parameters.....	49
Figure 3.19. AO connections to inversion parameters.....	51
Figure 4.1. CCSM3 fractional grid points.....	54
Figure 4.2. Display of model topography as resolution varies.....	55
Figure 4.3. MM5-NCEP in Fairbanks during December.....	59

	Page
Figure 4.4. MM5-NCEP in Fairbanks during January.....	60
Figure 4.5. MM5-NCEP in McGrath during December.....	62
Figure 4.6. MM5-NCEP in McGrath during January.....	63
Figure 4.7. MM5-NCEP in Anchorage during December.....	65
Figure 4.8. MM5-NCEP in Anchorage during January.....	66
Figure 4.9. MM5-NCEP in Barrow during December.....	68
Figure 4.10. MM5-NCEP in Barrow during January.....	69
Figure 4.11. Modeled and observed vertical temperature profiles in Fairbanks.....	75
Figure 4.12. Modeled and observed vertical temperature profiles in McGrath.....	76
Figure 4.13. Modeled and observed vertical temperature profiles in Anchorage.....	77
Figure 4.14. Modeled and observed vertical temperature profiles in Barrow.....	78
Figure 4.15. Future projected vertical temperature profiles in Fairbanks.....	84
Figure 4.16. Projected simulated vertical temperature profiles in McGrath.....	85
Figure 4.17. Future projected vertical temperature profiles in Anchorage.....	87
Figure 4.18. Future projected vertical temperature profiles in Barrow.....	88
Figure A.1. Surface temperature time series in McGrath and Fairbanks.....	102
Figure A.2. Urban heat island analysis of inversion parameters.....	103
Figure B.1. Cloud cover climatology.....	104
Figure B.2. Cloud cover and inversion strength (dT/dz) in Fairbanks.....	106

List of Tables

	Page
Table 3.1. Surface temperatures in Alaska during December and January.....	28
Table 3.2. Surface temperature time series correlation.....	28
Table 3.3. Inversion depth in Alaska during December and January.....	33
Table 3.4. Inversion depth time series correlation.....	33
Table 3.5. Inversion temperature difference in Alaska during December and January...	36
Table 3.6. Inversion temperature difference time series correlation.....	36
Table 3.7. Inversion strength in Alaska during December and January.....	41
Table 3.8. Inversion parameters correlated to wintertime PDO index from 1957-2008...	45
Table 3.9. Average DJF inversion parameters correlated to wintertime NAO index from 1957-2008.	50
Table 3.10. Average DJF inversion parameters correlated to wintertime AO index.....	52
Table 4.1. Downscaled model parameterizations.....	57
Table 4.2. MM5 inversion parameters downscaled from NCEP reanalysis data.....	71
Table 4.3. Inversion frequency.....	74
Table 4.4. 20 th century inversion parameters in Fairbanks.....	79
Table 4.5. 20 th century inversion parameters in McGrath.....	80
Table 4.6. 20 th century inversion parameters in Anchorage.....	81
Table 4.7. 20 th century inversion parameters in Barrow.....	82
Table 4.8. Average future projected inversion parameters in Fairbanks.....	89
Table 4.9. Average future projected inversion parameters in McGrath.....	89
Table 4.10. Average future projected inversion parameters in Anchorage.....	90
Table 4.11. Average future projected inversion parameters in Barrow.....	90

List of Appendices

	Page
Appendix A. Evaluating Fairbanks Radiosonde Data for the Urban Heat Island Effect (UHIE).....	101
Appendix B. Relationship Between Cloud Cover and Surface-based Inversions.....	104

Acknowledgements

First and foremost, I would like to express my sincere thanks to my advisor Uma Bhatt for the support, guidance, and encouragement during the course of this project. I would also like to thank my current and former committee members, Nicole Mölders, John Walsh, David Atkinson and Jing Zhang, for encouraging me and providing constructive criticism through this process. Richard Thoman and Ted Fathauer of the National Weather Service are acknowledged for their input and knowledge with respect to Alaska radiosonde observations, while Martha Shulski of the Alaska Climate Research Center is also thanked for providing various station data.

This work was partially funded by the Geophysical Institute and through a NOAA grant through the International Arctic Research Center titled "Social Vulnerability to Climate Change and Extreme Weather of Alaskan Coastal Communities". This research was also supported by a University of Alaska Fairbanks Center for Global Change Student Award funded by the Cooperative Institute for Arctic Research (CIFAR) through the National Oceanic and Atmospheric Administration under cooperative agreement NA17RJ1224 with the University of Alaska.

This work was supported in part, by a grant of high-performance computing (HPC) resources from the Arctic Region Supercomputing Center at the University of Alaska Fairbanks, as part of the US Department of Defense's HPC Modernization Program. The National Center for Environmental Prediction/National Center for Atmospheric Research (NCEP/NCAR) reanalysis data were provided by the Data Support Section of the Scientific Computing Division at the National Center for Atmospheric Research, which is supported by the US National Science Foundation (NSF). This research uses A1B scenario data from the Community Climate System Model project (www.cesm.ucar.edu), supported by the NSF Directorate for Geo- sciences and the US Department of Energy's Office of Biological and Environmental Research. Radiosonde and pilot balloon data

were provided by the National Climatic Data Center's Integrated Global Radiosonde Archive.

Lastly, I would like to thank my parents, Jim and Sandy, for encouraging me and providing unconditional support for all my dreams. My sisters Jaime and Jenna for listening to my problems no matter how late it was on the East Coast, and my brother Matt for calling me everyday to make sure I was still making time to have fun. My amazing boyfriend Colin for listening as best he could to my science rants and supporting me everyday without fail. I would also like to thank Morgan Brown, Julie Malingowski, and Michel Dos Santos Mesquita for their time and unbelievable assistance in preparing for my defense. Finally, I would like to thank all my friends, near and far, for making Fairbanks feel like home and for encouraging me to take a leap of faith in everything I do.

Chapter 1. Background and Justification

1.1 Introduction to Inversion Characteristics

The American Meteorological Society defines an inversion as a layer of the atmosphere where temperature increases with altitude. Perhaps the most prominent characteristic of an atmospheric temperature inversion is static stability, which prevents turbulent exchange and entrainment between the lower atmospheric boundary layer (ABL) and the free atmosphere aloft. Stable layers where temperature increases with height can be found at lower latitudes in the form of trade inversions that typically form in eastern regions of tropical oceans. Trade inversions form as the result of a balance between subsidence warming and radiative cooling and evaporation from the top of trade wind clouds (AMS 2000). In general, however, the mid-latitude troposphere is an unstable mixed layer where temperature decreases with height due to the abundance of radiation absorbed at the surface. At high latitudes however, the presence of a stable ABL is a result of a unique energy balance (Kadyrov and Viazankin 1999). In winter months, a deficit of net radiation makes the atmosphere become thermally stratified creating extremely stable conditions (Wendler 1975).

Physical controls of inversions are well documented and understood; Wexler (1936) and Bradley and Keimig (1992) found that temperature inversions are predominantly driven by a balance between radiative cooling and heat advection. In high latitude regions, radiative imbalance can occur in the presence of negative net radiation, when the surface cools to a temperature below that of the air above it. Through a deficit of solar radiation and longwave cooling, the surface loses more energy than it receives and its temperature decreases. This decrease in surface temperature subsequently cools the atmosphere above it, creating a thermally induced inversion. Warm air advection above the inversion layer can concurrently create a strong thermal stratification between layers, resulting in extremely stable conditions.

The existence of the Arctic temperature inversion has been recognized and studied for over a century by various scientists and explorers. Brooks (1931) demonstrated the high frequency of occurrence of inversions using kite ascents over Siberia. Detailed studies made over a broad region of the Arctic during the *Maud* expedition offered scientists new information on the structure of inversions (Sverdrup 1933). Wexler (1936) developed the idea of physical controls which affect inversion formation in a negative net-radiation environment. Later, Bilello (1966) performed statistical analysis on Arctic and subarctic inversions, focusing on characteristics such as frequency, base height, thickness, base temperature, and temperature gradient. Wendler (1975) investigated low-level inversions in Fairbanks, Alaska finding inversions present more than 95% of the time in the winter (November-February) with maximum temperature gradients of 20°C in 200m. More recently, Serreze et al. (1992) introduced the idea of the complexity of inversions, suggesting that inversions were not only affected by radiative cooling, but also by warm air advection, subsidence, radiative properties of ice crystals, surface melt, and topography. Subsequently, Hartmann and Wendler (2005a) examined the climatology of the wintertime surface-based inversion (SBI) and its importance for winter air quality in Fairbanks, Alaska.

1.2 Inversions in the Alaskan Interior

Fairbanks, Alaska is the largest community in the Interior of Alaska between the Brooks and Alaska Ranges (Wendler and Nicpon 1975), and according to 2007 Census Bureau estimates, the population of the city exceeds 30,000 individuals. The population of Fairbanks and vicinity exceeds 86,000 individuals. In the wintertime, temperature inversions are strong, stable, and semi-permanent (Hartmann and Wendler 2005a). According to a study performed by Bilello (1966) from November to April 1952-1961 in Fairbanks, Alaska, a surface-based inversion occurred 69% (day and night average) of the time with an average inversion thickness of 430m and an average inversion temperature difference of 2°C for a measurement period of nine years. Comparatively, Hartmann and

Wendler (2005a) found that throughout the winter season (considered December to February), a surface-based inversion occurred 77% of the time, with the remaining 23% frequently displaying elevated inversions. Wintertime inversions in the Interior are certainly a prominent characteristic and affect the lives of citizens in the local community.

Regardless of what one deems “wintertime” in Fairbanks, it is clear that inversions have serious implications for air quality on a regional scale. In 1972, Fairbanks exceeded federal air quality regulations for carbon monoxide pollution on 168 days of the year (Rozell 2002). According to the U.S. Environmental Protection Agency (EPA), the Fairbanks North Star Borough was a ‘serious’ nonattainment area for CO from 1992-2004. Today, Fairbanks is listed as a ‘maintenance’ area for carbon monoxide and exceeds acceptable levels on many days in the colder months. According to the EPA, a nonattainment area is a geographic area that violates National Ambient Air Quality Standards, while a ‘maintenance’ area is a geographic region previously designated as a nonattainment area and subsequently redesignated to attainment (subject to the requirement to develop a maintenance plan for the pollutant in question).

The role surface-based inversions play in regional air quality is well documented in the literature (Wendler and Jayaweera 1972; Wendler 1975; Bowling 1986). Fairbanks’ inversions are among the most extreme in the world not only due to their ability to last several days (or sometimes even weeks), but also because temperature gradients are large, with temperature increases of 9°C with each 30m increase in altitude (Bowling 1979). Extreme inversion events typically occur in the coldest months. In Fairbanks, Alaska, December and January are the coldest months and have strong inversions (Fig. 1.1).

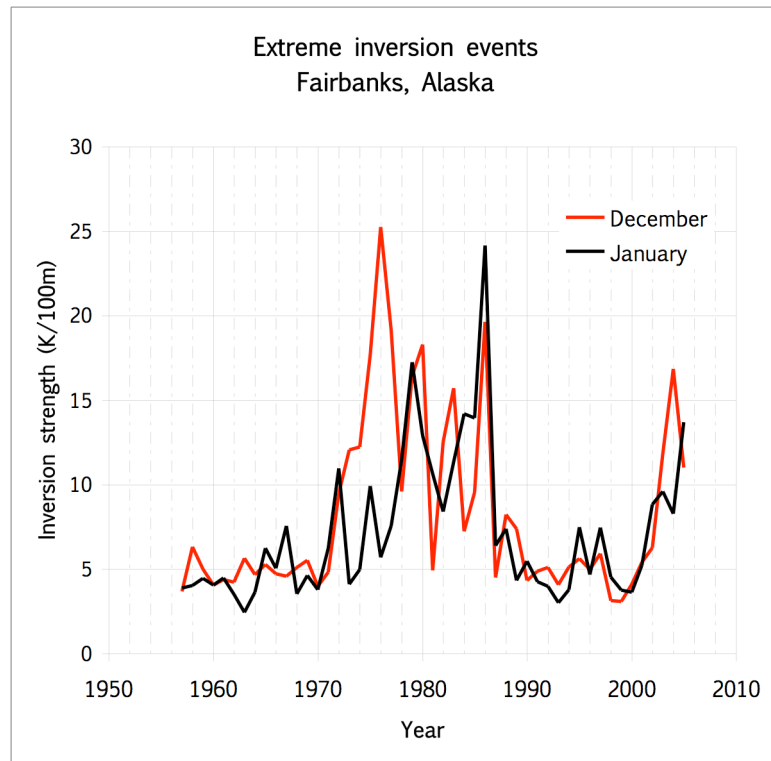


Figure 1.1. Extreme inversion events in Fairbanks, AK. Maximum observed inversion strength values for each year are shown as a function of time in December and January in Fairbanks, Alaska.

Due to inversion stability and resistance to vertical mixing, pollution released close to the surface tends to remain in the layer it enters. Strong winds can break up inversions, but in a orographically sheltered region such as Fairbanks that does not receive strong winds during winter months, pollutants move away from their sources horizontally and therefore fairly slowly, leading to unusually high pollution levels (Bowling 1979). As a result of the presence and behavior of wintertime inversions, levels of criteria pollutants, as designated by the Environmental Protection Agency, in Fairbanks are comparable with those of a much larger metropolitan area in the contiguous U.S. such as Los Angeles (Holty 1973; Bowling 1979).

In the future, the effect inversions have on air pollutants and their subsequent effect in society and industry could become a problem in Fairbanks, as well as other high latitude communities. Increasing surface temperatures for example, would imply decreasing inversion depths. Over time, if pollution levels remain constant and temperature inversions become shallower, the concentration of pollutants in the stable ABL will increase. Therefore, it is important to determine the effect a changing climate will have on surface-based temperature inversions in urban arctic areas such as Anchorage, McGrath, Fairbanks, and Barrow.

In addition to their detrimental effect on arctic urban air quality, temperature inversions are also relevant for other topics of research. Studies have shown that the altitude of the base of the inversion can be used to estimate the geostrophic drag coefficient, which is needed in sea-ice models to simulate motion (Overland 1985; Overland and Guest 1991; Overland and Davidson 1992). Additionally, inversion strength has been suggested to be an influencing factor in Arctic energy budgets, specifically the advection of heat and moisture through leads and polynyas (Andreas and Murphy 1986). This suggests that the frequency at which these events may occur must depend on temporal and spatial variability of inversion strength (Serreze et al. 1992). Temperature inversions in the Arctic also have implications for atmospheric chemistry. According to Bridgman et al. (1989), high concentrations of pollutants and aerosols can be found at the top of the inversion layer. Scientists have also linked the inversion layer to destruction of certain chemicals in the ABL during high latitude Arctic sunrise. These changes in the composition of the lower Arctic atmosphere are important for the oxidizing capacity of the ABL and for tropospheric cycles of ozone and other gases (Barrie et al. 1988; Oltmans et al. 1989).

Fairbanks has been the primary focus of this study due to the wintertime presence of surface-based temperature inversions and the associated air quality issues. However, primary pollutants are prevalent throughout Arctic and Subarctic regions and have the

potential to react chemically with trace species in the atmosphere. The resulting secondary pollutants could potentially be transported to other Arctic regions causing subsequent air quality problems in more remote areas. Not only does this problem present the need for source-reduction efforts in urban areas, but also for research efforts aimed at the evaluation of surface-based temperature inversions in other areas of Alaska and the Arctic. For this reason, Anchorage, McGrath, and Barrow were also considered as regions where surface-based temperature inversions are prevalent (Fig. 1.2). In addition, the spatial and temporal variability of Arctic temperature inversions, especially across the state of Alaska is largely unknown and needs to be established.



Figure 1.2. Alaska radiosonde observation (RAOB) stations. RAOB data was processed at four Alaskan stations representing 3 regions of the state: Southcentral, the Interior, and the Far North (Image modified from Kerski 2005, USGS).

Alaska geography is complex and varies regionally. This study will characterize inversion characteristics at different geographic regions in Alaska and determines the climatic components that influence their variability. In addition, dynamically downscaled model output will be analyzed to determine if this technique can capture the characteristics of surface-based temperature inversions across complex Alaska orography.

1.3 The Need for Simulating the Earth's System

In 2007 the Intergovernmental Panel on Climate Change (IPCC) released the Fourth Assessment Report (AR4) to summarize the current state of understanding of natural and human induced climate change. According to this report, “Warming of the climate system is unequivocal” (Solomon et al. 2007) and it has become evident through direct observations that the climate system is undergoing unprecedented changes, which have severe implications globally and in Arctic regions. Already, studies have demonstrated increased atmospheric water vapor content, increased mixed layer temperature of the oceans, decreased mountain glaciers and snow cover in both hemispheres, global sea level rise, decreased sea ice extent in both winter and summer seasons, and increased duration and intensity of drought and cyclone activity (Solomon et al. 2007).

Observed data is ideal when studying the Earth's climate, but due to spatial and temporal gaps in station data and observations, there comes a need for scientists to simulate physical components using computer models. Today, climate models are important tools for simulating past, present, and future climates on Earth. Climate models can vary in complexity from simple box model approximations to more complex coupled Atmosphere-Ocean General Circulation Models (AOGCMs) that apply fundamental physical relationships to quantify different climate parameters.

Generally, General Circulation Models (GCMs) are able to capture the global distribution of basic climate parameters. Yet, in recent years the validity of GCMs has come into question due to changes in the Earth's climate system. In addition, the role of the cryosphere is poorly understood because most Regional Climate Models (RCMs) cannot accurately capture important drivers of regional climate (Leung et al. 2006). In the AR4, the IPCC claims that "climate models are based on well-established physical principles and have been demonstrated to reproduce observed features of recent climate and past climate changes..." but "...Confidence in these estimates is higher for some climate variables (e.g. temperature) than for others (e.g. precipitation)." Therefore, there is a need to not only verify GCM output with observed data, but also enhance the resolution of the output. A useful method to attain regional-scale climate information from GCM data is called downscaling (Wigley 2004). Typically, GCM output has a coarse resolution that inadequately captures regional climate parameters which brings about the need to apply various methods of downscaling in order to accurately quantify regional climate dynamics (Bengtsson et al. 1996). Generally, uncertainties in model simulations can be addressed by evaluating the agreement between observational data and the model simulated output of the present climate.

1.4 Downscaling Options and Successes

GCMs offer a feasible approach for simulating future climate scenarios. However, changes in regional forcing factors that are important for mitigation and impact studies are not adequately resolved by global simulations. GCM output is produced for model grid-cell areas that can be several hundred kilometers on a side, which is far too coarse for regional climate change assessments. More importantly, GCM resolution creates altered topography over Alaska with distorted coastlines and an elevation maximum over the state's interior, which actually has low elevations between the Alaska and Brooks ranges.

Therefore, due to complex orography in regions such as Alaska, GCMs are unable to resolve local climate conditions. Therefore, a method is needed to convert coarse GCM output to finer spatial scales in order to capture mesoscale climate change and assess regional impacts of climate change. According to Spak et al. (2007), there are two methods available to estimate climate variables at a higher resolution: dynamical downscaling and statistical downscaling.

RCMs are appropriate dynamical downscaling tools and their validity is highly reliant on large-scale boundary conditions and local forcings (Leung et al. 2003, Chun-Fung Lo et al. 2008). Although computationally intensive, dynamical downscaling is unique in that it describes the physical processes of climate using fundamental conservation laws for mass, energy and momentum.

Comparatively, statistical downscaling is relatively fast, inexpensive, and requires far fewer computational resources. Additionally, unlike dynamical downscaling, statistical downscaling uses multivariate regressions to determine the correspondence between large-scale and regional climate. However, due to the lack of comprehensive station data and the orographic complexity of the region, statistical downscaling is not as applicable in Alaska as it may be in the continental United States (Bhatt et al. 2007). For this reason, dynamical downscaling was the technique chosen for this particular project.

Dynamical downscaling has proven to be successful in numerous studies in complex orographic regions. Schmidli et al. (2005) evaluated the current climate over the European Alps and found that statistical downscaling not only drastically underestimates the magnitude of interannual variations, but also that RCMs can “achieve significantly higher skills than the statistically downscaled models” during the winter. Zhang et al. (2007a) found that downscaled meteorological variables (temperature, pressure, humidity, and precipitation), which were provided as input for a glacier mass balance model, agreed reasonably well with observed station data when using a hierarchical

modeling approach. The Hubbard and Bering Glaciers in Alaska were simulated well for downscaled and observed data, and any systematic biases that existed could be removed by simple calibration techniques.

1.5 Goals of this Research

This work aims to investigate the following aspects and questions with regards to surface-based temperature inversions in Alaska:

- Evaluate the observed characteristics during winter months in Fairbanks, McGrath, Anchorage, and Barrow.
- Are there significant trends in inversion parameters such as inversion depth, inversion temperature difference, and inversion strength?
- How are Alaskan inversions related to the large-scale climate?
- Evaluate how well models, both global climate models and regional models, simulate inversions.
- Estimate future projections of Alaskan inversions

In order to evaluate observed characteristics during winter months at each station, it is important to explain the methods used to obtain and process observed data, where the data originates, and the tools used for the modeling component of the project (Chapter 2). Once the sources of data have been explained and a methodology established, surface-based inversions in Alaska are discussed with respect to their climatology in Fairbanks, and their trends and variability in winter months at all stations, and their connections to large-scale climate variability (Chapter 3). Once statistically significant relationships have been established between various inversion parameters and modes of large-scale climate variability, inversions are investigated in 20th century model simulations and future scenarios using the IPCC middle-of-the-road A1B scenario (Chapter 4). Lastly, the overall outcome of this research is examined including the main findings of this study and a discussion of caveats to future work (Chapter 5).

Chapter 2. Methods, Data, and Modeling Tools

2.1 Data Sources and Selection

Observational data from 1957-2008 was provided by the National Climatic Data Center (NCDC). The Integrated Global Radiosonde Archive (IGRA) consists of twice daily, quality-controlled radiosonde and pilot balloon observations at more than 1500 globally distributed stations, seventeen of which are located in Alaska. Data for Alaskan stations is available beginning in 1948 with observations including pressure, temperature, geopotential height, dewpoint depression, wind direction, and wind speed (Durre et al. 2006). Each data set from IGRA is subject to quality assurance algorithms, which include but are not limited to checks for format problems, physically implausible values, climatological outliers, and temporal and spatial inconsistencies in temperature. A series of specialized algorithms are applied successively to raw data that remove values that exceed all known world extremes (i.e. temperatures less than -120°C or greater than 70°C). According to Durre et al. (2006), 0.025% of all global data values were found to be invalid.

A two-tiered system of climatological checks was also implemented to remove geopotential height, temperature, and pressure values that deviate a given number of standard deviations from their long-term means. Tier-1 checks are primarily calculated for the entire period of record for a given station, while tier-2 statistics are quantified using time of year and time of day. According to Durre et al. (2006), a threshold of six standard deviations was used for tier-1 statistics, while a five standard deviation threshold was applied to tier-2 which removed a total of 0.1% of all geopotential height, temperature and pressure values globally.

Radiosondes in Fairbanks have been launched at Fairbanks International Airport since 1951. According to Mahesh et al. (1997), temperatures recorded by radiosondes are

subject to many sources of error. Vertical profiles collected before 1957 include measurements with considerable time lag and with long periods of no measurement, which would sometimes cause the instrument to not detect smaller layers of atmosphere with negative lapse rates (Huovila and Tuominen 1989). Therefore, as a result of concern over instrumentation error, data before 1957 was not used for this study in order to minimize data inconsistencies.

An additional concern arises as a result of urban development and human activities around the city of Fairbanks (Mölders and Olson 2004). Magee et al. (1999) define the urban heat island as the temperature difference between a city and the same location if the city were not present. The presence of an urban heat island is of concern for surface-based temperature inversions because lower level temperatures will affect inversion structure and strength. Additionally, urban heat sources and the relatively low surface albedo when compared to that of snow may enhance the UHIE in the boundary layer. One technique used to approximate the urban heat island effect (UHIE) is to compare temperatures between the urban location in question, and a nearby location with similar orographic features. McGrath, Alaska was chosen as the rural location due to similar orographic features and because it has not grown considerably in the past 50 years. In this particular study it was determined that the temperature difference between Fairbanks and McGrath was negligible and UHIE adjustments were not necessary (for details see Appendix A).

2.1.2 Inversion Detection Algorithm

The existence of the Arctic temperature inversion has been recognized for more than a century, and subsequent research has been performed on various aspects of this atmospheric phenomenon. Because Arctic temperature inversion profiles often exhibit complicated vertical structures, they have been classified using various different methods. The classification method used to detect an inversion is important because it affects the associated statistics such as the frequency, height of inversion top, base height, depth,

inversion strength, and inversion temperature difference. Bilello (1966) determined any layer having greater than 1 K temperature increase per kilometer is an inversion, (implying isothermal layers were not included in the classification). In contrast, Maxwell (1982) included isothermal layers saying that the rate of temperature increase must be greater than 2 K per 100 meters, but any decrease in temperature is seen as the top of the inversion. Bradley and Keimig (1992) argued the top of the inversion is the height of the last temperature measurement which exceeds or is equal to the preceding measurement, including isothermal layers. The algorithm used to detect inversions for this study was based on the definition developed by Kahl (1990) and Serreze et al. (1992) which defined an inversion as a layer where temperature increases with altitude, including embedded layers with negative lapse rates, provided they are no more than 100 meters in extent.

Initial data analysis was performed on radiosonde observation (RAOB) data from Fairbanks. Once the inversion detection algorithm was modified to capture all inversions of interest and evaluation procedures were streamlined, analysis was also performed on McGrath, Anchorage, and Barrow station data. Each station has very unique climatological characteristics, and it was expected that these features would have an impact on and be reflected in the inversion characteristics.

Analysis of observed data began with a series of steps that enabled efficient parsing of the twice-daily RAOBs for each month. After vertical pressure was converted to geometric height, inversion parameters such as depth (dz), temperature difference (dT), and strength (dT/dz) were calculated for each of the two daily soundings from 1957-2008. Inversion parameters were averaged to create overall average values for each day (prior, there were two soundings per day measured at 0000 UTC and 1200 UTC). Data was then averaged on a daily and monthly basis for each winter month.

Monthly average data values from 1957-2008 were then analyzed to determine average values of inversion depth, temperature difference, and strength. Standard deviation was

also calculated from monthly averaged data. Additionally, prior to any time series and correlation analysis, data was detrended. Detrending is a process that aims to “remove linear variation in a time series by computing a linear regression and subtracting it from the data” (AMS 2000).

Observed vertical profiles were also examined and linearly interpolated with height to establish whether there was evidence that profiles were changing in a discernable pattern on both a monthly and daily basis. Vertical temperature profiles were interpolated using the following algorithm:

$$T = \frac{z - z_0}{z_1 - z_0} (T_1 - T_0) + T_0 \quad (1)$$

In Equation 1, T is the interpolated temperature (K), T₀ is lower level temperature (K), T₁ is the upper level temperature (K), z is the interpolated height (m), z₀ is the lower level height (m), and z₁ is the upper level height (m).

2.2 Global and Regional Climate Models

Each component of the hierarchical modeling strategy has specific goals. According to Li et al. (2008), global and regional climate change are observed quite differently. For example, while global climate change can most often be observed as a secular warming, regional climate change manifests itself through shifts in circulation and precipitation. Therefore, the global climate component will characterize the large-scale circulation and the climate parameters that are important for determining climate-forcing of environmental variables, while the regional component will simulate events on a local scale and account for orographic complexity. GCM output will serve as boundary conditions for the regional model (mesoscale component). Downscaling will integrate

large-scale climate information with local topography and land surface conditions to provide details of meteorological variables on the mesoscale.

We have employed the National Center for Atmospheric Research (NCAR) Community Climate System Model Version 3 (CCSM3) for the global scale and a sophisticated Arctic regional modeling system, the NCAR-PSU 5th generation mesoscale model (Polar MM5) for the high-resolution simulations. We have chosen not to include the Weather Research and Forecasting (WRF) Model in this particular application due to current limitations with respect to long-term climate studies. Currently, the WRF model is calibrated for short-term weather analysis and lacks a necessary ice/ocean model component needed for long-term studies in Alaska. A diagram of the downscaling procedure and sequence is shown in Fig. 2.1.

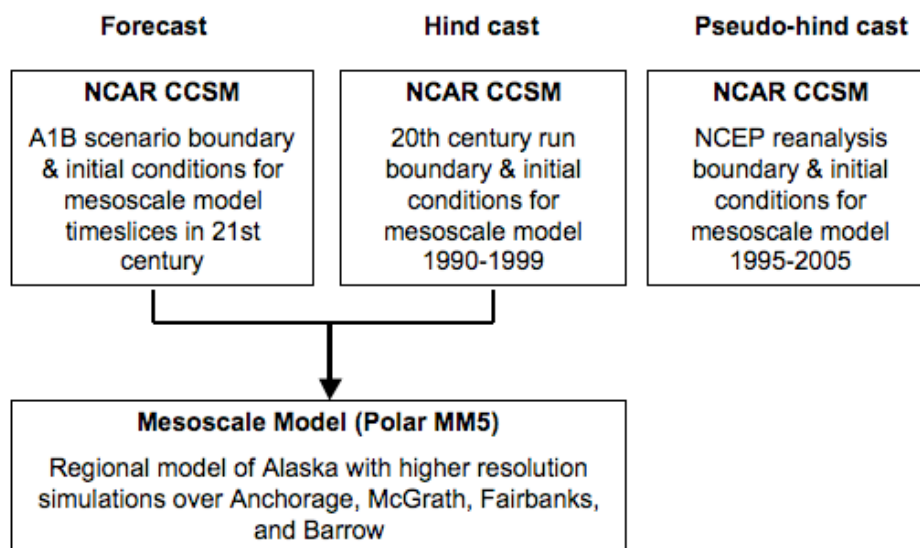


Figure 2.1. Modeling hierarchy diagram. Flow diagram outlining the modeling hierarchy and sequence. The top row shows global component simulations and projections. All global components are downscaled using the Polar MM5 model. The term “pseudo-hind cast” was used to describe the NCEP/NCAR Reanalysis dataset due to the integration of observations.

CCSM3 consists of four component models that represent the atmosphere, ocean, cryosphere, and land surface at T85 truncation (approximately 1.4° resolution) with 26 vertical levels. These component models are linked through a flux coupler where no corrections are applied to the fluxes (Collins et al. 2006). There have been major improvements from previous versions of the CCSM family in the parameterizations of cloud processes, aerosol radiative forcing, land-atmosphere fluxes, and sea-ice dynamics. However, it is important to consider that although performance of CCSM3 has improved compared to earlier versions, large biases exist in the 2-m air temperature for sub-Arctic continental regions in the winter months (Collins et al. 2006). CCSM3 simulated DJF temperature relative to the observed dataset from Willmott and Matsuura (2000) was found to be too warm by as much as 10 K in parts of Alaska (Collins et al. 2006). Model biases and systematic errors are taken into consideration by comparing a 20th century control run to local station observations.

The Polar MM5, which includes a thermodynamic sea ice model (Zhang and Zhang 2001) and a mixed layer ocean model (Kantha and Clayson 1994), is a three dimensional non-hydrostatic regional model with a terrain following sigma vertical coordinate, a choice of multiple options of physical parameterization schemes, and a nested-domain design. This model allows for high-resolution simulations over a specific area of interest, which efficiently utilizes computer resources.

This project applies a timeslice downscaling approach (Bengtsson et al. 1996). The first step in this process is model hind casting, which is a technique used to estimate biases in the NCAR CCSM3. The model hind cast will use the long record of observational data from four stations in Alaska to validate CCSM3 20th century simulation model output. A pseudo hind cast will also be performed using NCEP reanalysis data for validation purposes which involves a synthesis of observational data from a variety of available sources. The 20th century model simulation is then employed to provide boundary and initial conditions for the RCM component. The general climatology of surface-based

temperature inversions is evaluated to determine trends and variability with observations, and this comparison provides a measure with which to estimate errors due to CCSM3 biases in the downscaled future CCSM3 scenario. The future time-slice integrations provide changes for the 21st century based on the A1B scenario, which represents balanced fossil and non-fossil fuel use. Simulation details including model parameterizations (Table 4.1) are provided in Chapter 4, where model results are discussed.

Chapter 3. Variability and Trends of Observed Surface-based Temperature Inversions in Alaska

3.1 Data Analysis

Twice-daily RAOB data was analyzed from 1957 to 2008 to investigate the variability and trends of surface-based inversions from October through March at each station. In Alaska, the vertical structure of inversions varies due to external factors such as orography, radiation, and wind. Often times, inversions can become elevated from the surface and may contain embedded layers where temperature decreases with height. An algorithm was developed to capture inversions that originate at the surface and that have such complex structures. For this particular study, an inversion was defined as a layer where temperature decreases with height, including layers with a negative lapse rate if the layers are less than 100 meters thick (Kahl 1990 and Serreze et al. 1992). This definition of an inversion would also include small isothermal layers (Fig. 3.1).

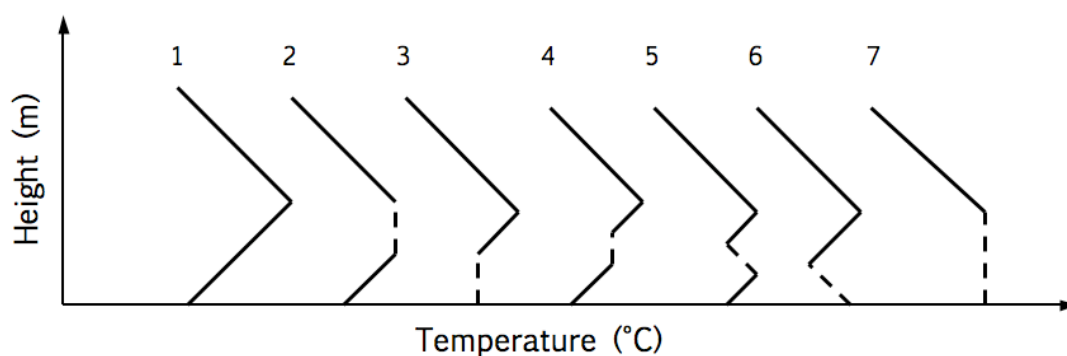


Figure 3.1. Inversion profile possibilities. This diagram schematically shows types of surface-based inversions considered during statistical analysis. Dashed regions represent layers less than 100 meters in depth. All dashed regions were included as part of the inversion, this includes isothermal layers (Figure adapted from Bradley et al. 1992).

The inversion algorithm detects surface-based temperature inversions in the RAOB data, as well as inversions that would inhibit vertical mixing and keep pollutants near the surface. Therefore, although small layers with negative lapse rates may be embedded in the inversion profile, the overall state of the atmosphere is stable. In Fig. 3.1, profiles 1-6 are all considered surface-based inversions, while profile 7 is not because it will not inhibit vertical mixing.

3.1.1 Inversion Climatology

Profiles and their characteristics display a seasonal progression which are summarized on a monthly basis. Inversion parameters of interest include inversion depth, inversion temperature difference, and inversion strength. Inversion depth is the height from the bottom of the inversion (including isothermal layers and layers with negative lapse rates if they are less than 100 m) to the top where the lapse rate begins decreasing for more than 100 m. The inversion temperature difference is therefore the temperature gradient between the top and bottom of the inversion, as defined by the inversion depth. Inversion strength in this study is defined as the temperature difference over the inversion depth (dT/dZ).

Inversion characteristics vary from month to month, and have unique relationships (Fig 3.2). For example, in the absence of synoptic forcing inversion depth and temperature difference are largely a function of surface temperature, as will be shown later. Climatological (average from 1957-2008) monthly vertical temperature profiles for Fairbanks are shown in Fig. 3.2. Although warmer months such as October and March typically have inversions some days of the month, on average their vertical profiles have negative lapse rates. Cooler months (November-February) have strong semi-permanent inversions that, when averaged over a long time period, are about 1000-1500 meters thick with 5-10 K temperature difference from the base to the top of the inversion. Additionally, as one might expect, variations in inversion characteristics are largest in the coldest months (Fig. 3.3). The coldest surface temperatures, and greatest deviations from

mean values occur in January. One exception is evident in Fairbanks during December, when inversion strength displays the largest variability of any other winter month.

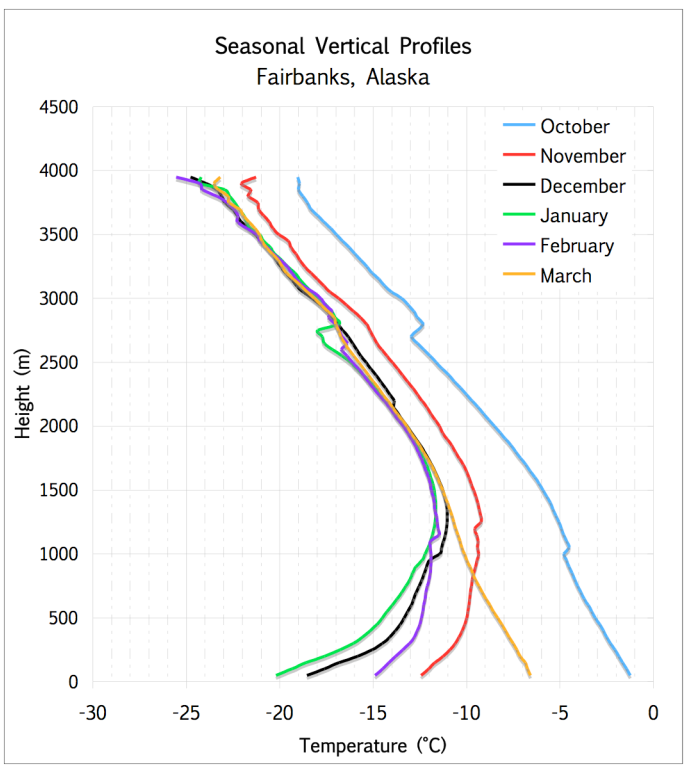


Figure 3.2. Monthly average vertical temperature profiles in Fairbanks, AK. There is a monthly progression of average inversion profiles during the wintertime in Fairbanks, Alaska from 1957-2008.

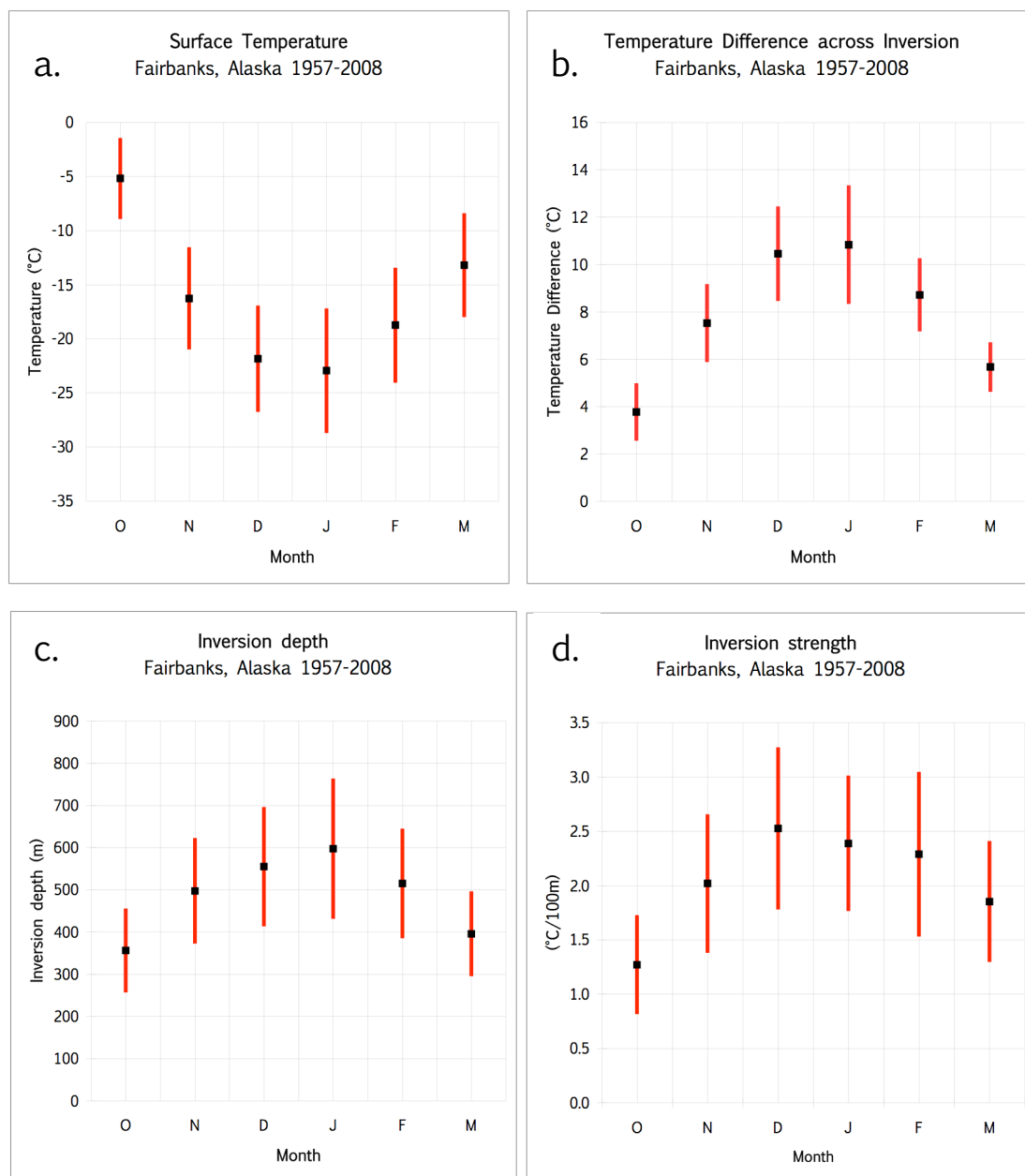


Figure 3.3. Seasonal variation of inversion parameters in Fairbanks, AK. Inversion characteristics follow monthly regimes through the winter season, with the greatest variability in the coldest months. The black markers represent the long-term mean during each month from 1957-2008, while the red bars show the range of variability based 1-sigma of standard deviation values.

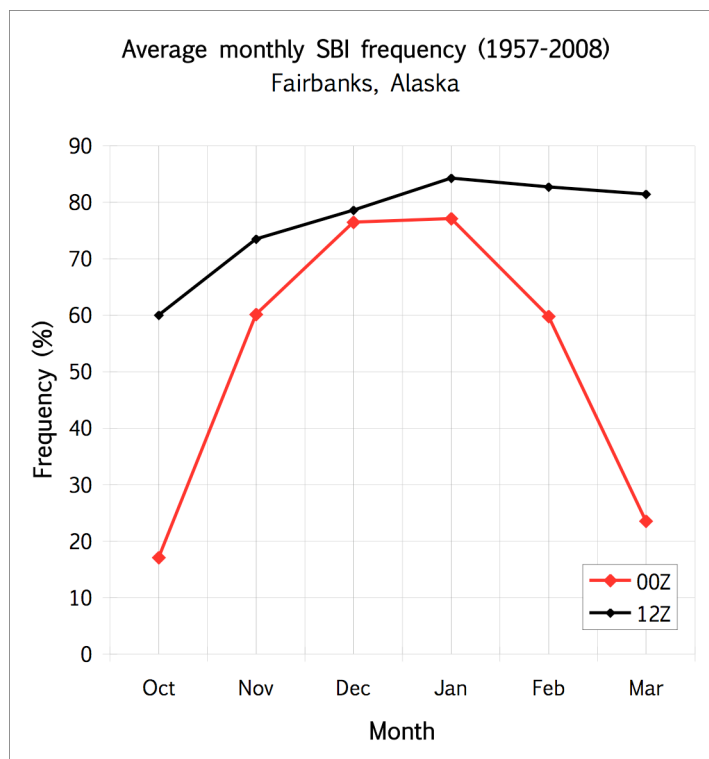


Figure 3.4. Wintertime inversion frequency in Fairbanks, AK. Long-term mean frequency of inversions shown as a percentage of days of the month in Fairbanks, Alaska. 0000 UTC represents 1500 hrs LST in Fairbanks, while 1200 UTC represents 0300 hrs LST inversions.

Inversion frequency varies with time of day and time of year. The 1200 UTC profiles (Fig. 3.4, black line) are taken at 0300 hrs LST and display little change with month, while the 0000 UTC (Fig. 3.4, red line) or 1500 hrs LST, profiles are impacted by the stronger diurnal cycle during the warmer months. During warmer months, the diurnal cycle has a greater impact on inversion frequency. During cooler months such as December and January, the solar radiation deficit creates an environment where inversion frequency does not vary with the diurnal cycle (Fig. 3.4).

In addition to their seasonal patterns, inversion characteristics also differ geographically across Alaska. For this particular study, four stations were chosen that represent three of

the six distinct regions of the state. Anchorage represents the Southcentral region, Fairbanks and McGrath represent the Interior, and Barrow represents the North Slope (Fig. 1.2). Factors that influence climate are different in each area which subsequently affects inversion frequency, depth, temperature difference, and strength.

Variability of inversion profiles as a function of height is different at each station. Non-local forcing in a particular region such as synoptic events will affect daily variability of vertical temperature profiles. However, while inversion profiles may be complex and vary on a day-to-day basis, overall average monthly profiles appear smooth. The daily standard deviation for each height is shown in Fig. 3.5. The variability is smallest in Anchorage and greatest for the Interior stations of Fairbanks and McGrath.

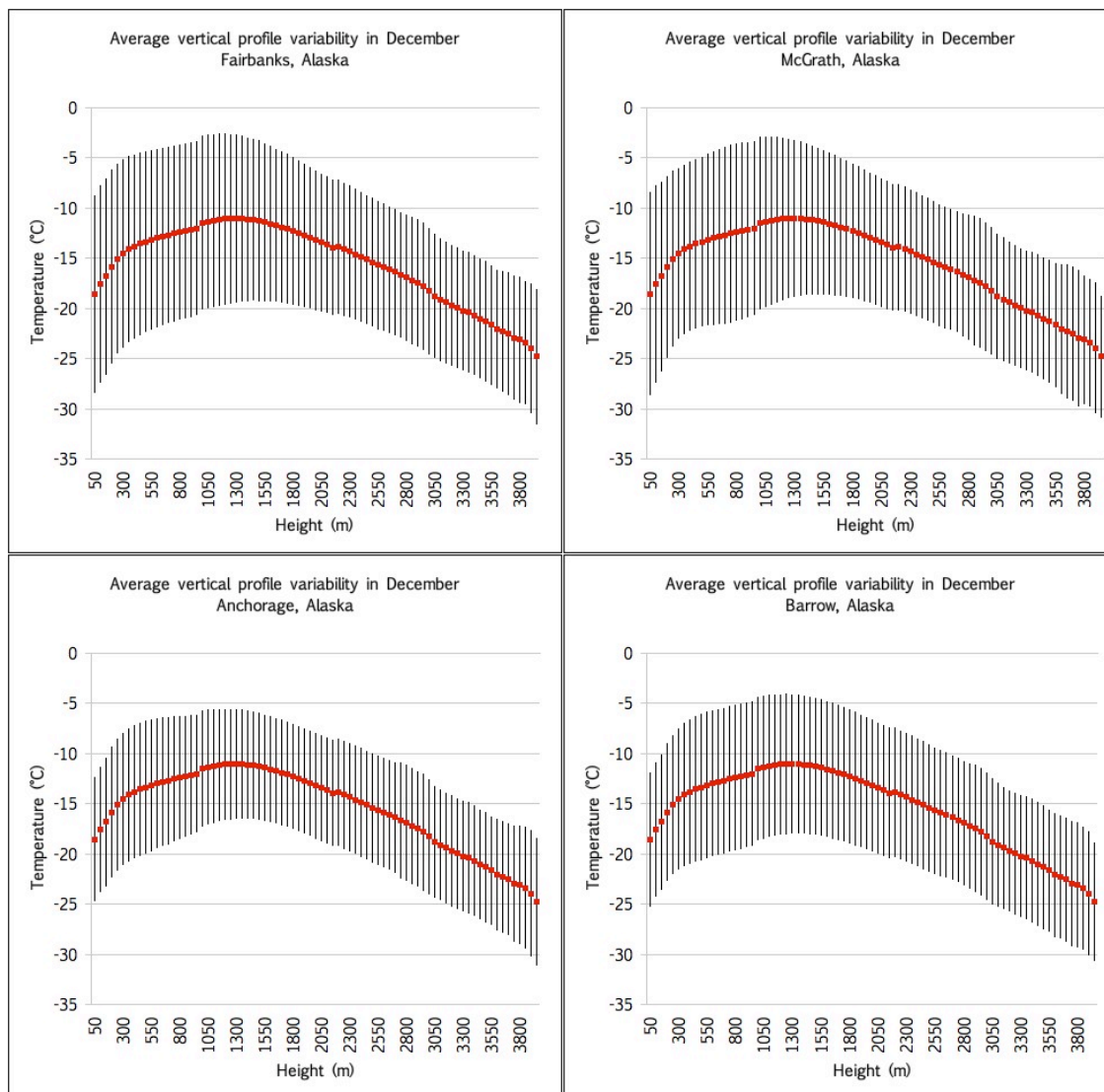


Figure 3.5. Average vertical profile variability in December. Fairbanks, McGrath, Anchorage, and Barrow vertical profile variability in December. The variability is represented by 1-sigma of standard deviation from the mean values.

Fig. 3.6 shows the long-term mean vertical temperature profiles at each station during December, typically one of the colder months of the year. Important features to note are the differences in surface temperature, inversion depth and temperature difference, and inversion strength. When compared to the three other stations, Anchorage has the

shallowest inversion with the smallest temperature difference from the base to the top during December. Fairbanks and McGrath exhibit similar inversion characteristics, which is attributed to their similar geography and surrounding orography. Both Interior stations display relatively large average inversion depths and temperature differences. Barrow's inversion has the coldest surface temperature, but has a depth that is a few hundred meters shallower than inversions in the Interior on average.

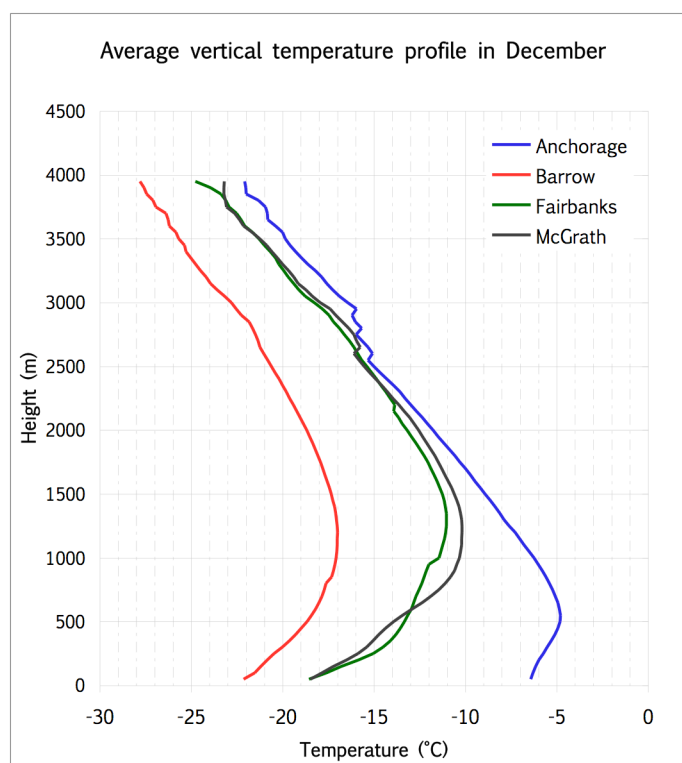


Figure 3.6. Monthly averaged vertical temperature profiles at Alaska stations in December. Average vertical temperature profiles from 1957-2008 in Alaska vary with geographic region during the winter months.

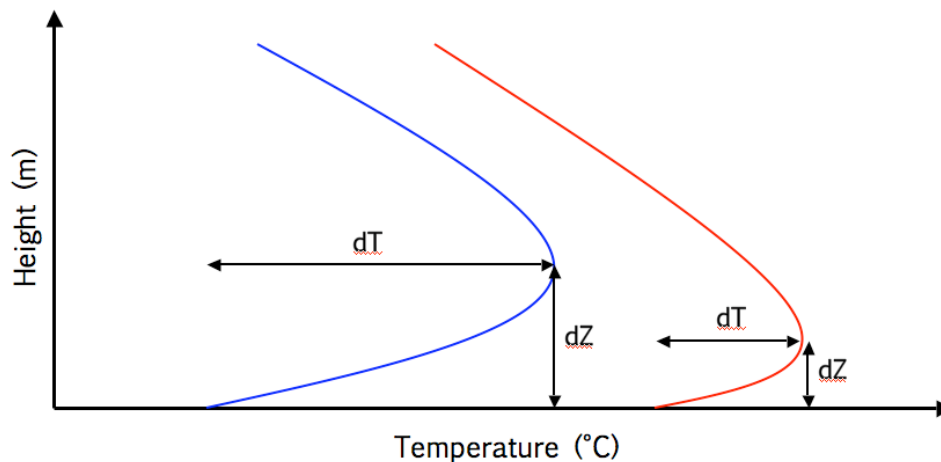


Figure 3.7. Relationship between inversion depth and temperature difference. Surface-based temperature inversions in Alaska are largely a function of surface temperature. When surface temperatures are warm (cold), inversion depth and temperature difference is small (large).

The inversion profiles shown in Fig. 3.6 are not simply a result of geography, but are significantly correlated with surface temperature at each particular station. It should be mentioned that any reference to the phrase “significant” hereafter implies statistical significance at 95% unless specified otherwise. An analysis of RAOB data in Fairbanks showed that warmer surface temperatures were negatively correlated to inversion depth and temperature difference (Fig. 3.7). In other words, when the surface is warm, inversions are shallow with a small temperature difference but when the surface is cool, inversions are deep with a great temperature difference. This notion holds true for all stations in the study and makes physical sense because inversions develop from surface cooling due to longwave radiative losses.

3.1.2 Surface Temperature

The range of surface temperatures across Alaska vary largely as a function of geographic region. Anchorage overall has the warmest surface temperatures in December and January (Table 3.1), while McGrath, Fairbanks, and Barrow exhibit cooler temperatures

with similar ranges (Fig. 3.8). Warmer temperatures in Anchorage are not only a function of the comparably lower latitude, but also the proximity to the ocean. McGrath and Fairbanks are characterized by their continental climates, which are inland and cut off from the moderating influence of the oceans. Continental climates are characterized by great daily and annual temperature ranges, low humidity and relatively light and irregular precipitation (Shulski and Wendler 2007). Yet, while the range of temperatures may vary from region to region across Alaska, surface temperatures have similar patterns of interannual variability at each station and are positively correlated (Table 3.2). These similar patterns of interannual variability suggest that climatic regions across the state may be influenced by similar large-scale forcing as evident in the temperature observations (Fig. 3.8) as well as temperature anomalies (Fig. 3.9). This suggests that if Fairbanks experiences a warmer than average winter then McGrath, Anchorage and Barrow are likely to have an anomalously warm winter.

Surface temperatures have increased at all four stations in Alaska between 1957-2008 (Table 3.1). On average, they have increased at a rate of 0.11 K/decade in December and 0.05 K/decade in January over the 1957-2008 period. In December the trend is similar at all four stations but the trend varies considerably in January, with Barrow displaying essentially no trend.

Table 3.1. Surface temperatures in Alaska during December and January. Due to availability of data, December values represent an average from 1957-2007, while January values are an average from 1957-2008. Bold values listed indicate trends significant at 95% or greater based on a t-test. Any italicized values indicate a trend significant at 90% or greater.

Surface Temperature				
	December		January	
	Average (K)	Trend (K/decade)	Average (K)	Trend (K/decade)
Anchorage	265.2	0.96	264.3	<i>0.69</i>
McGrath	250.5	1.02	249.2	0.38
Fairbanks	251.3	1.05	250.2	0.87
Barrow	248.3	0.91	247.1	-0.03

Table 3.2. Surface temperature time series correlation. Anchorage, McGrath, and Barrow time series were detrended and correlated to Fairbanks surface temperature data from 1957-2008. Statistical significance of correlations at the 95% level or greater based on Student's t-test is indicated in bold.

Correlation to Fairbanks Surface Temperatures		
	December	January
Anchorage	0.888	0.875
McGrath	0.795	0.889
Barrow	0.466	0.452

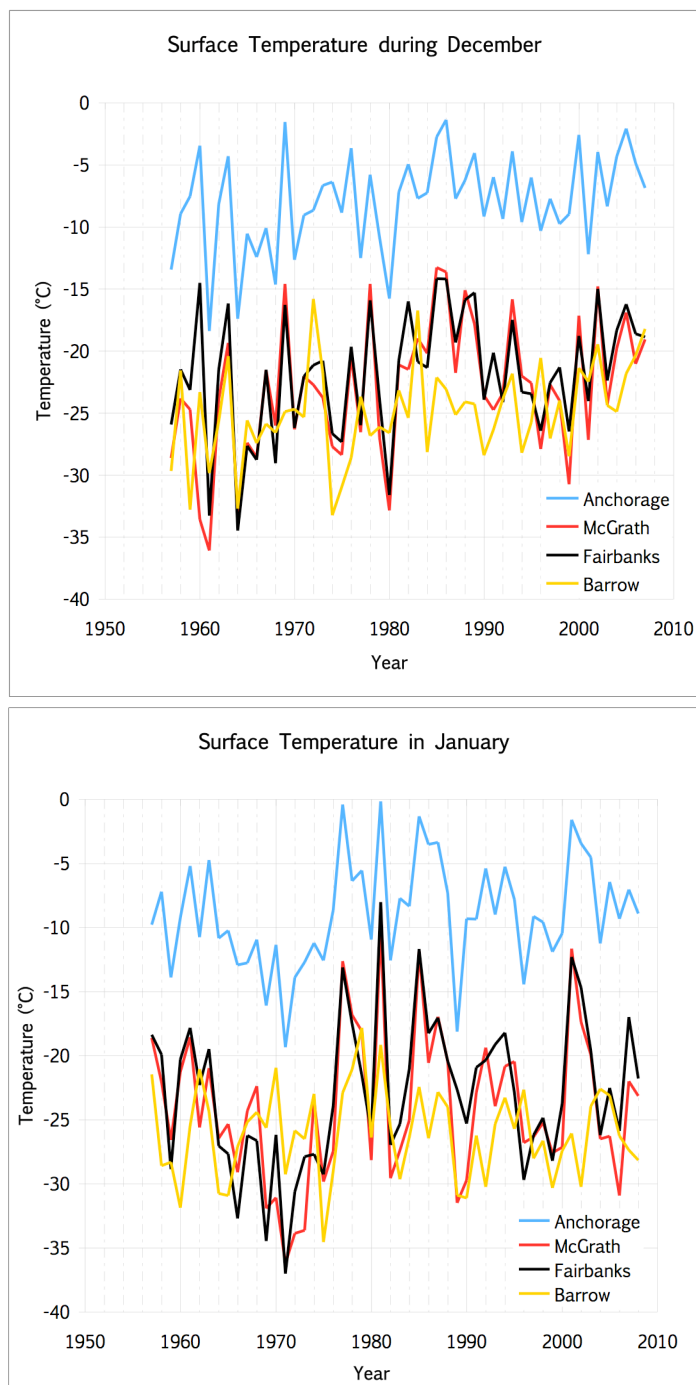


Figure 3.8. Wintertime surface temperatures in Alaska. Surface temperatures for Anchorage (blue), McGrath (red), Fairbanks (black), and Barrow (yellow) have an increasing trend from 1957-2008. On average, surface temperatures have increased at a rate of 0.11 K/decade in December and 0.05 K/decade in January.

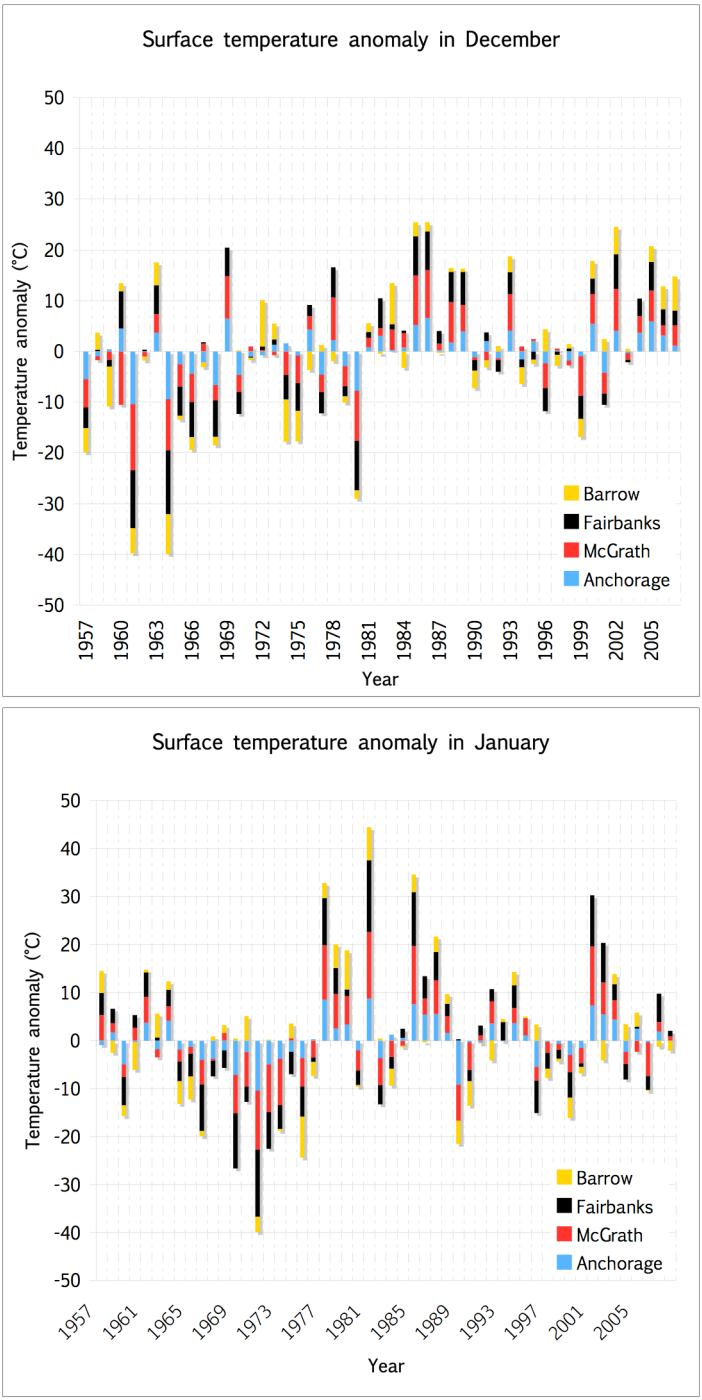


Figure 3.9. Wintertime surface temperature anomalies in Alaska. December and January surface temperature anomalies for Anchorage (blue), McGrath (red), Fairbanks (black), and Barrow (yellow) from 1957-2008.

3.1.3 Inversion Depth

Inversion depth displays a decrease from 1950 to the late 1980s and an increase in the last 20 years at all four Alaska stations (Fig. 3.10). Inversion depth in the early part of the record was between 800 and 1000 meters at Interior stations but is between 400-600m towards the end of the study period. On average, inversion depth is decreasing at a rate of 7.3m/decade in December and 7.9m/decade in January. Individual trends and long-term mean inversion depths vary at each location (Table 3.3). Note that the trends are quite large compared to the mean depths because of the large decrease in inversion depth during the early part of the record. In addition, inversion depth has similar patterns of interannual variability at each station and is quantified by the significant positive correlations of depth in Fairbanks with that at other stations (Table 3.4). The strongest correlations are between Fairbanks and McGrath, the two Interior stations. Recall that for surface-based temperature inversions, the depth is defined as the difference in height between the surface and the height at which the lapse rate is negative for more than 100 meters.

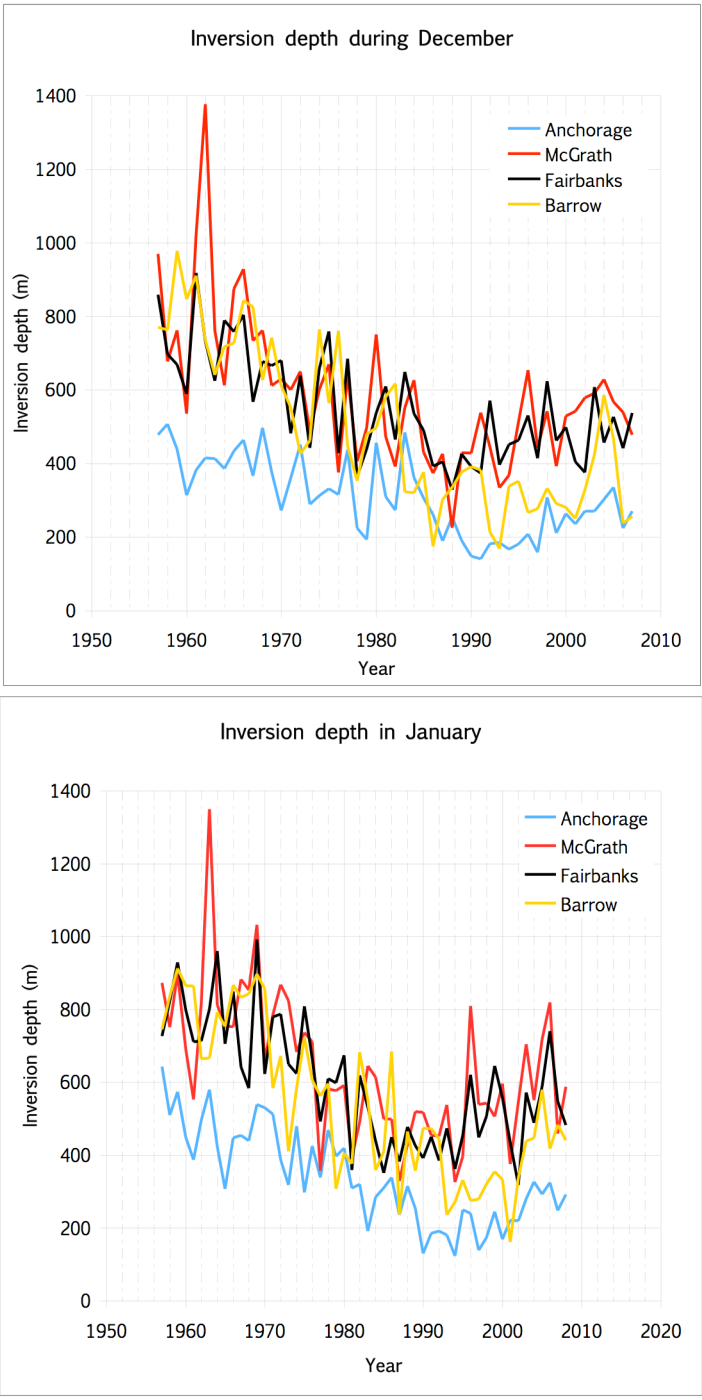


Figure 3.10. Wintertime inversion depth in Alaska. December and January inversion depth for Anchorage (blue), McGrath (red), Fairbanks (black), and Barrow (yellow) show decreasing trends. On average, inversion depth is decreasing at a rate of 7.3m/decade in December and 7.9m/decade in January.

Table 3.3. Inversion depth in Alaska during December and January. Due to availability of data, December values represent an average from 1957-2007, while January values are an average from 1957-2008. Bold values listed indicate trends significant at 95% or greater based on a t-test. Any italicized values indicate a trend significant at 90% or greater.

Inversion Depth (m)				
	December		January	
	Average (m)	Trend (m/decade)	Average (m)	Trend (m/decade)
Anchorage	310	-47.1	339	-66.3
McGrath	587	-74.7	639	-70.6
Fairbanks	555	-62.8	597	-72.7
Barrow	496	-117.7	540	-107.7

Table 3.4. Inversion depth time series correlation. Correlation of Anchorage, McGrath, and Barrow inversion depth with Fairbanks inversion depths from 1957-2008. Time series were linearly detrended before performing correlation analysis. Statistical significance at the 95% level or greater based on Student's t-test is indicated in bold.

Correlation to Fairbanks Inversion Depths		
	December	January
Anchorage	0.536	0.396
McGrath	0.624	0.641
Barrow	0.342	0.455

Surface temperatures display an increasing trend from 1957-2008 (Fig. 3.8), which is consistent with the trend in inversion depth. Recall, the earlier discussion that demonstrated that Fairbanks inversion depths are negatively correlated with surface temperatures. Inversion depth anomalies (not detrended) display a clear transition from primarily positive to negative anomalies around 1975 (Fig. 3.11). This transition appears to occur at all stations and is consistent with previous studies that show a strong relationship between the shift in the Pacific Decadal Oscillation (PDO) and climate variations across the entire state (Papineau 2001; Hartmann and Wendler 2005b).

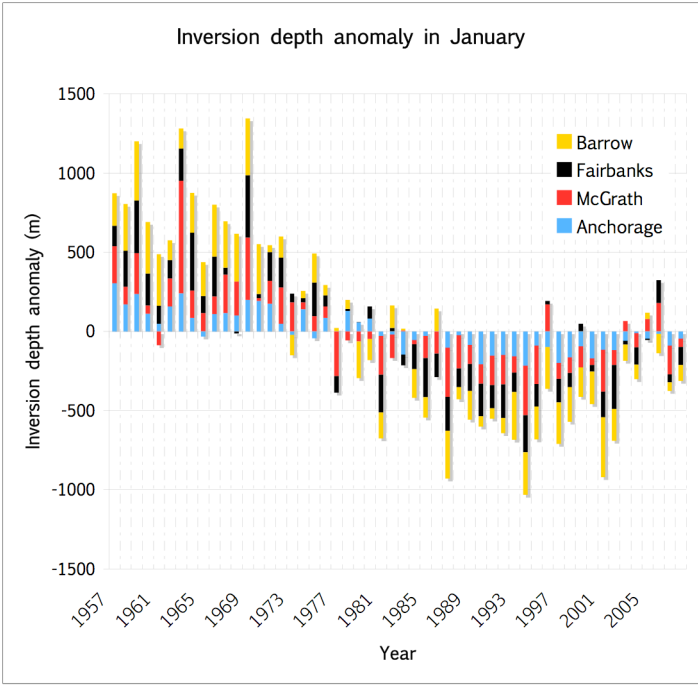
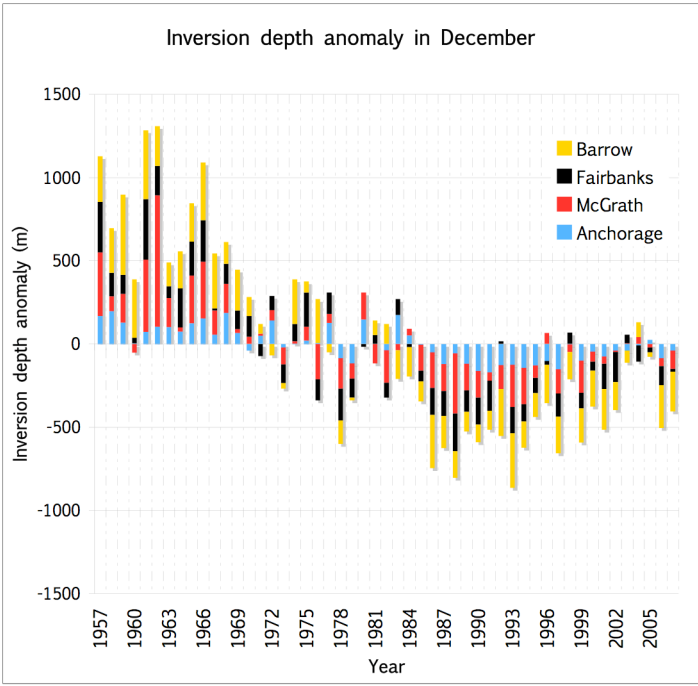


Figure 3.11. Wintertime inversion depth anomalies in Alaska. December and January inversion depth anomalies for Anchorage (blue), McGrath (red), Fairbanks (black), and Barrow (yellow) from 1957-2008.

3.1.4 Inversion Temperature Difference

The inversion temperature difference is defined as the temperature gradient that exists from the surface to the top of the inversion. Anchorage has the smallest average temperature difference of the four stations, while Fairbanks and McGrath have the greatest temperature difference (Table 3.5). Despite these dissimilarities however, Anchorage, McGrath, and Barrow show statistically significant correlation to patterns of interannual variability in inversion temperature difference in Fairbanks from 1957-2008 (Table 3.6). In addition, December and January inversion temperature differences have weak negative trends from 1957-2008 in each of the four stations (Fig. 3.12). Thus, just as inversion depth, inversion temperature difference decreases over time are consistent with increasing surface temperatures trends across the state. On average, inversion temperature difference is decreasing at a rate of 0.08 K/decade in December and 0.09 K/decade in January. Individual trends in inversion temperature difference for each station are shown in Table 3.5.

The overall shape of the inversion temperature difference (Fig. 3.12) is similar to that of inversion depth (Fig. 3.10), with large values early in the study period, decreasing until the late 1980's and subsequently increasing over the last 20 years. This characteristic curve shape resembles some elements of multidecadal variability. A comparison of inversion depth anomalies (Fig. 3.11) with inversion temperature difference anomalies (Fig. 3.13), suggests that there is a transition from generally positive to negative anomalies during the mid-1970s.

Table 3.5. Inversion temperature difference in Alaska during December and January. Due to availability of data, December values represent an average from 1957-2007, while January values are an average from 1957-2008. Bold values listed indicate trends significant at 95% or greater based on a t-test. Any italicized values indicate a trend significant at 90% or greater.

Inversion Temperature Difference (°C)				
	December		January	
	Average (K)	Trend (K/decade)	Average (K)	Trend (K/decade)
Anchorage	3.9	-0.53	4.5	-0.73
McGrath	10.6	-0.74	11.7	-0.75
Fairbanks	10.5	-0.46	10.8	-0.89
Barrow	6.6	-0.98	7.8	-0.96

Table 3.6. Inversion temperature difference time series correlation. Anchorage, McGrath, and Barrow time series were detrended and correlated to Fairbanks inversion temperature differences from 1957-2008. Statistical significance at the 95% level or greater based on Student's t-test is indicated in bold.

Correlation to Fairbanks Inversion Temperature Differences		
	December	January
Anchorage	0.517	0.362
McGrath	0.461	0.625
Barrow	0.020	0.391

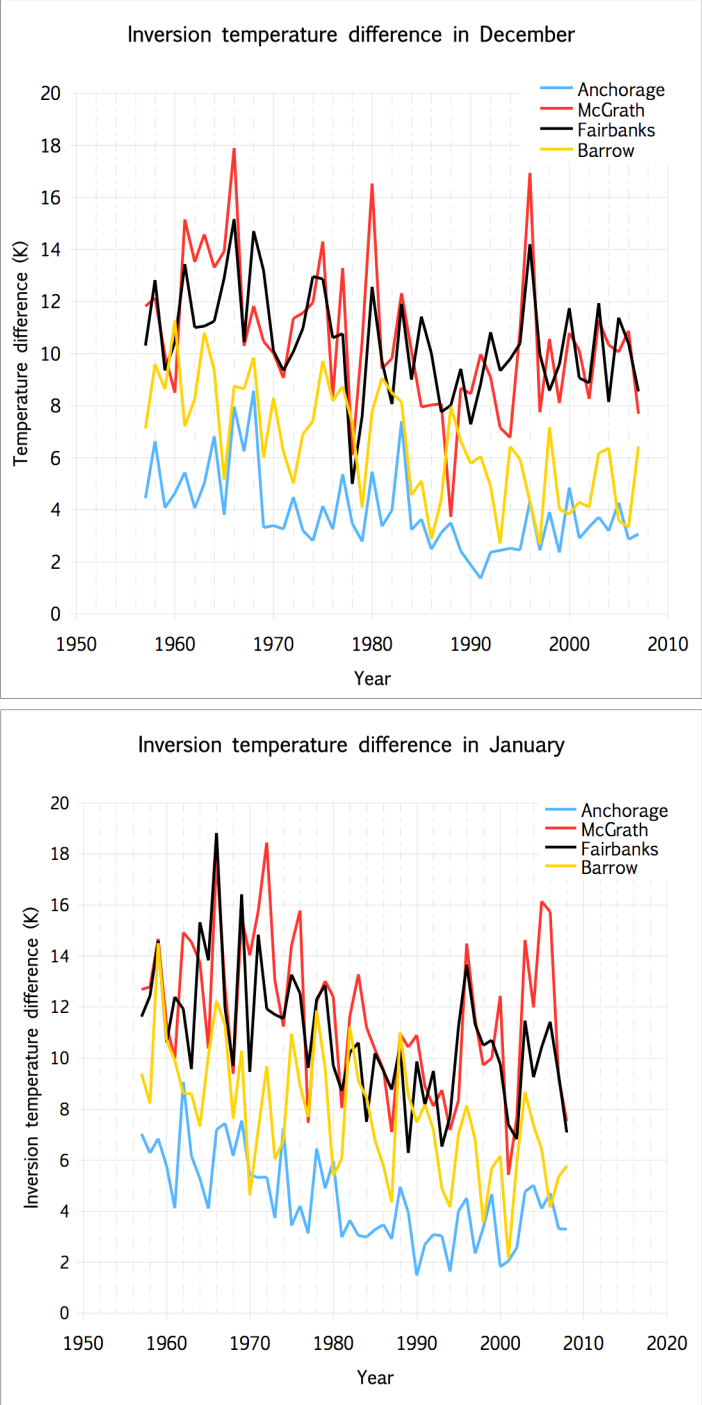


Figure 3.12. Wintertime inversion temperature difference in Alaska. December and January temperature difference in Anchorage (blue), McGrath (red), Fairbanks (black), and Barrow (yellow) show decreasing trends from 1957-2008. On average, temperature difference is decreasing at a rate of 0.08 K/decade in December and 0.09 K/decade.

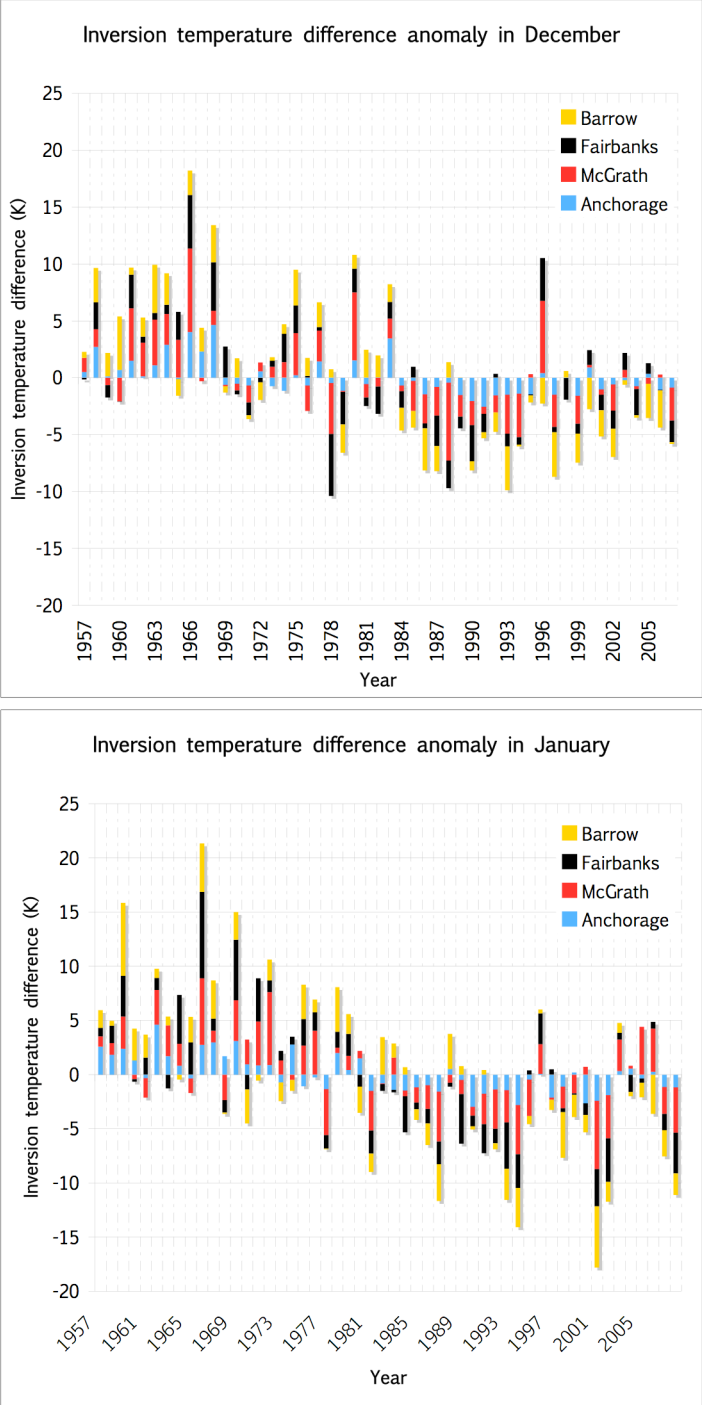


Figure 3.13. Wintertime inversion temperature difference anomalies in Alaska. December and January inversion temperature difference anomalies for Anchorage (blue), McGrath (red), Fairbanks (black), and Barrow (yellow) from 1957-2008.

3.1.5 Inversion Strength

The strength of a surface-based temperature inversion is defined as the temperature difference divided by the inversion depth (dT/dZ). Although inversion depth and temperature difference are positively correlated, inversion strength is highly dependent on the behavior and magnitude of the numerator (dT) and the denominator (dz) making interpretation not simple. In December and January, inversion strength displays changing variability (Fig. 3.14) over the analysis period, with the largest variations during the middle part of the record (~1972-1988). On average, inversion strength has increased at a rate of $0.002 \frac{K/100m}{year}$ in December and $0.003 \frac{K/100m}{year}$ in January over the study period. Overall the average inversion strength is weakest in Anchorage and strongest in Fairbanks (Table 3.7), which is consistent with the analysis of surface temperature, inversion depth, and inversion temperature difference.

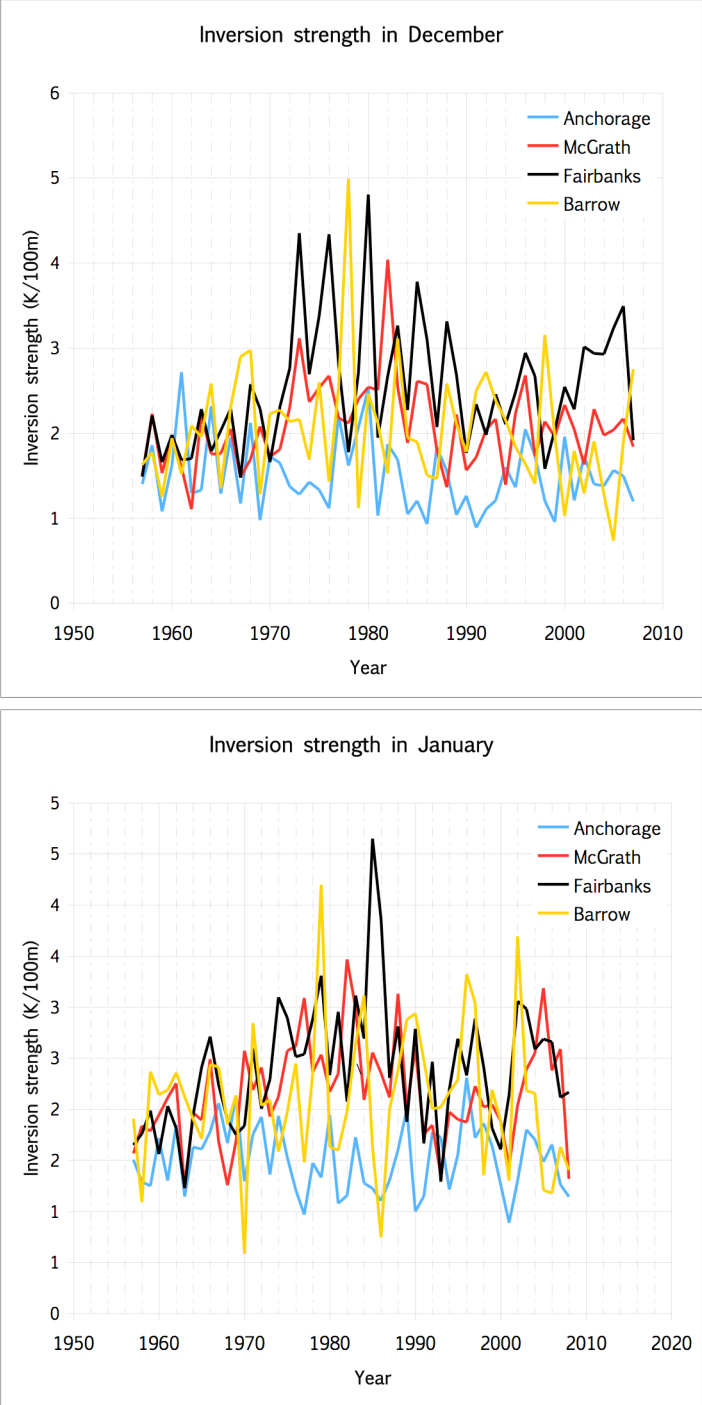


Figure 3.14. Wintertime inversion strength in Alaska. Inversion strength in Anchorage (blue), McGrath (red), Fairbanks (black), and Barrow (yellow) shows high variability from the early 1970s until the late 1980s. On average, inversion strength is increasing at a rate of $0.002 \text{ K}/100\text{m}\text{-decade}^{-1}$ in December and $0.003 \text{ K}/100\text{m}\text{-decade}^{-1}$ in January.

Table 3.7. Inversion strength in Alaska during December and January. Due to availability of data, December values represent an average from 1957-2007, while January values are an average from 1957-2008. Bold values listed indicate trends significant at 95% or greater based on a t-test. Any italicized values indicate a trend significant at 90% or greater.

Inversion Strength ($^{\circ}\text{C}/100\text{m}$)				
	December		January	
	Average (K/100m)	Trend ($\frac{K/100m}{year}$)	Average (K/100m)	Trend ($\frac{K/100m}{year}$)
Anchorage	1.5	-0.06	1.5	-0.02
McGrath	2.1	0.04	2.2	0.05
Fairbanks	2.5	<i>0.13</i>	2.4	0.11
Barrow	2.0	-0.04	2.1	0.01

In Fairbanks, surface-based temperature inversions are believed to be the strongest found anywhere with “temperature differences of 20 K in the lowest 200m not uncommon” (Wendler and Nicpon 1975). On average however, McGrath, Fairbanks, and Barrow have inversions that increase approximately 2 K per 100 meters. This may be due in part to the orographic effects of the Brooks and Alaska Ranges. The Canadian Arctic exhibits similar inversion strength magnitudes of approximately 1.5 K per 100 meters (Kahl et al. 1992). The Eurasian Arctic also experiences strong low-level inversions. According to Serreze et al. (1992), the strongest inversions in Eurasia are found in Verkhoyansk in the Yana River valley with inversion strengths averaging about 1.5 K per 100 meters.

Prior to 1970, inversion strength at all stations in both December and January was anomalously low (Fig. 3.15). Beginning in 1971, however, there is a period where inversion strength became highly variable. This trend is evident in all months (October-March) at each station. In general, inversion strength anomalies vary more between stations for a given year than was seen for surface temperature, inversion depth, and inversion strength anomalies. This behavior is likely due to the derivative nature of inversion strength anomaly. Patterns of interannual variability in inversion strength likely

vary in large part due to synoptic-scale forcing or influences from modes of multi-decadal climate variability, which alter synoptic variability.

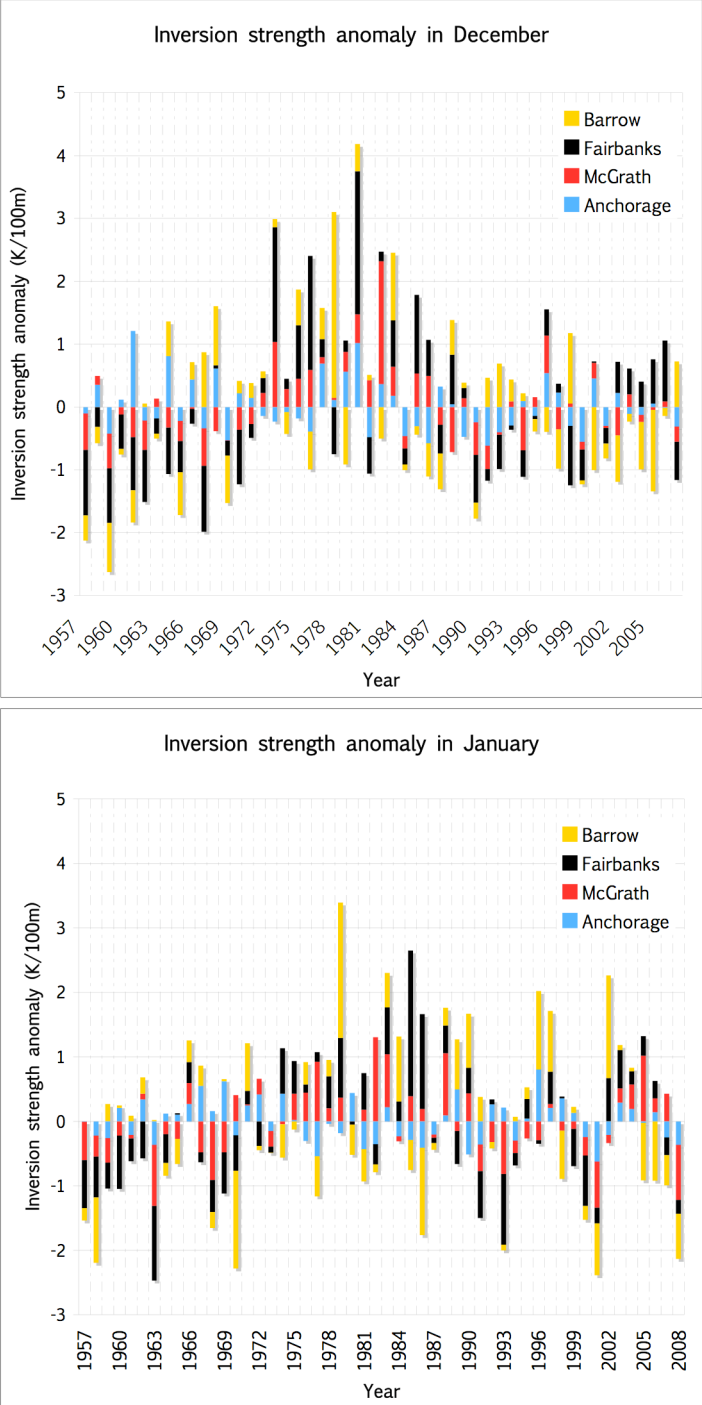


Figure 3.15. Wintertime inversion strength anomalies in Alaska. December and January inversion strength anomalies for Anchorage (blue), McGrath (red), Fairbanks (black), and Barrow (yellow) from 1957-2008.

3.2 Connections to Large-scale Climate Variability

Inversion depth and temperature difference anomalies exhibit similar behavior over the observation period. Inversion depth (Fig. 3.11) and temperature difference (Fig. 3.13) show a distinct shift from positive to negative anomalies in the late 1970s. Positive anomalies of inversion depth and temperature difference indicate inversions that are cold and deep, while negative anomalies indicate warm, shallow inversions. The shift in inversion strength anomalies is not as distinct, however. This behavior could be due to the proportional relationship between temperature difference and depth in the inversion strength parameter. In other words, because the magnitude of inversion strength is affected by both the depth and the temperature difference, climate variability may not be as evident in such a parameter and requires interpretation (Fig. 3.15).

The change from generally positive to generally negative anomalies of inversion depth and temperature difference anomalies in the late 1970s is concurrent with the shift of the Pacific Decadal Oscillation (PDO) from a negative to a positive phase. In an attempt to explain this shift, multidecadal climate oscillations were compared to RAOB data from the stations in Alaska.

The PDO is a 20-30 year pattern of Pacific climate variability that displays warm and cool anomalies in sea surface temperature (SST) north of 20°N in the central basin.

The PDO index (Mantua et al. 1997, Minobe 1997) is the principle component associated with the first empirical orthogonal function (EOF) of Pacific SST poleward of 20°N after the global SST trend is removed (Trenberth 1990, Trenberth and Hurrell 1994, Zhang et al. 1997, Mantua et al. 1997). The positive (negative) phase of the PDO is characterized by anomalously cool (warm) SSTs in the mid-North Pacific, above average (below average) SSTs along the Pacific Coast, and below average (above average) SLP over the North Pacific.

The PDO index shifted around 1976 from a dominantly negative phase (1951-1975) to a dominantly positive phase. According to Hartmann and Wendler (2005b), “mean annual and seasonal temperatures for the positive phase were up to 3.1 K higher than for the negative phase.” Therefore, positive values of the PDO index are positively correlated with surface temperatures and negatively correlated with mean SLP (Fig 3.16) in Alaska. Decreased SLP results in a deepening of the Aleutian low and increased warm, moist air advection into Alaska.

Table 3.8. Inversion parameters correlated to wintertime PDO index from 1957-2008. Time series of inversion parameters averaged during DJF and detrended in Fairbanks have high correlation to the PDO index. Bold values are statistically significant at 95% or greater, while italicized values are statistically significant at 90% confidence.

Parameter	Correlation with PDO
Surface temperature	0.494
Inversion depth	-0.358
Inversion temperature difference	-0.219
Inversion strength	<i>0.233</i>

The PDO index was compared with inversion parameters in Fairbanks during the winter months (Table 3.8). Surface temperature is positively correlated to the PDO index, consistent with the notion that the positive phase of the PDO implies warmer than average surface air temperatures in Alaska. The inversion depth is negatively correlated with the PDO index and suggests that during the positive phase there are shallower inversions. Inversion temperature difference and strength are weakly correlated with the PDO index. Since the inversion depth and temperature difference are negatively correlated with the PDO, then a positive PDO index implies that inversion depth and temperature difference are anomalously low (Fig. 3.17).

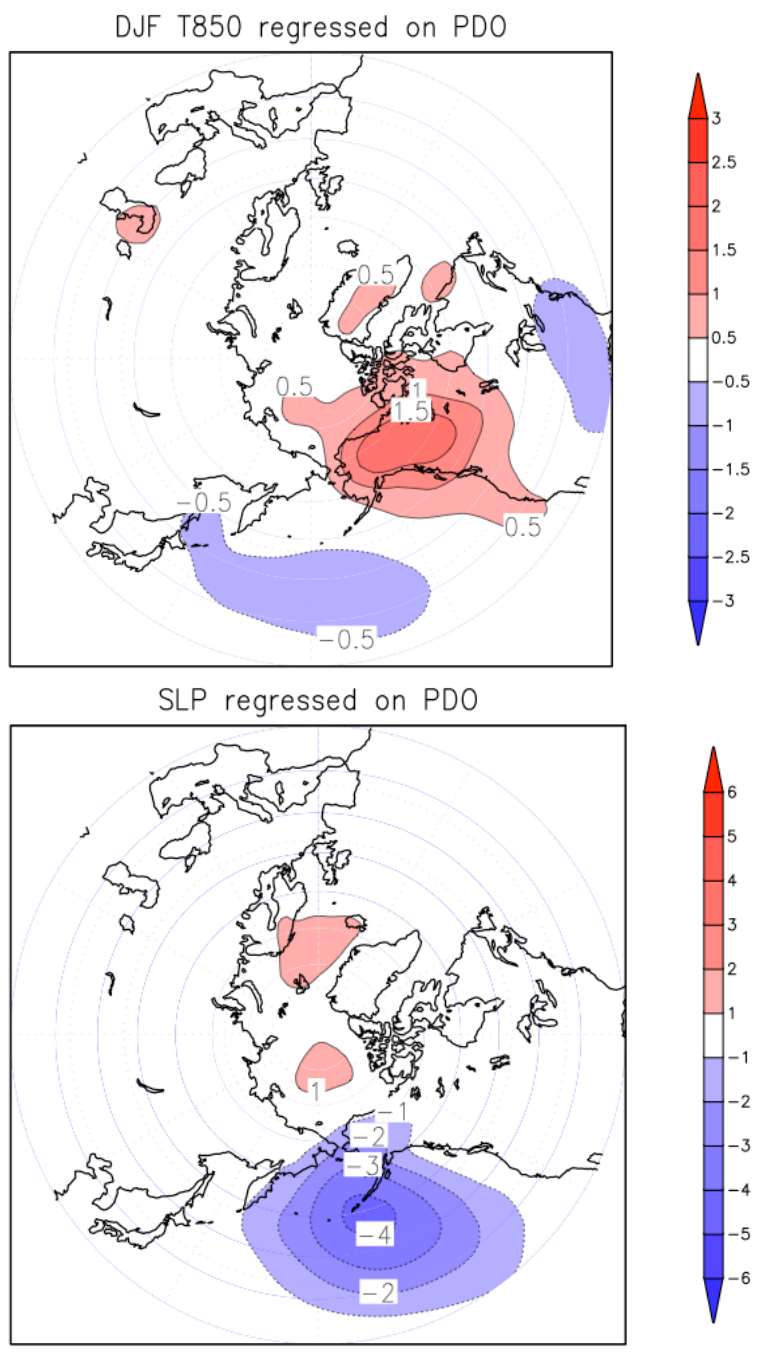


Figure 3.16. PDO connections to inversion parameters. DJF 850 mb temperature regressed on the PDO (top) SLP regressed on the PDO (bottom). For every unit change in the PDO index, the plots show the change in magnitude of air temperature in °K at 850 mb and SLP in hPa the Northern Hemisphere.

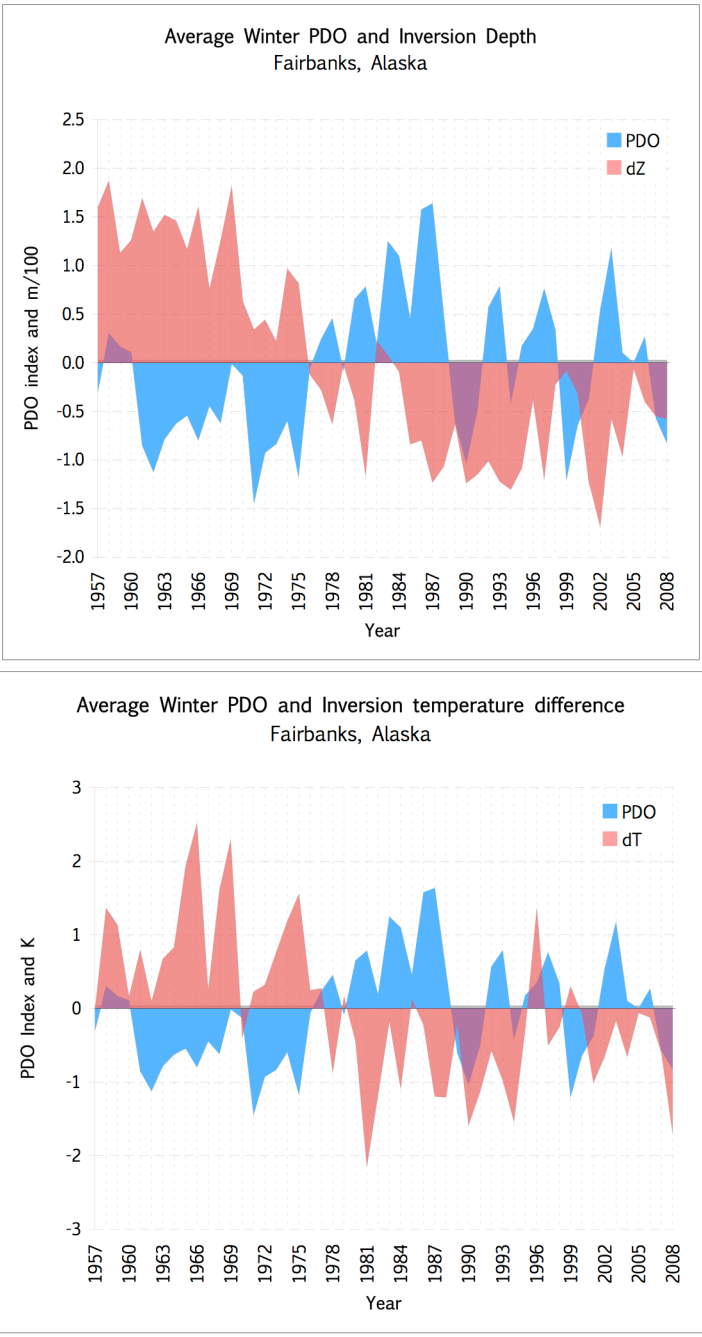


Figure 3.17. Inversion parameters correlated to wintertime PDO index. The average winter PDO index (October-March) is negatively correlated to inversion depth and temperature difference in Fairbanks, Alaska from October-March.

According to Papineau (2001), synoptic-scale forcings resulting from large-scale climate oscillations have a considerable effect on temperature anomalies over Alaska. Surface temperature changes that occur as a result of synoptic-scale flow are inhibited by the development of strong, stable inversions. Additionally, warm anomalies are primarily a function of advection, therefore temperatures during warm anomalies oscillate in phase with changes in the synoptic-scale flow.

For this reason, it is important to determine the effect other modes of natural climate variability have on inversion characteristics in Alaska. The North Atlantic Oscillation (NAO) is a climate index that describes the gradient of SLP between the Icelandic Low and the Azores High. The NAO index is the normalized SLP difference between a station in Iceland and the Azores. The positive phase of the NAO is characterized by a stronger than average pressure gradient between the subtropical and mid-latitude North Atlantic (Fig. 3.18). In addition, during the positive NAO phase the strength and intensity of storms penetrating into the Arctic increases (Zhang et al. 2004). Table 3.9 shows the correlation of the wintertime index of the NAO to inversion parameters in Alaska. Overall the correlations, while consistent among stations, are fairly weak between the NAO and surface inversion parameters in Alaska. The correlations indicate that during the positive phase of the NAO, Alaska surface temperatures are cooler than normal, inversion depths are shallower than normal, and inversion temperature differences are weaker than normal. This relationship is somewhat confusing, but is consistent with the notion that temperatures aloft are warmer than normal during the positive phase of the NAO. This fact requires further analysis to tease out the details of this relationship.

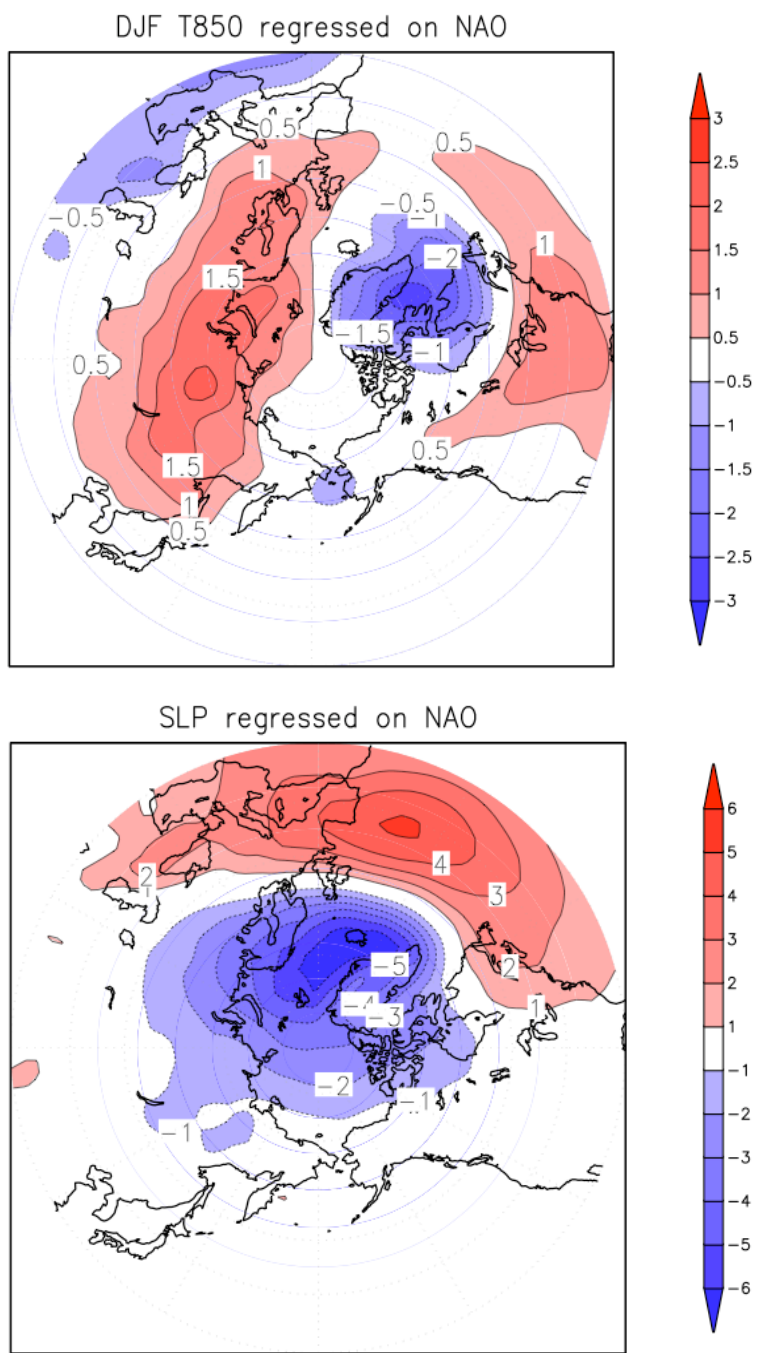


Figure 3.18. NAO connections to inversion parameters. DJF 850 mb temperature regressed on the NAO (top) SLP regressed on the NAO (bottom). For every unit change in the NAO index, the plots show the change in magnitude of temperature at 850 mb and SLP in the Northern Hemisphere.

Table 3.9. Average DJF inversion parameters correlated to wintertime NAO index from 1957-2008. Bold values listed indicate correlations significant at 95% or greater based on a t-test. Any italicized values indicate a correlation significant at 90% or greater.

Location	Surface temperature	Inversion depth	Inversion temperature difference	Inversion strength
Anchorage	-0.204	-0.140	-0.140	-0.138
McGrath	-0.132	-0.280	<i>-0.257</i>	-0.085
Fairbanks	-0.102	-0.22	-0.343	-0.040
Barrow	-0.127	-0.213	-0.020	-0.083

Another mode of climate variability describing large-scale climate in the Arctic is the Arctic Oscillation (AO). While the AO and NAO display large covariability, the AO is associated with atmospheric variability from the surface to the stratosphere while the NAO with air-sea interaction. The AO describes a pattern of sea level pressure of one sign over the Arctic and opposite sign in the midlatitudes. The AO index is defined as the principle component of the first EOF of 1000mb height (or SLP) anomalies poleward of 20°N (Thompson and Wallace 1998). The positive (negative) phase of the AO is characterized by negative (positive) SLP anomalies in the Arctic and with positive (negative) SLP anomalies in the midlatitudes (Fig. 3.19). Table 3.10 shows the correlation of the wintertime index of the AO to inversion parameters in Alaska. The correlations are general weak but display a consistent pattern between stations. Correlations are negative with surface temperature, inversion depth and inversion temperature difference. The sign of the correlations also indicates that the relationship with the AO is complex since the positive phase of the AO implies cooler than normal surface temperatures yet shallower than normal inversion depths. This behavior is opposite the relationship between the surface temperature and inversion depth noted earlier in this chapter. This suggests that the interactions are complex and require additional analysis that is beyond the scope of the current project.

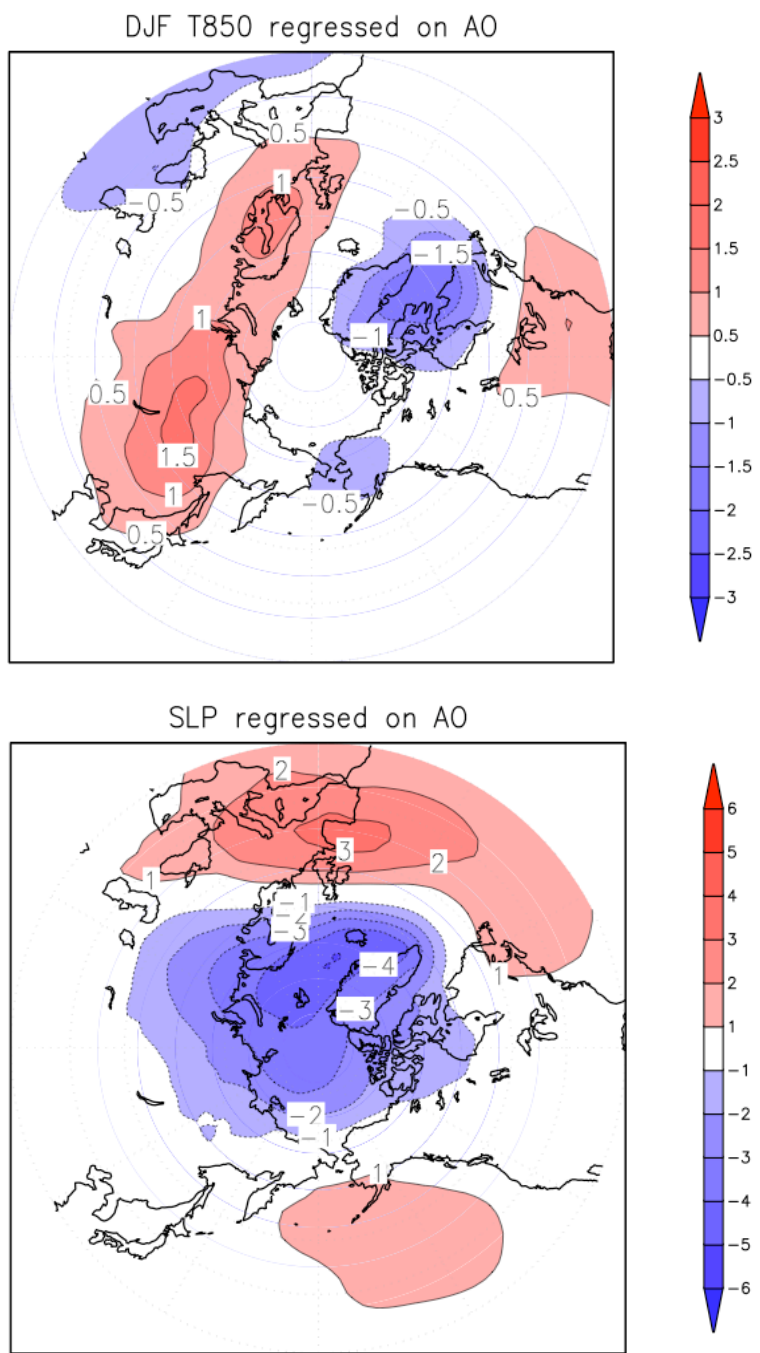


Figure 3.19. AO connections to inversion parameters. DJF 850 mb temperature regressed on the AO (top) SLP regressed on the AO (bottom). For every unit change in the AO index, the plots show the change in magnitude of temperature at 850 mb and SLP in the Northern Hemisphere.

Table 3.10. Average DJF inversion parameters correlated to wintertime AO index. Bold values listed indicate correlations significant at 95% or greater based on a t-test. Any italicized values indicate a correlation significant at 90% or greater.

Location	Surface temperature	Inversion depth	Inversion temperature difference	Inversion strength
Anchorage	-0.394	<i>-0.239</i>	-0.156	-0.034
McGrath	-0.304	-0.127	-0.158	-0.017
Fairbanks	-0.209	<i>-0.246</i>	-0.293	-0.036
Barrow	<i>-0.233</i>	<i>-0.248</i>	-0.181	-0.304

Chapter 4. 20th Century Model Simulations and Future Scenarios

4.1 Introduction to Modeling Schemes

In order to determine how well climate models capture surface-based temperature inversions in Alaska, both regional and global climate models are investigated in Alaska. Four stations were chosen in Alaska, representing different climatic regions of the state. The analysis of observations (see Chapter 3) shows that surface-based inversions at each station vary substantially due to geographic location, surrounding orography, and the influence of the large-scale synoptic flow. Simulating such complex conditions poses a challenge for coarse models due to the complexity of terrain and the general circulation. Therefore, a model downscaling technique was employed in an attempt to more accurately capture characteristics of surface-based temperature inversions in Alaska.

The effect on model performance due to varying resolution is an important factor to consider. In some circumstances, increased resolution will not necessarily increase the accuracy of a model's simulation. For example, it is important to note that CCSM3 has partial grid points that may contain fractional ocean and land components (Fig. 4.1), while the Polar MM5 does not. Therefore, coastal regions must be run at fairly high resolutions to be accurately resolved by a model that does not have mixed ocean/land grid points. Model scenarios used in this particular application have varying degrees of resolution. The global component, CCSM3, has an approximate resolution of 1.4° in latitude and longitude (T85 truncation). The two downscaled model scenarios, MM5 downscaled from CCSM3 and MM5 downscaled from NCEP Reanalysis data, have resolutions of 30km and 54km respectively (Fig. 4.2a). MM5 downscaled from CCSM3 covers all of Alaska, western Canada and parts of the Canadian archipelago, and much of eastern Russia (Fig. 4.2b), while MM5 downscaled from NCEP captures Alaska, parts of

western Canada, and only a small portion of eastern Russia near the Bering Strait (Fig. 4.2c).

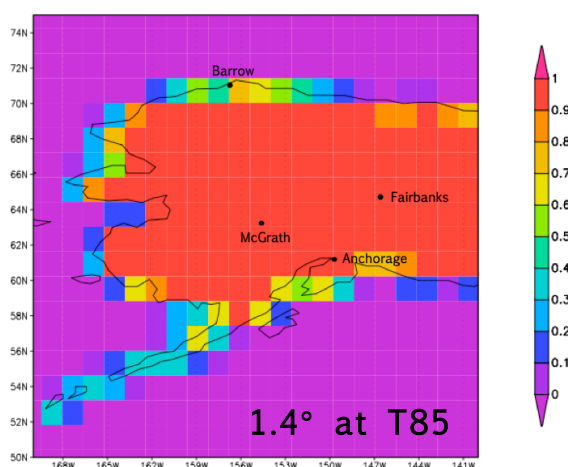


Figure 4.1. CCSM3 fractional grid points. Shading displays the fraction of grid point that is land CCSM3. A value of 0 means the entire grid point is ocean, while a value of 1 indicates a complete land grid point.

Model simulations were not projected specifically for this study. Instead, availability of model output was available from other projects that spanned the observation area of this study. For this reason, model simulations were prepared at varying resolutions. Therefore, it is important to note that no attempt is made to compare various simulations with one another, but instead to show how each simulation with its specific parameterizations, captures surface-based temperature inversions at stations in Alaska. In this respect, strengths and weaknesses of each simulation can be evaluated.

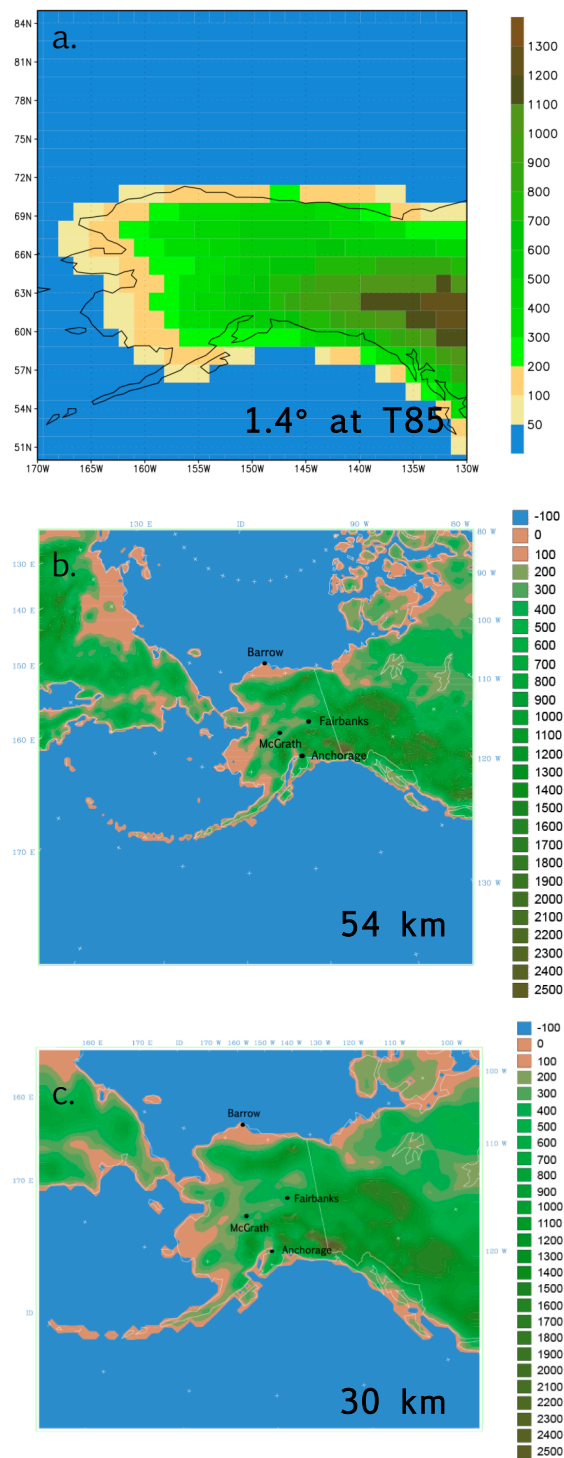


Figure 4.2. Display of model topography as resolution varies. Images showing topographical resolution and land-sea mask of CCSM3 (a), MM5 downscaled from CCSM3 (b), and MM5 downscaled from NCEP Reanalysis (c).

A 10-year pseudo-hind cast downscaling simulation was conducted using MM5 forced by NCEP/NCAR Reanalysis data over the period 1994-2004. These simulations were originally applied by Zhang et al. (2007a,b) and Bhatt et al. (2007) to develop a downscaling methodology for constructing temperature and precipitation station data to force a glacier mass balance model. The NCEP/NCAR downscaling simulation employed the model configuration shown in Figure 4.1b and employed the model physics listed in the right hand column of Table 4.1.

A simulation was also conducted by downscaling a CCSM3 20th century simulation using the higher resolution domain shown in Fig. 4.1c. The model period used for this study covers 1979-1999. Note that these years refer to CCSM3 model years and do not exactly correspond to observations during this period. Different model physics were used in these MM5 simulations than for the earlier NCEP/NCAR downscaling because a higher vertical and horizontal resolution required a different radiation scheme. The NCAR/CCM2 radiation scheme led to numerical instabilities so the RRTM scheme was used. Other choices of model physics are listed in the center column of Table 4.1. It should be reiterated that the differences in model physics for each model component of this study were due to the adoption of model simulations intended for other projects. Lastly, three decades of future scenario (A1B) projections were downscaled at 30km resolution using the model physics listed for CCSM3 in Table 4.1. The A1B scenario, which employs a balanced mix of fossil fuel and non-fossil fuels was used to force the Arctic MM5 for a forecast simulation in 2010-2019, 2050-2059, and 2090-2099.

Table 4.1. Downscaled model parameterizations. Input variables used to run model simulations in downscaled modeling schemes.

Physical component	MM5 downscaled from CCSM3	MM5 downscaled from NCEP Reanalysis
Cumulus parameterization	Grell cumulus	Kain/Fritsch cumulus
Resolvable-scale microphysics parameterization	Reisner-1 microphysics (modified by Thompson et al. 2004)	NASA/Goddard microphysics with hail/graupel
Planetary boundary layer process parameterization	MRF-PBL	Eta-Mellor-Yamada PBL
Atmospheric radiation parameterization	RRTM long-wave radiation	NCAR/CCM2 radiation
Land surface parameterization	NOAH land-surface model	NOAH land-surface model

Model biases were evaluated but not corrected for in this analysis. MM5 downscaled from NCEP Reanalysis data is used to estimate biases in the Polar MM5 model based on the assumption that the reanalysis is identical to observations. The CCSM3 20th century simulation serves as a measure of the GCM biases for the current climate. Future downscaled projections of surface-based inversions should be examined in light of the biases of the model when simulating the present day climate.

4.2 MM5 Downscaled from NCEP Reanalysis

MM5 downscaled from NCEP reanalysis data is used in this application to estimate biases in the Polar MM5 based on the assumption that NCEP represents the exact observations. Determining biases in the Polar MM5 model is important because biases in the regional model component will impact downscaled variables, regardless of the forcing component. The NCEP reanalysis data set is a 40-year record of global analyses

of atmospheric fields that uses a state-of-the-art data assimilation system (Kalnay et al. 1996; Kistler et al. 2001). The reanalysis procedure has assimilated many sources of observations from various countries and organizations (i.e., it can be viewed as an intelligent interpolation procedure for all available quality controlled data).

The average vertical temperature profile in December as simulated by MM5 downscaled from NCEP (1994-2004) compares well to the monthly averaged observed profile in Fairbanks (Fig. 4.3). Note that this is not unexpected because when regional models are run in ‘climate mode’ the large scale variables (winds, temperature, humidity) are nudged to the large-scale forcing to reduce the departure from mass and energy conservation. The modeled temperature is 5 K cooler at the surface and shows a very sharp increase in temperature in the first 100 meters. However, these findings can be explained by the fact that MM5, like all mesoscale models, smoothes the terrain and hence underestimates the actual impact of local terrain. Overall, the observed profile is somewhat smoother than the modeled profile. The annual variations of the modeled time series (Fig. 4.3) display similar interannual variability when compared to observations, indicating that MM5 can capture the large-scale forcing of inversion parameters. Modeled surface temperature, inversion depth, and temperature difference have comparable interannual variability in December. However, simulated inversion strength is much more variable in the model than what was observed in Fairbanks during December.

The average vertical temperature profile in Fairbanks during January as simulated by MM5 downscaled from NCEP (1994-2004) also compares well to the observed profile, with a similar sharp temperature increase in the first 100 meters that is not evident in observations (Fig. 4.4). Time series analysis in Fairbanks in January shows very similar interannual variability in all inversion parameters (Fig. 4.4).

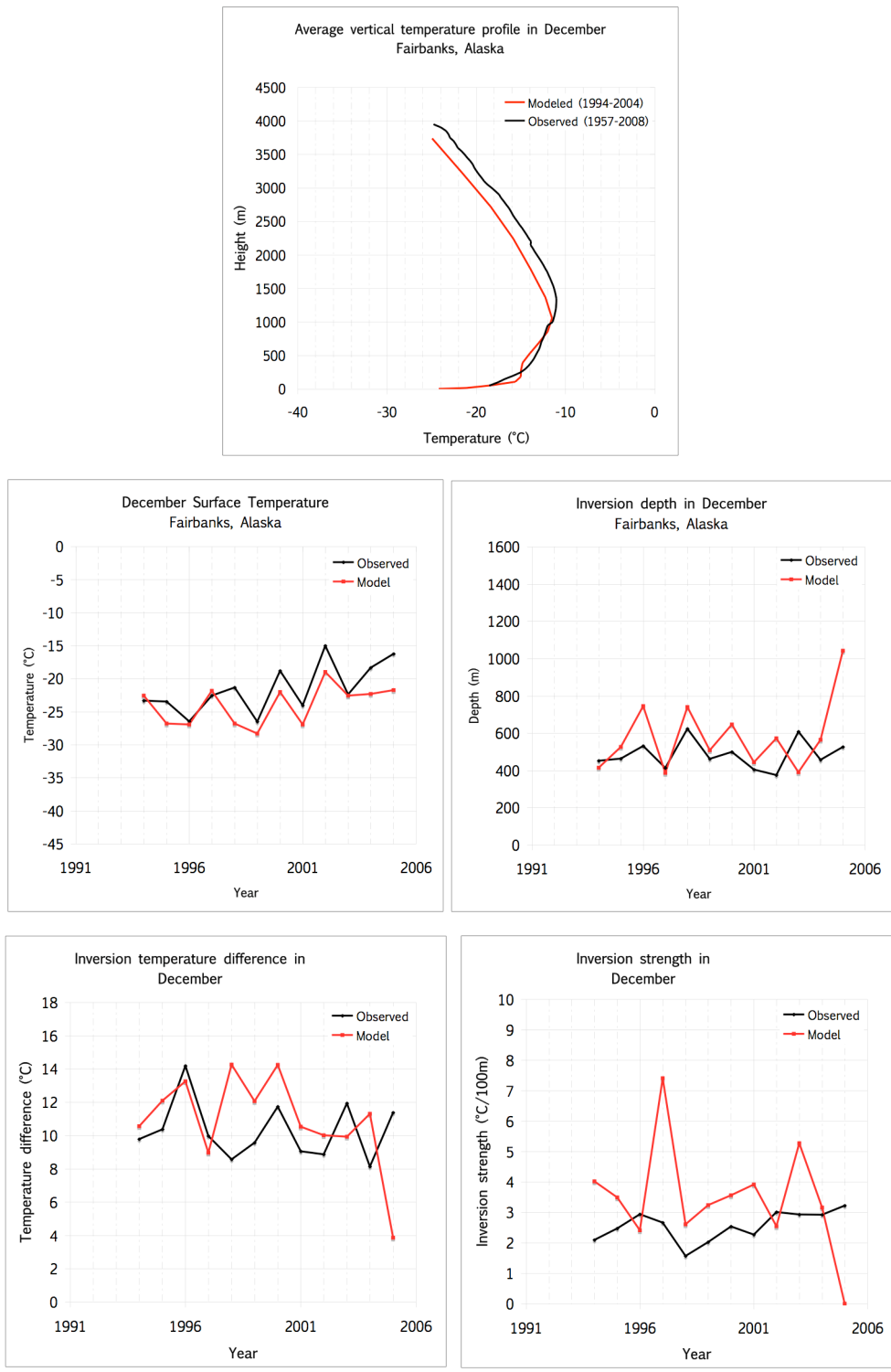


Figure 4.3. MM5-NCEP in Fairbanks during December. Inversion parameters as simulated by MM5 downscaled from NCEP Reanalysis data.

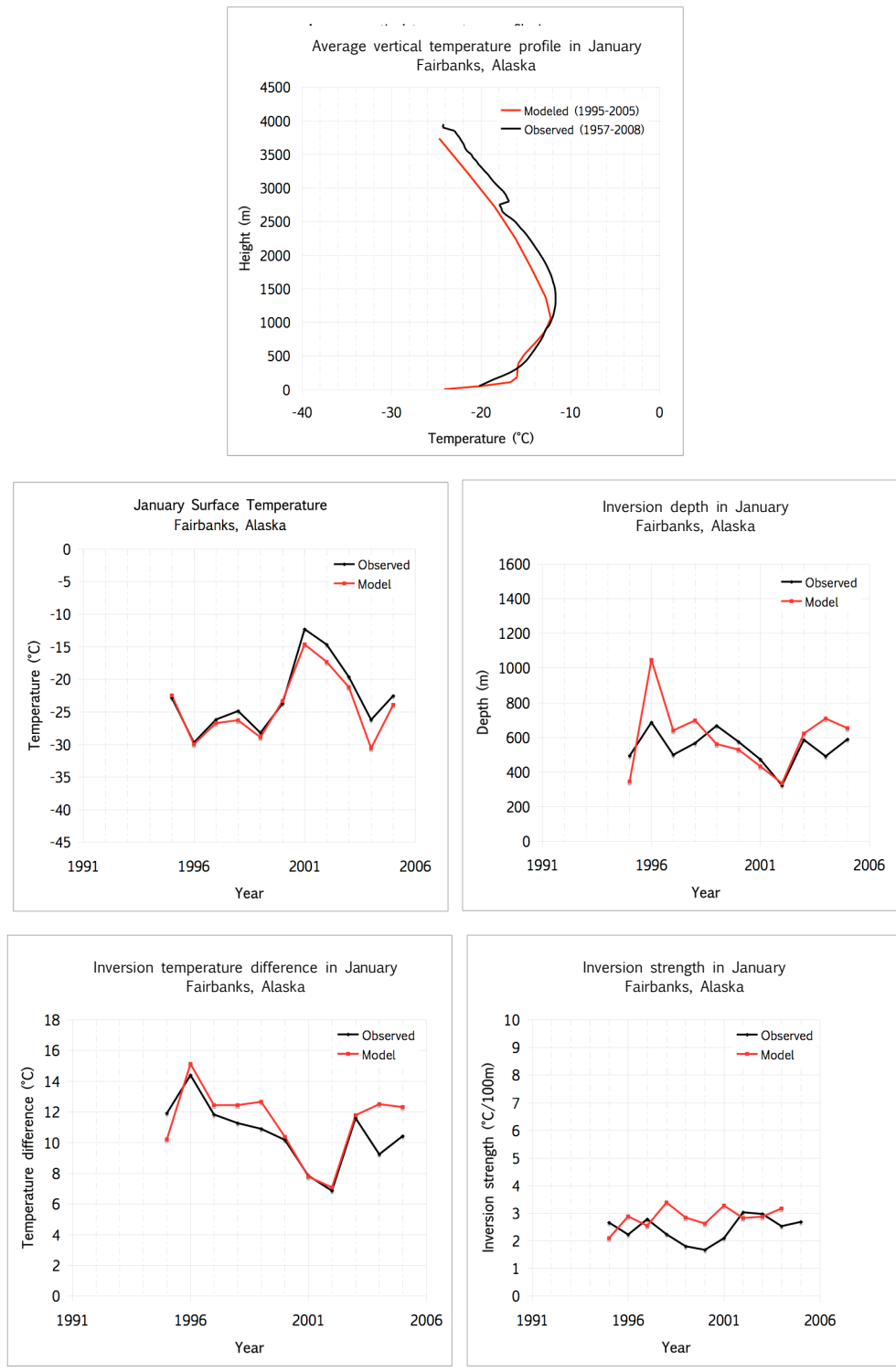


Figure 4.4. MM5-NCEP in Fairbanks during January. Inversion parameters as simulated by MM5 downscaled from NCEP Reanalysis data.

The average vertical temperature profile simulated in McGrath during December by MM5 forced with NCEP is similar to the observed vertical temperature profile (Fig. 4.5). The model seems to be approximately 5 K cooler at the surface, similar to Fairbanks in December (Fig. 4.3), and exhibits the sharp increase in temperature within the first 100 meters. Time series of each inversion parameter agrees well with model simulations. However, the model overestimates inversion depth and temperature difference in McGrath during December each year, which may translate into inaccuracies in the inversion strength time series (Fig. 4.5).

The average vertical temperature profile simulated in McGrath during January shows a very sharp increase in temperature (~ 10 K) in the first 100 meters (Fig. 4.6), which is not evident in the observed profile. The simulated time series for surface temperature displays similar interannual variability when compared to observations, while inversion depth and temperature difference were slightly overestimated. Simulated inversion strength was slightly offset from observed values, due in part to variability in inversion depth and temperature difference (Fig. 4.6).

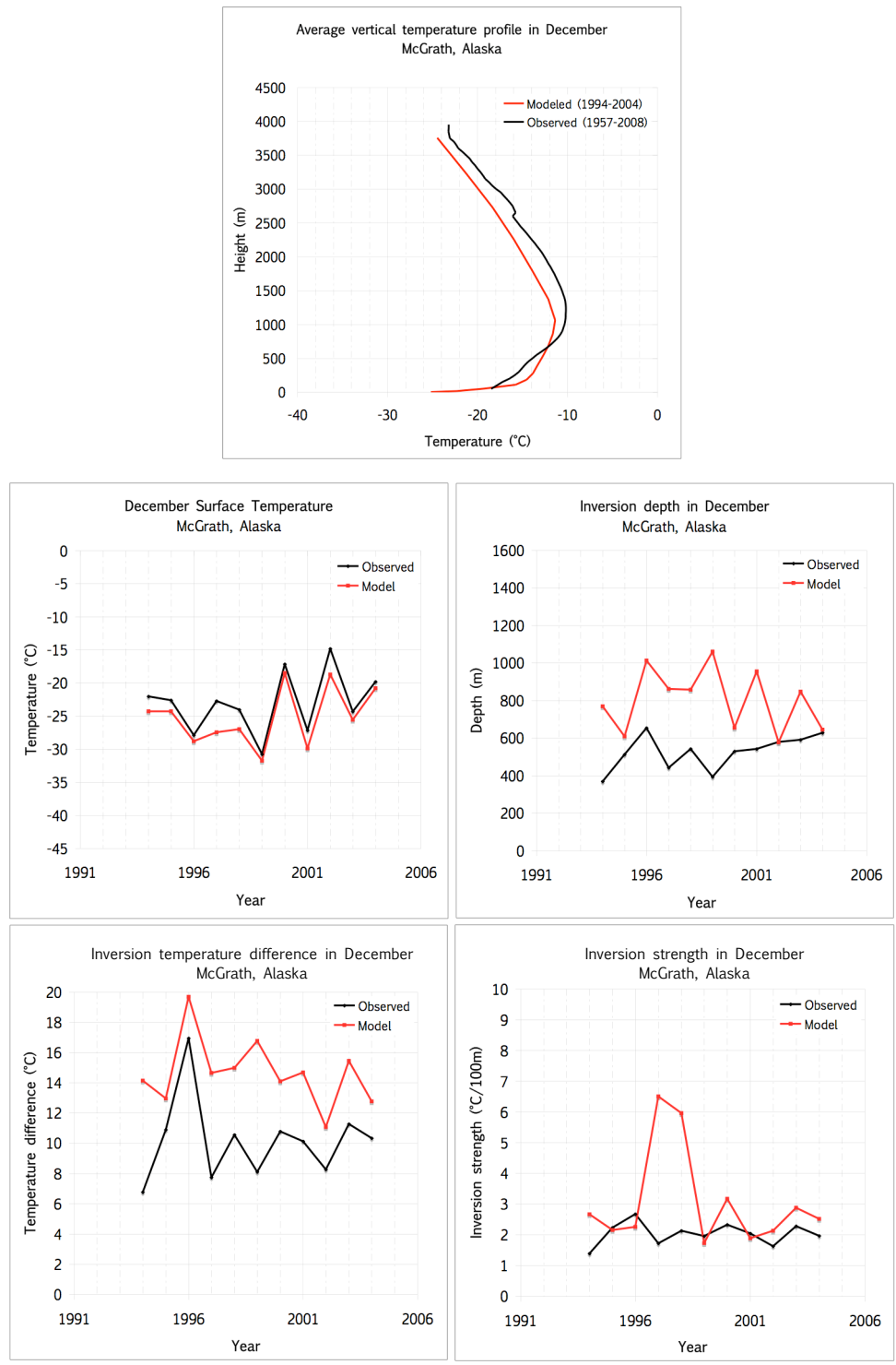


Figure 4.5. MM5-NCEP in McGrath during December. Inversion parameters as simulated by MM5 downscaled from NCEP Reanalysis data.

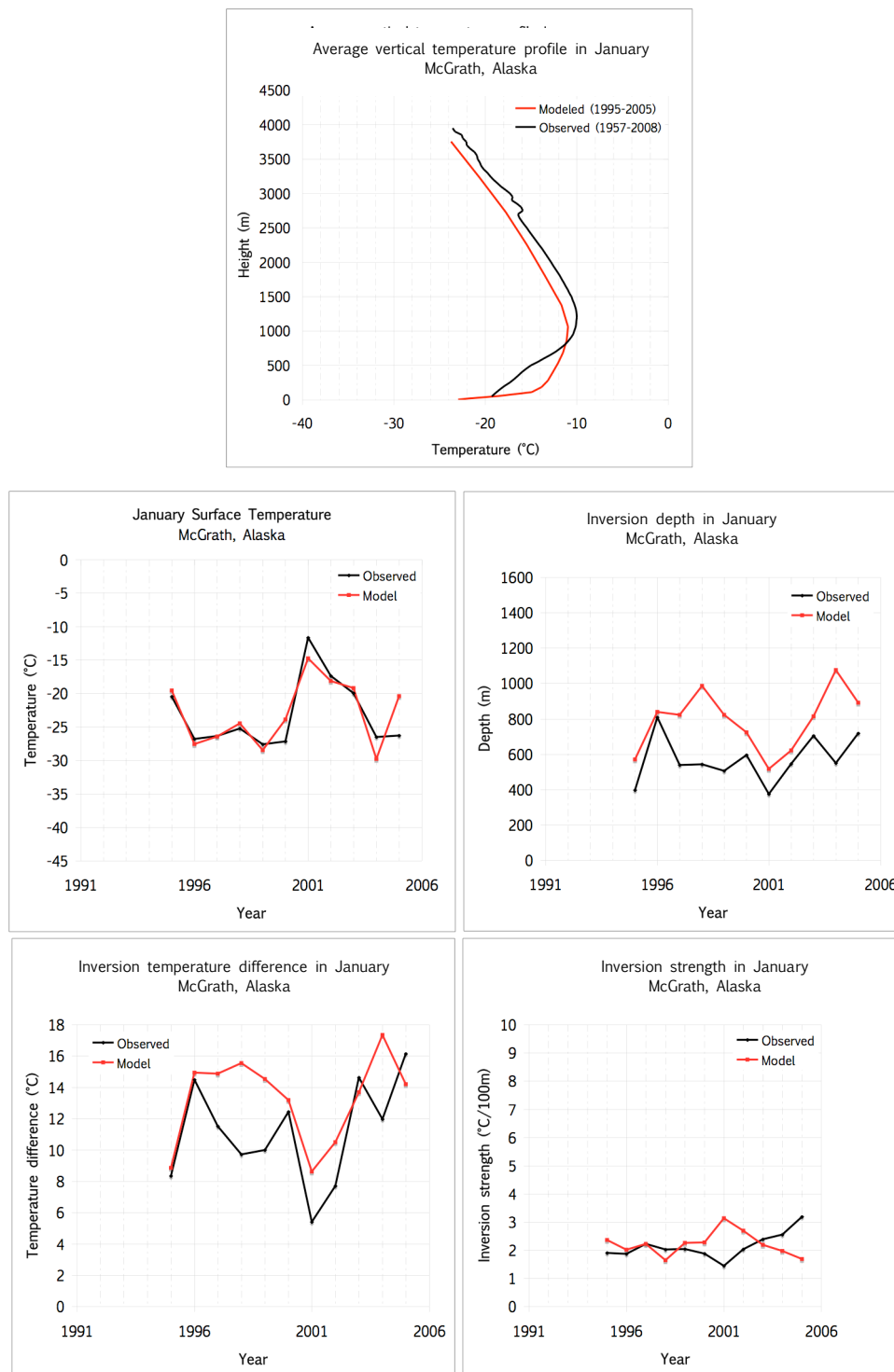


Figure 4.6. MM5-NCEP in McGrath during January. Inversion parameters as simulated by MM5 downscaled from NCEP Reanalysis data.

The average vertical temperature profile simulated in Anchorage during December differs in the lower thousand meters with the observed, but becomes more accurate with height. The simulated profile is cooler at the surface (~ 10 K) and has a sharp increase in temperature in the first 100 meters. The observed profile is less severe with a smaller temperature difference and depth (Fig. 4.7). Much of the differences between actual and modeled inversion parameters are a result of the differences between actual and modeled terrain height. The topography around Anchorage is unique because it is a mix of ocean and mountains. Mountains in South Central Alaska around the Anchorage area are high, while the altitude of Anchorage is comparatively low. Therefore when simulated with MM5, mountains in this region yield a much higher mean terrain height than the grid cell site falls into. As a result, time series simulations of inversion parameters shows similar interannual variations, but inaccurately captures the magnitude of surface temperature, temperature difference, and inversion strength. Model simulations of inversion depth, however, are captured well (Fig 4.7).

The average vertical temperature profile in Anchorage during January is similar to the profile simulated in December. The model simulates a much cooler surface temperature with a sharp increase in temperature in the first 100 meters (Fig. 4.8). Time series simulations of surface temperature, inversion temperature difference, and inversion strength are all accurate with respect to interannual variability, but do not capture the observed magnitude of each parameter. However similar to December, inversion depth is captured well in January (Fig. 4.8).

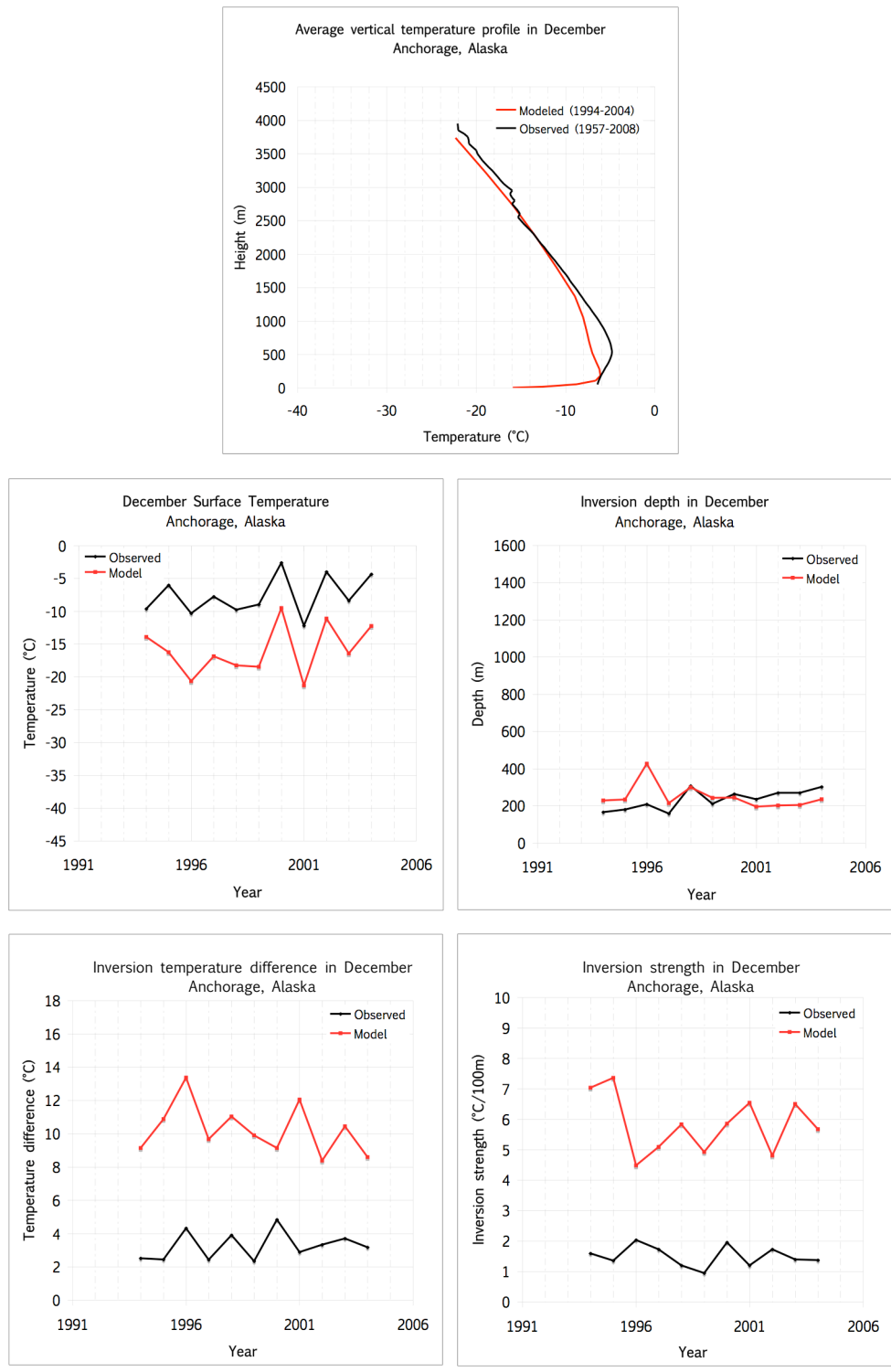


Figure 4.7. MM5-NCEP in Anchorage during December. Inversion parameters as simulated by MM5 downscaled from NCEP Reanalysis data.

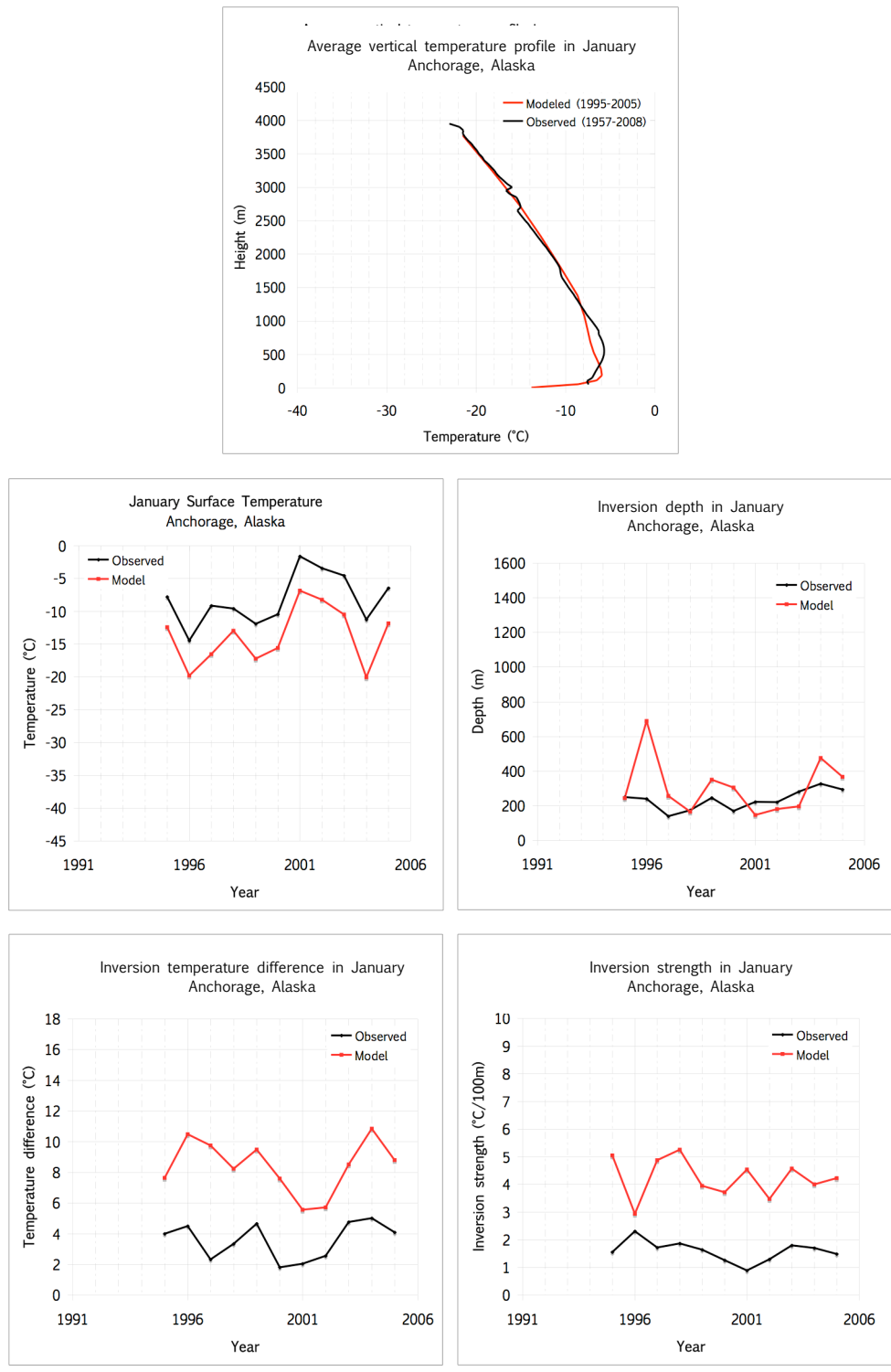


Figure 4.8. MM5-NCEP in Anchorage during January. Inversion parameters as simulated by MM5 downscaled from NCEP Reanalysis data.

The average simulated vertical temperature profile in Barrow during December is fairly accurate. However, the simulated profile drastically underestimates the surface temperature and shows a very steep increase in temperature in the first 100 meters, whereas the observed profile has a much smaller inversion temperature difference (Fig. 4.9). Potential reasons are that the Polar MM5 does not consider a partially ice-covered ocean. Instead, it assumes sea ice all along the Barrow coast. However, there is typically open water at ± 2 K and heat fluxes from open water are much higher than from sea ice. Furthermore, albedo of the open ocean is much lower (i.e., temperature-albedo feedback will be simulated incorrectly leading also to too low near-surface air temperatures if sea ice instead of open ocean is considered) (Narapusetty and Mölders 2005). The time series simulation of surface temperature is underestimated but displays fairly accurate interannual variability. However, other simulated inversion parameters such as inversion depth and temperature difference, are overestimated and fail to capture interannual variability. Simulated inversion strength also has too much variability that is not evident in observations (Fig. 4.9).

Similar to Barrow in December, the average simulated vertical temperature profile in January is also fairly accurate but exhibits the sharp increase in temperature in the first 100 meters, which does not appear in observations (Fig. 4.10). Time series simulations of surface temperature are accurate with respect to interannual variability, but not with respect to magnitude. Surface temperatures throughout the observation period are underestimated in the model. Inversion depth and temperature difference are overestimated, while inversion depth seems to correlate well with observations (Fig. 4.10).

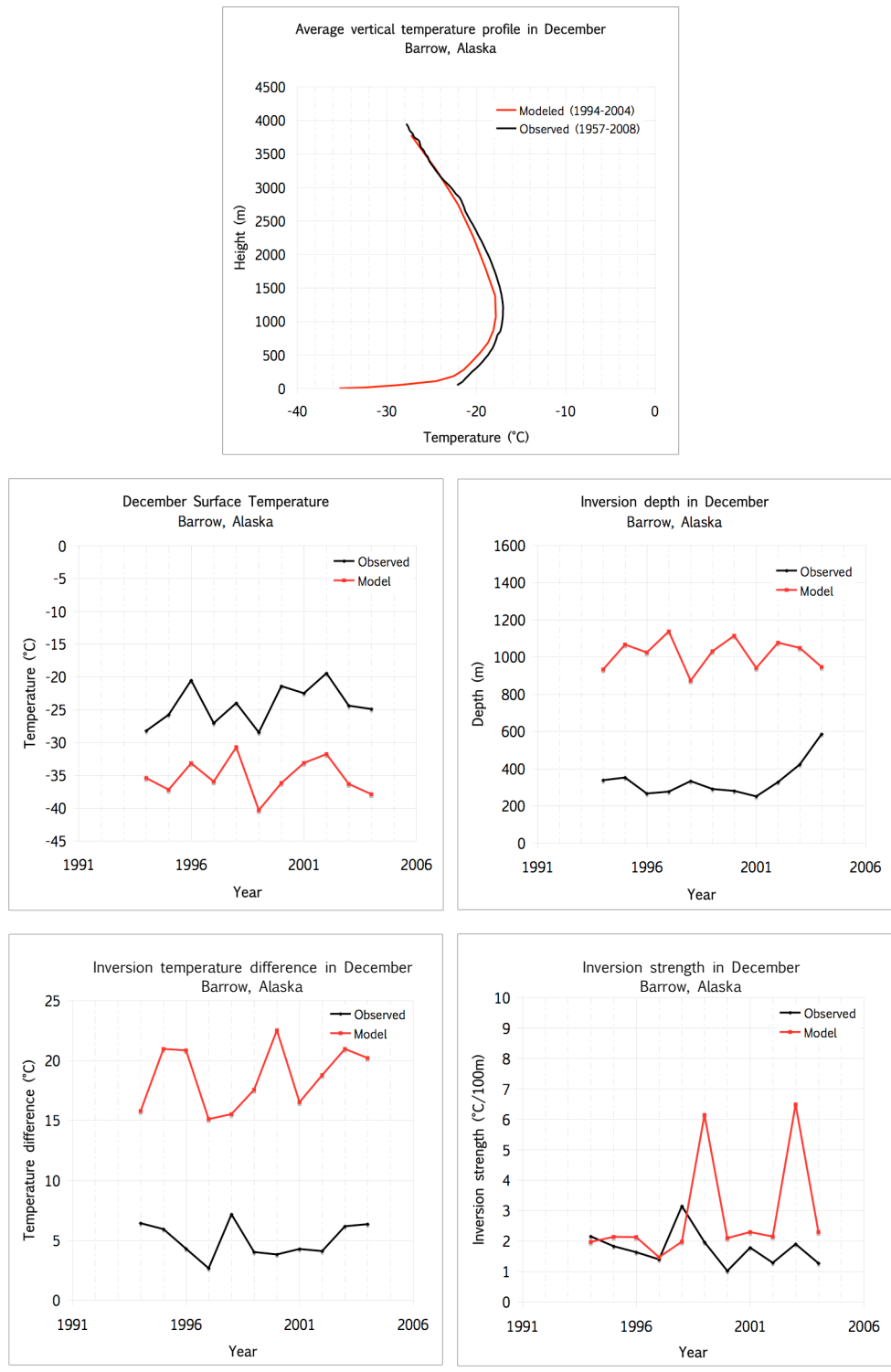


Figure 4.9. MM5-NCEP in Barrow during December. Inversion parameters as simulated by MM5 downscaled from NCEP Reanalysis data.

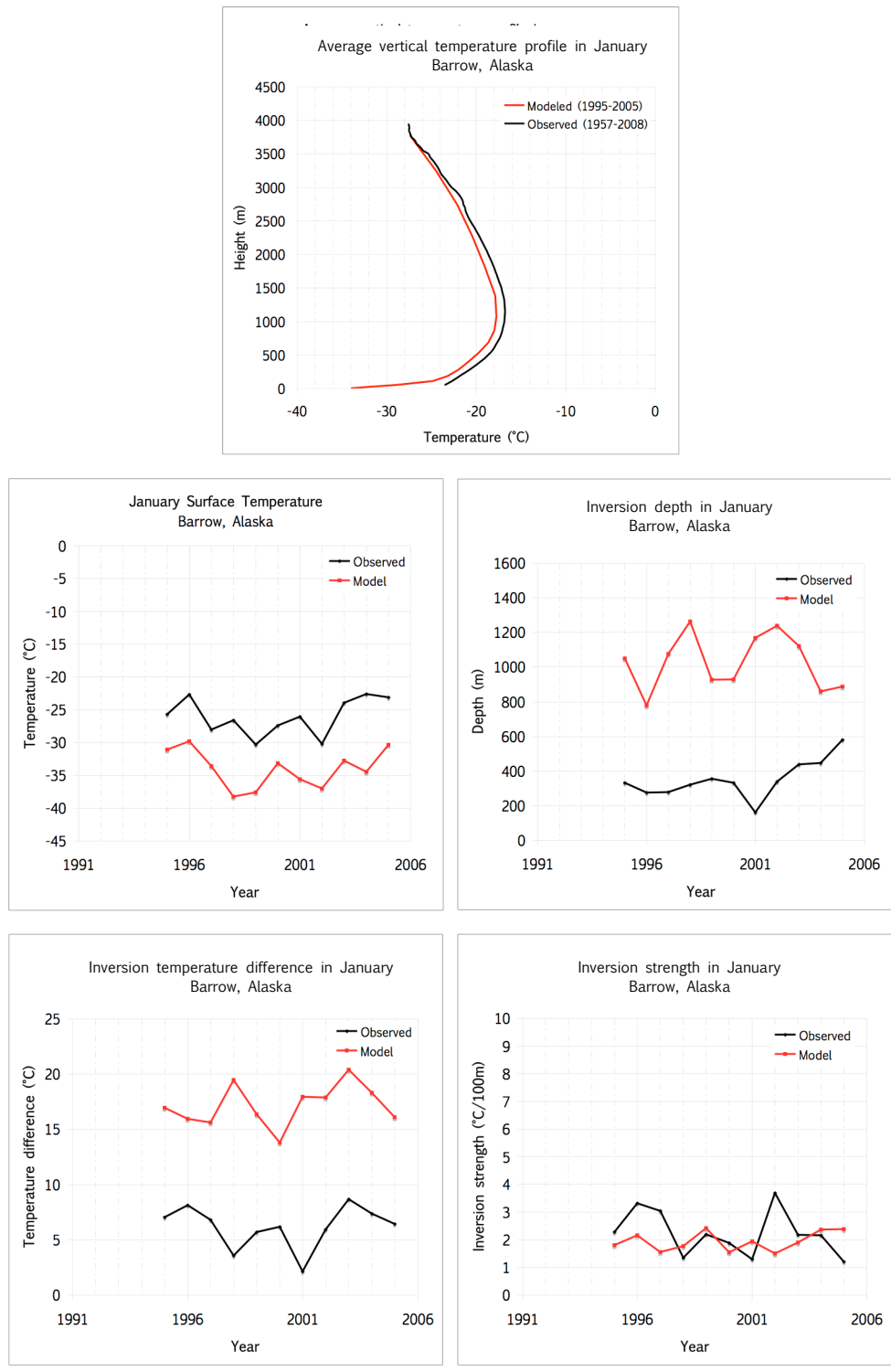


Figure 4.10. MM5-NCEP in Barrow during January. Inversion parameters as simulated by MM5 downscaled from NCEP Reanalysis data.

MM5-NCEP profiles in Barrow (Fig. 4.9 and 4.10) exhibit profiles that are the most similar to observed vertical temperature profiles. However, MM5 downscaled from NCEP simulates comparable inversion depths and temperature differences at all stations in Alaska (Table 4.2). When compared to time series of observed inversion parameters in December and January at each station, MM5 output downscaled from NCEP reanalysis data follows similar patterns of variability from year to year but is not always highly correlated. MM5-NCEP simulations capture the large-scale circulation, which influences inversion variability in Alaska, hence the year-to-year similarity. Since interannual variations are captured well and the primary weakness in these simulations are the mean, it can be concluded that downscaling is appropriate to study inversions, but may require a simple bias correction to more accurately simulate mean quantities.

An examination of daily vertical temperature profiles simulated by MM5 forced with NCEP reanalysis yields similar profile structures that persisted throughout the month at each station. In other words, the variability in depth of inversions and strength is lower in the downscaled model data than observations. In contrast, the analysis of daily observed temperature profiles display greater day-to-day variability in a given month. Therefore, when modeled profiles are averaged over monthly time periods, the overall average vertical temperature profile does not look very different than any individual daily profile. In contrast, observed profiles have larger day-to-day variability than the model. Thus, when observed daily profiles are averaged to obtain a monthly average profile, distinct individual characteristics of each day's profile are smoothed. It is important to note that the accuracy of simulated vertical profiles is partially achieved by the nudging process. While the downscaling in this section can provide us with an estimate of MM5 biases for the particular MM5 configuration used (54km, see Fig. 4.2b), these biases are not clearly translatable for the 30km resolution downscaling results of CCSM3. So these results are presented here for completeness.

Table 4.2. MM5 inversion parameters downscaled from NCEP reanalysis data. Average values for temperature $-(T)$, inversion depth $-(dz)$, inversion temperature difference $-(dT)$, and inversion strength $-(Inv)$. Standard deviations are shown in parenthesis.

Fairbanks	December		January	
	MM5-NCEP	Observed	MM5-NCEP	Observed
T (°C)	-24.2 (2.9)	-21.9 (4.9)	-24.1 (4.9)	-23.0 (5.8)
dz (m)	540.2 (123.3)	554.9 (141.4)	597.4 (189.9)	597.1 (166.2)
dT (K)	11.6 (1.7)	10.4 (2.0)	11.3 (2.2)	10.8 (2.5)
Inv (K/100m)	3.8 (1.4)	2.5 (0.01)	2.4 (0.6)	2.4 (0.01)

McGrath	December		January	
	MM5-NCEP	Observed	MM5-NCEP	Observed
T (°C)	-25.2 (4.2)	-23.0 (5.4)	-23.0 (4.6)	-24.0 (5.8)
dz (m)	804.4 (159.1)	587.9 (196.9)	789.6 (163)	639.4 (194.6)
dT (K)	14.7 (2.1)	11.0 (3.7)	13.3 (2.7)	11.7 (3.0)
Inv (K/100m)	3.1 (1.5)	2.1 (0.01)	2.2 (0.4)	2.2 (0.004)

Anchorage	December		January	
	MM5-NCEP	Observed	MM5-NCEP	Observed
T (°C)	-15.9 (3.6)	-8.0 (3.9)	-13.8 (4.2)	-8.9 (4.2)
dz (m)	248.7 (62.5)	310.1 (102.7)	306.8 (153.9)	334.7 (132.7)
dT (K)	10.2 (1.4)	3.9 (1.5)	8.4 (1.7)	4.5 (1.7)
Inv (K/100m)	5.8 (0.9)	1.5 (0.004)	4.2 (0.7)	1.5 (0.003)

Barrow	December		January	
	MM5-NCEP	Observed	MM5-NCEP	Observed
T (°C)	-35.3 (2.7)	-24.9 (3.7)	-34.0 (2.8)	-26.5 (5.0)
dz (m)	1017.3 (79.6)	478.2 (221.4)	1027.4 (154.2)	539.2 (208)
dT (K)	18.6 (2.5)	6.6 (2.2)	17.2 (1.8)	8.2 (3.9)
Inv (K/100m)	2.8 (1.7)	2.0 (0.01)	1.9 (0.3)	2.2 (0.01)

4.3 Downscaled from Model

Climate change is expected to impact surface-based inversions at different temporal and spatial scales. Therefore, there is a need to develop strategies for downscaling GCM simulations of climate change to relatively small spatial scales (e.g. Bengtsson et al. 1996). Dynamical downscaling from large-scale GCM data (CCSM3) is carried out in order to evaluate how well this technique can capture characteristics of surface-based temperature inversions in Alaska. The goal of this section is to first evaluate downscaled 20th century CCSM3 simulations to qualitatively estimate biases. Next, future scenarios are downscaled to estimate the impact a changing climate will have on inversion parameters during three decades of the 21st century.

4.3.1 CCSM3 20th Century Simulation

While many features of the climate are simulated well by CCSM3 and other global climate models, substantial biases still exist. Systematic errors can be evaluated through a comparison of CCSM3 20th century integration with observations. GCM simulations (model years 1978-1999) during the winter months (October-March) were compared to RAOBs to estimate regional biases in CCSM3 over Fairbanks, Alaska.

When configured for climate change simulations of the 20th century using a T85 grid for atmosphere and land, CCSM3 cannot capture the overall average vertical temperature profile in cold winter months in Alaska (Figs. 4.11-4.14, blue lines). The coarse vertical resolution in the near-surface layer, coarse horizontal resolution, and associated topography in a GCM make it difficult to accurately resolve vertical temperature profiles.

The GCM simulation underestimates inversion depth, temperature difference and strength, and overestimates surface temperature. At global-scale, temperature inversions cannot be adequately resolved because output is too coarse to capture local features that lead to the formation of inversions. Inversion characteristics such as depth, temperature

difference, and strength have unique characteristics and were evaluated in the model output to determine how well GCM model simulations can capture individual inversion parameters. Surface temperatures simulated by CCSM3 are accurate with respect to wintertime surface temperature variations in Fairbanks, but do not capture the mean values.

4.3.2. 20th Century Downscaled Simulation

MM5 downscaled from CCSM3 provides climatic data in Alaska at 30km resolution. Model output creates profiles that vary station-to-station. Overall however, there is very little day-to-day variation in profile structure (therefore, not shown). For example, in Fairbanks downscaled profiles have a shallow inversion (<500m) each day, which translates to an overall average profile with similar characteristics (Fig. 4.11). This quality holds true for each of the four stations.

The downscaled model data captures inversion profiles in Barrow (Fig 4.14) well when compared to other stations (Figs. 4.11-4.13 and Tables 4.4-4.7).

In summary, the GCM is too coarse to characterize surface temperature characteristics. It has been established in literature (Chapman and Walsh 2007), that surface air temperature biases exist in the Arctic. According to Chapman and Walsh (2007), mean winter root-mean square (rms) errors average 3 times larger than summer values. Yet, while NCAR CCSM3 is in the category of “notably good performers”, the range of rms error in surface air temperature is 2.5-11 K over the Arctic. The dynamically downscaled GCM results compare better with observations, indicating that they are valuable for inversion studies. For Interior stations, the downscaled surface temperatures are too warm and the inversion depths are too shallow compared to observations. In Anchorage and Barrow, the average surface temperature is close to observed but the inversion depths are too shallow in Anchorage and too deep in Barrow. The temperature difference (dT) for

the inversions is typically weaker in the downscaled model output than observed, leading to inversion strengths (dT/dz) that are in general weaker in the downscaled model output.

The monthly frequency of inversions (Table 4.3) is overestimated in both the GCM simulations and the MM5 output downscaled from CCSM3.

Table 4.3. Inversion frequency. Inversion frequency shown as a percentage of days per month in December. January is shown in parenthesis. Significance tests were not performed on means and standard deviations of inversions frequency.

	Inversion frequency (%)		
	1978-1999	1979-1999	1957-2008
	CCSM3 20 th century simulation	MM5 downscaled from CCSM3	Observations
Fairbanks	75 (85)	95 (95)	79 (84)
McGrath	87 (84)	73 (74)	69 (65)
Anchorage	83 (82)	78 (75)	48 (44)
Barrow	98 (97)	88 (92)	53 (57)

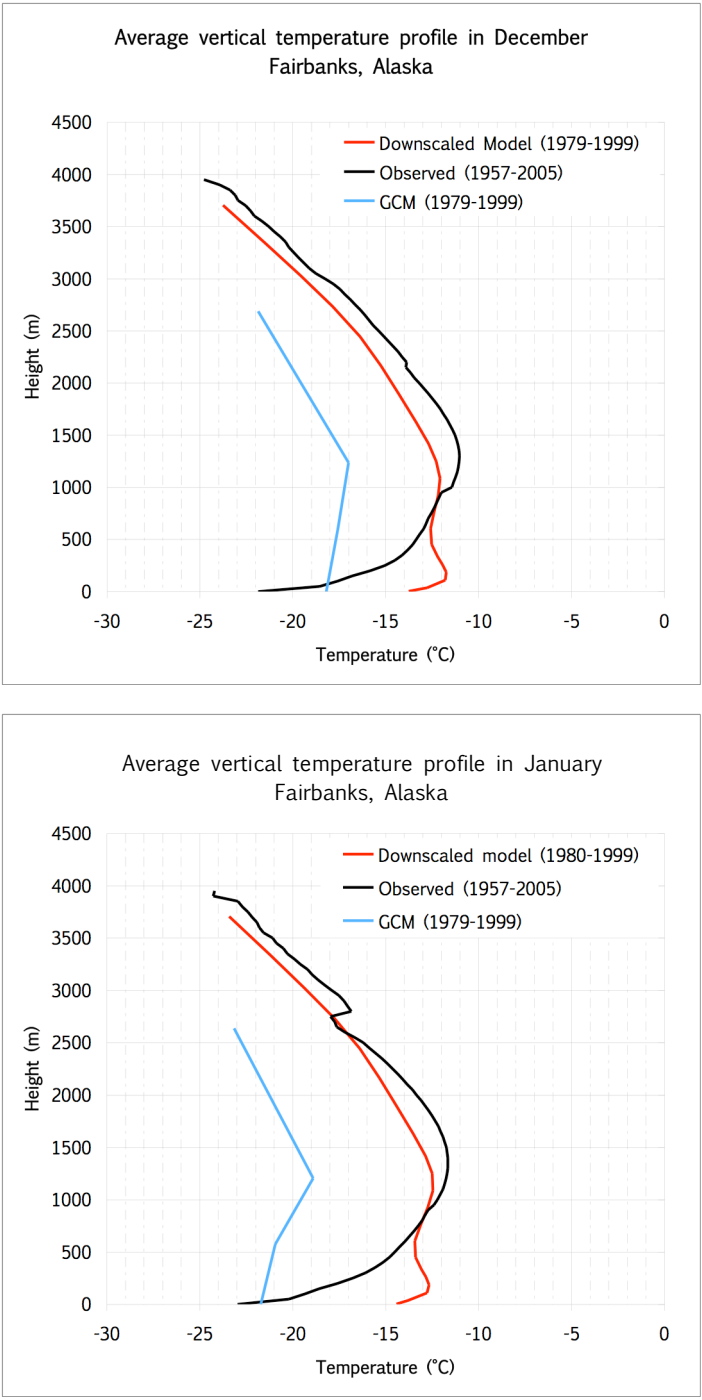


Figure 4.11. Modeled and observed vertical temperature profiles in Fairbanks. MM5 downscaled from CCSM3 (1979-1999), observed (1957-2008), and GCM simulated profiles (1979-1999).

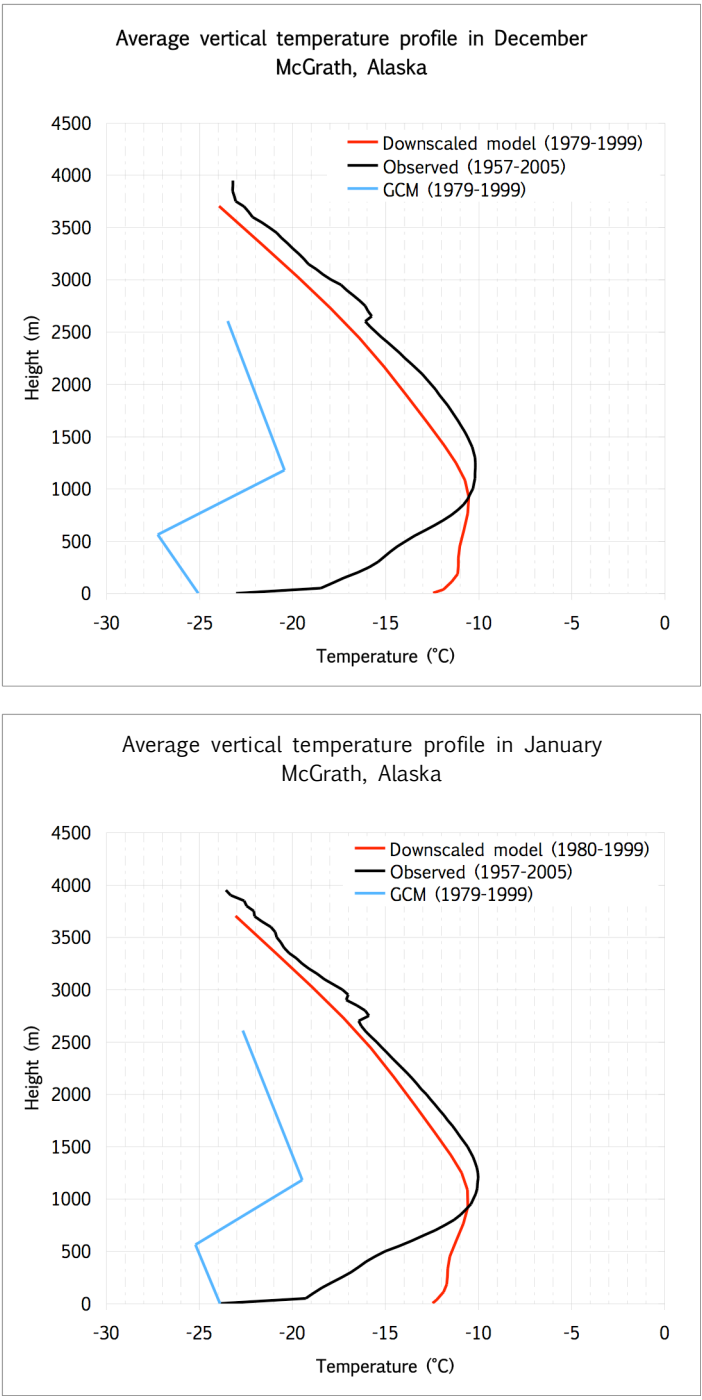


Figure 4.12. Modeled and observed vertical temperature profiles in McGrath. MM5 downscaled from CCSM3 (1979-1999), observed (1957-2008), and GCM simulated profiles (1979-1999).

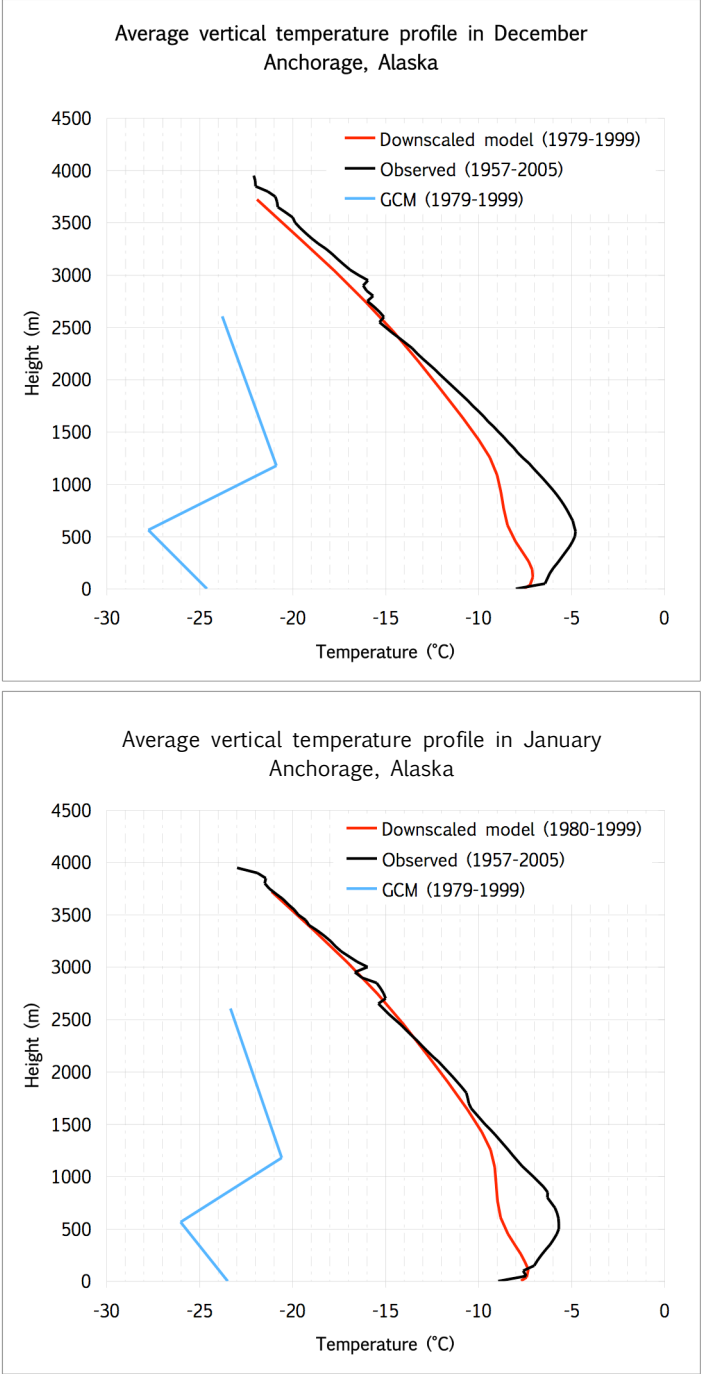


Figure 4.13. Modeled and observed vertical temperature profiles in Anchorage. MM5 downscaled from CCSM3 (1979-1999), observed (1957-2008), and GCM simulated profiles (1979-1999).

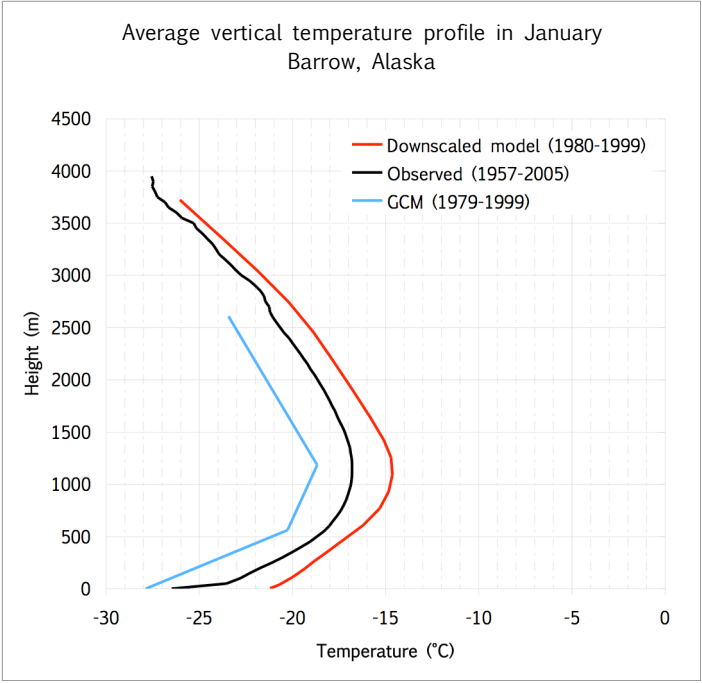
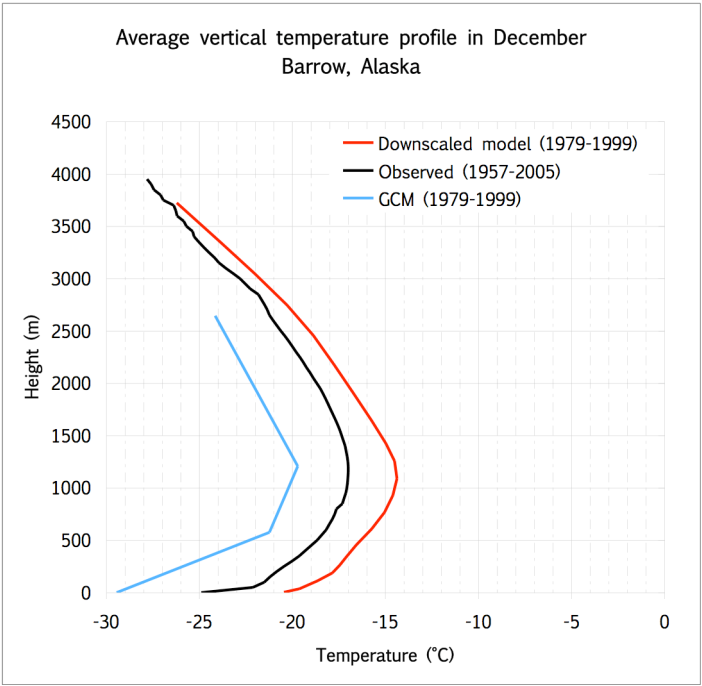


Figure 4.14. Modeled and observed vertical temperature profiles in Barrow. MM5 downscaled from CCSM3 (1979-1999), observed (1957-2008), and GCM simulated profiles (1979-1999).

Table 4.4. 20th century inversion parameters in Fairbanks. Average inversion parameters in 20th century model simulations and observations. Standard deviations shown in parenthesis. Significance tests were not performed on means and standard deviations of inversion parameters.

	Fairbanks - December		
	1978-1999	1979-1999	1957-2007
	CCSM3 20th century simulation	MM5 downscaled from CCSM3	Observed
T (°C)	-20.7 (2.7)	-13.4 (6.8)	-21.9 (4.9)
dZ (m)	863.9 (154.5)	182.4 (86.1)	554.9 (141.4)
dT (K)	4.4 (0.8)	2.3 (0.9)	10.4 (2.0)
Inv (K/100m)	0.6 (0.002)	1.4 (0.2)	2.5 (0.01)

	Fairbanks - January		
	1979-1999	1980-1999	1957-2008
	CCSM3 20th century simulation	MM5 downscaled from CCSM3	Observed
T (°C)	-23.0 (3.8)	-14.4 (8.8)	-23.0 (5.8)
dZ (m)	909.9 (133.1)	205.6 (124.3)	597.1 (166.2)
dT (K)	5.4 (0.6)	2.6 (1.3)	10.8 (2.5)
Inv (K/100m)	0.69 (0.001)	1.4 (0.3)	2.4 (0.01)

Table 4.5. 20th century inversion parameters in McGrath. Average inversion parameters in 20th century model simulations and observations. Standard deviations shown in parenthesis. Significance tests were not performed on means and standard deviations of inversion parameters.

	McGrath - December		
	1978-1999	1979-1999	1957-2007
	CCSM3 20 th century simulation	MM5 downscaled from CCSM3	Observed
T (°C)	-26.7 (3.6)	-12.1 (4.5)	-23.0 (5.4)
dZ (m)	1137.3 (133.3)	312.0 (130.7)	587.9 (196.9)
dT (K)	9.1 (1.3)	2.8 (1.3)	11.0 (3.7)
Inv (K/100m)	0.9 (0.001)	0.7 (0.1)	2.1 (0.01)

	McGrath - January		
	1979-1999	1980-1999	1957-2008
	CCSM3 20 th century simulation	MM5 downscaled from CCSM3	Observed
T (°C)	-26.5 (3.1)	-12.5 (7.9)	-24.0 (5.8)
dZ (m)	1188.3 (179.2)	339.6 (218.6)	639.4 (194.6)
dT (K)	9.3 (1.2)	2.9 (2.2)	11.7 (3.0)
Inv (K/100m)	0.9 (0.001)	0.7 (0.2)	2.2 (0.004)

Table 4.6. 20th century inversion parameters in Anchorage. Average inversion parameters in 20th century model simulations and observations. Standard deviations shown in parenthesis. Significance tests were not performed on means and standard deviations of inversion parameters.

	Anchorage - December		
	1978-1999	1979-1999	1957-2007
	CCSM3 20th century simulation	MM5 downscaled from CCSM3	Observed
T (°C)	-26.5 (3.1)	-7.4 (5.8)	-8.0 (3.9)
dZ (m)	1157.3 (146.8)	161.5 (131.3)	310.1 (102.7)
dT (K)	9.1 (1.6)	1.2 (1.1)	3.9 (1.5)
Inv (K/100m)	0.9 (0.001)	0.8 (0.2)	1.5 (0.004)

	Anchorage - January		
	1979-1999	1980-1999	1957-2008
	CCSM3 20th century simulation	MM5 downscaled from CCSM3	Observed
T (°C)	-25.7 (2.4)	-7.7 (7.9)	-8.9 (4.2)
dZ (m)	1185.5 (152.1)	139.9 (89.4)	334.7 (132.7)
dT (K)	8.2 (1.3)	1.1 (0.8)	4.5 (1.7)
Inv (K/100m)	0.8 (0.001)	0.8 (0.2)	1.5 (0.003)

Table 4.7. 20th century inversion parameters in Barrow. Average inversion parameters in 20th century model simulations and observations. Standard deviations shown in parenthesis. Significance tests were not performed on means and standard deviations of inversion parameters.

	Barrow - December		
	1978-1999	1979-1999	1957-2007
	CCSM3 20th century simulation	MM5 downscaled from CCSM3	Observed
T (°C)	-29.8 (4.6)	-20.1 (6.1)	-24.9 (3.7)
dZ (m)	833.4 (137.2)	646.0 (229.4)	478.2 (221.4)
dT (K)	10.6 (1.9)	6.0 (2.5)	6.6 (2.2)
Inv (K/100m)	1.6 (0.002)	0.9 (0.2)	2.0 (0.01)

	Barrow - January		
	1979-1999	1980-1999	1957-2008
	CCSM3 20th century simulation	MM5 downscaled from CCSM3	Observed
T (°C)	-28.5 (3.5)	-21.2 (6.8)	-26.5 (5.0)
dZ (m)	814.8 (102.9)	654.4 (211.0)	539.2 (208)
dT (K)	10.2 (1.8)	6.1 (2.2)	8.2 (3.9)
Inv (K/100m)	1.5 (0.003)	0.9 (0.1)	2.2 (0.01)

4.3.2 MM5 Downscaled from CCSM3-A1B

A changing climate can have significant implications for the strength, variability, and persistence of surface-based temperature inversions in Alaska. The Fourth Assessment Report organized by the Intergovernmental Panel on Climate Change predicts warming temperatures across the globe, and enhanced warming at high latitudes (Solomon et al. 2007). Since temperature inversions seem to be largely moderated by surface temperatures under relatively quiet synoptic conditions, and large-scale circulation under strong synoptic conditions, changes in both surface temperatures and general circulation could have implications for the strength, variability, and persistence of inversions during the winter months. Additionally, changes in surface-based inversions on the regional

scale could have strong implications with regards to boundary layer air quality. Therefore, there is strong motivation to investigate inversion parameters under changing climate scenarios.

The middle-of-the-road A1B 21st century scenario of CCSM 21st was used to force MM5 to construct downscaled information over Alaska for three decades: 2010-2019, 2050-2059, and 2090-2099. MM5 was employed to downscale results to a 30km resolution over Alaska (Fig 4.2c) and temperature inversion characteristics were investigated at the four Alaskan stations.

CCSM3 21st century simulated profiles in Fairbanks have shallow inversions in December and January which begin in the 20th century simulation and project forward to future decades (Fig. 4.15). Overall, trends in surface temperature are positive over time while inversion depth, temperature difference and strength are negative. This finding is consistent with the notion that increases in surface temperature are associated with shallower inversion depths. As the decades progress the entire vertical profile gets warmer. In January, there appears to be a larger change in column temperature between 2010-2019 and 2050-2059 than in December.

CCSM3 21st century simulated profiles in McGrath have inversions that are slightly deeper than those found in Fairbanks (Fig. 4.16). However, inversions in McGrath become notably weaker over the 21st century. The weakening of inversions in McGrath is greater than in Fairbanks. Additionally, similar to Fairbanks, there appears to be a larger change in January column temperature between 2010-2019 and 2050-2059 than in December. The elevated inversions (not analyzed in this study) evident at around 1200 m in the 20th century downscaled profile is much weaker by the end of the 21st century (Fig. 4.16).

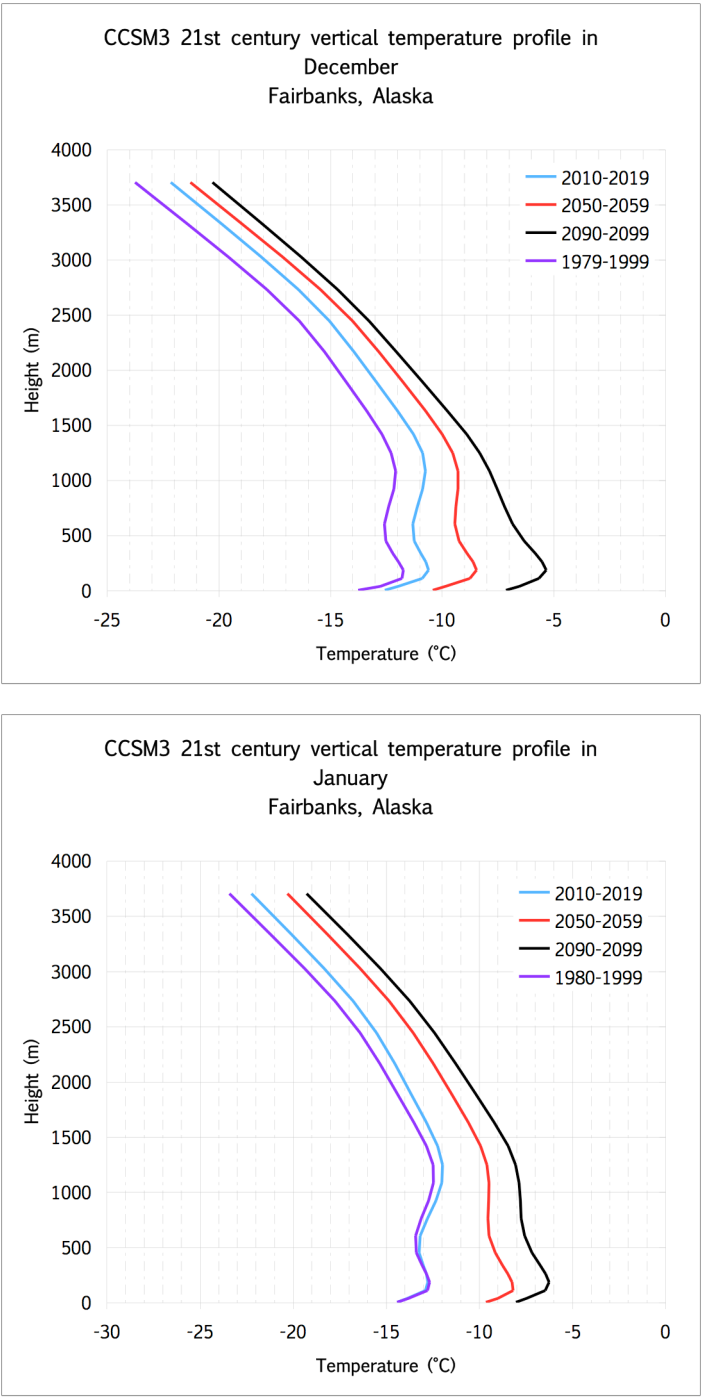


Figure 4.15. Future projected vertical temperature profiles in Fairbanks. Projected profiles are downscaled using CCSM3 and the A1B scenario, and are shown for 2010-2019, 2050-2059, and 2090-2099. The 20th century simulation (1979-1991) is also shown for comparison.

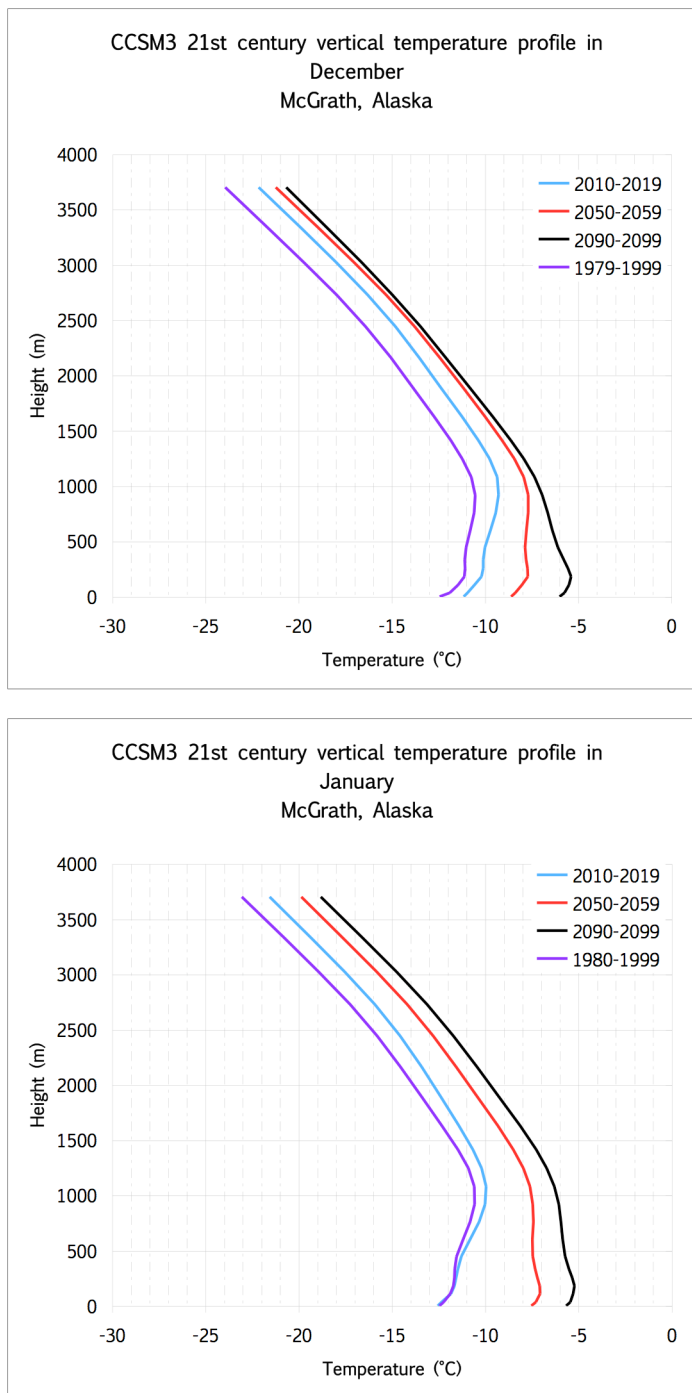


Figure 4.16. Projected simulated vertical temperature profiles in McGrath. Simulated profiles are downscaled using CCSM3 and the A1B scenario, and are shown for 2010-2019, 2050-2059, and 2090-2099. The 20th century simulation (1979-1991) is also shown for comparison.

CCSM3 21st century projected profiles in Anchorage have shallow inversions that decrease in depth with each progressing decade (Fig. 4.17 and Table 4.10). However, the inversion strength in the 20th century simulation is stronger than future projections of inversion strength. Additionally, the change in profile temperature from 2010-2019 to 2050-2059 is greater in January than in December, which also occurs in Fairbanks and McGrath.

CCSM3 21st projected profiles in Barrow have deeper inversions than other locations and overall have the coolest surface temperatures (Table 4.11). Projected profiles in Barrow vary from other stations since the profile is smooth in 2010-2019, and becomes sharper with each progressing decade (Fig. 4.18). Thus, as other stations show a nearly constant inversion strength, Barrow's projected profile creates a positive trend in inversion strength from 2010-2019 to 2090-2099, indicating an increasing inversion strength as climate warms. Lastly, the 20th century inversion profile matches up well with the vertical profile in 2010-2019, which suggests that the predicted warming over this time period is small in Barrow in January.

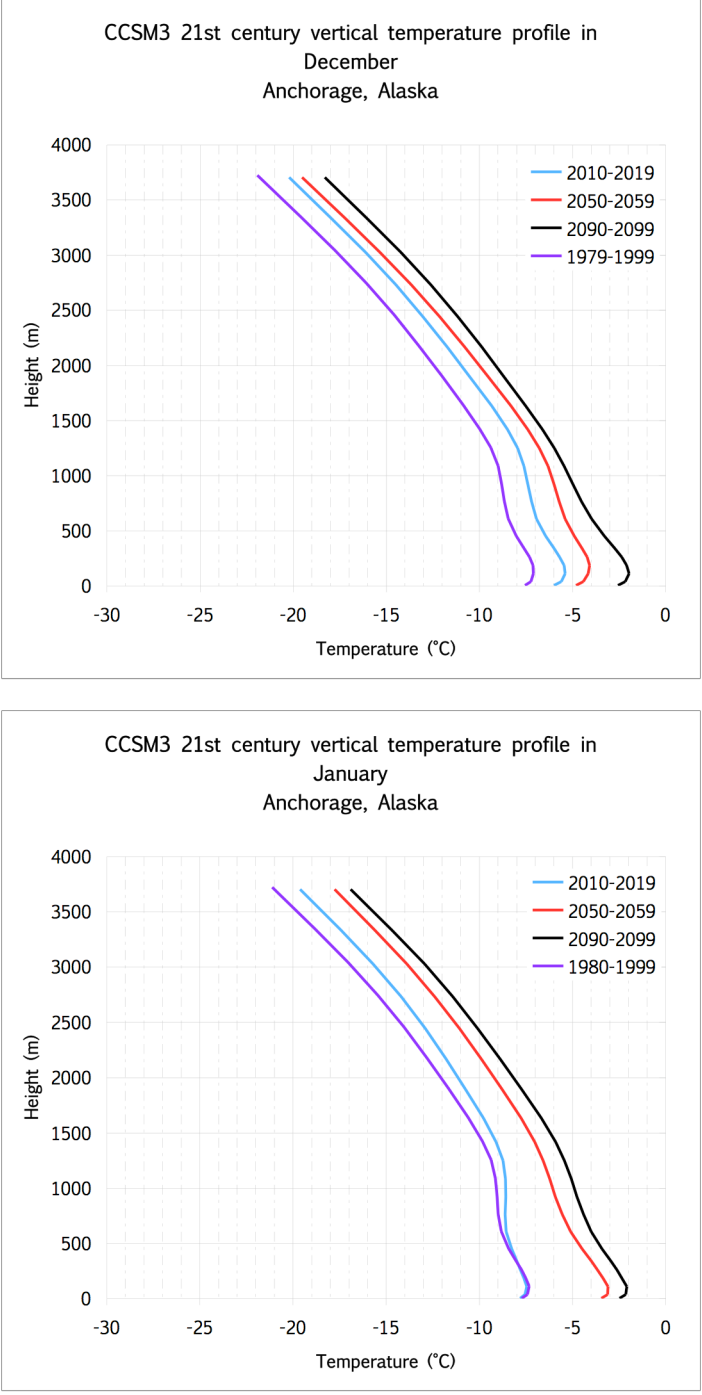


Figure 4.17. Future projected vertical temperature profiles in Anchorage. Projected profiles are downscaled using CCSM3 and the A1B scenario, and are shown for 2010-2019, 2050-2059, and 2090-2099. The 20th century simulation (1979-1991) is also shown for comparison.

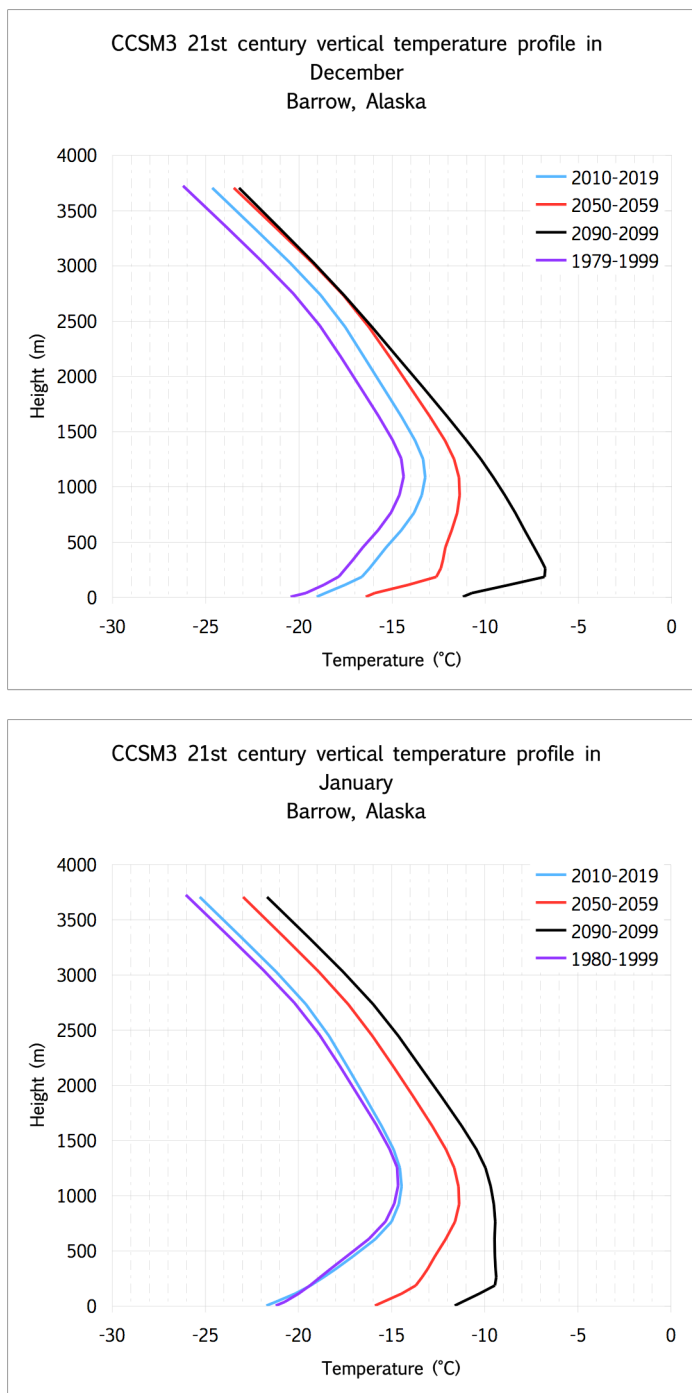


Figure 4.18. Future projected vertical temperature profiles in Barrow. Projected profiles are downscaled using CCSM3 and the A1B scenario, and are shown for 2010-2019, 2050-2059, and 2090-2099. The 20th century simulation (1979-1991) is also shown for comparison.

At all four stations, model projections in each subsequent decade indicate surface warming in December and January (Figs. 4.15-4.18). Vertical profiles in Fairbanks, McGrath, and Anchorage have similar inversion parameters with each progressing decade (Tables 4.8-4.11). Yet, although profiles in these locations are similar in vertical structure, the overall surface and column temperature is warming with slight decreases in inversion depth and temperature difference. In the future, Barrow the surface warms significantly as does the entire vertical temperature profile. This behavior has the overall impact of making the inversion strength increase over the 21st century (Fig. 4.18 and Table 4.11). Overall, these results suggest that inversions strengths will weaken slightly in Fairbanks, McGrath and Anchorage and slightly strengthen in Barrow.

Table 4.8. Average future projected inversion parameters in Fairbanks. Average values for temperature -T, inversion depth -dZ, inversion temperature difference -dT, and inversion strength -Inv. Average values for December (January). Significance tests were not performed on means and standard deviations of inversion parameters.

	CCSM3 21 st century projection - Fairbanks			
	1979-1991	2010-2019	2050-2059	2090-2099
T (°C)	-13.8 (-15.3)	-12.6 (-14.4)	-10.4 (-9.6)	-7.1 (-8.0)
dZ (m)	191.1 (197.5)	187.5 (232.5)	177.1 (161.2)	169.2 (170.8)
dT (K)	2.8 (2.7)	2.8 (2.9)	2.4 (2.0)	2.2 (2.3)
Inv (K/100m)	1.9 (1.5)	1.5 (1.3)	1.4 (1.4)	1.3 (1.4)

Table 4.9. Average future projected inversion parameters in McGrath. Average values for temperature -T, inversion depth -dZ, inversion temperature difference -dT, and inversion strength -Inv. Average values for December (January). Significance tests were not performed on means and standard deviations of inversion parameters.

	CCSM3 21 st century projection - McGrath			
	1979-1991	2010-2019	2050-2059	2090-2099
T (°C)	-13.2 (-13.6)	-11.1 (-12.6)	-8.6 (-7.5)	-6.0 (-5.7)
dZ (m)	325.8 (403.3)	347 (378)	218.7 (183.6)	152.9 (154.2)
dT (K)	3.6 (3.5)	3.2 (3.8)	1.9 (1.5)	1.1 (1.1)
Inv (K/100m)	1.8 (0.7)	0.7 (0.8)	0.7 (0.8)	0.7 (0.7)

Table 4.10. Average future projected inversion parameters in Anchorage. Average values for temperature -T, inversion depth -dZ, inversion temperature difference -dT, and inversion strength -Inv. Average values for December (January). Significance tests were not performed on means and standard deviations of inversion parameters.

	CCSM3 21 st century projection - Anchorage			
	1979-1991	2010-2019	2050-2059	2090-2099
T (°C)	-8.2 (-8.2)	-6.0 (-7.8)	-4.8 (-3.4)	-2.5 (-2.5)
dZ (m)	129.3 (147.3)	165.7 (209.8)	163.2 (106.7)	130.6 (115.3)
dT (K)	1.9 (1.2)	1.3 (1.7)	1.4 (0.8)	1.0 (0.9)
Inv (K/100m)	2.2 (0.8)	0.9 (0.8)	0.9 (0.8)	0.8 (0.8)

Table 4.11. Average future projected inversion parameters in Barrow. Average values for temperature -T, inversion depth -dZ, inversion temperature difference -dT, and inversion strength -Inv. Average values for December (January). Significance tests were not performed on means and standard deviations of inversion parameters.

	CCSM3 21 st century projection - Barrow			
	1979-1991	2010-2019	2050-2059	2090-2099
T (°C)	-22.2 (-20.1)	-19.0 (-21.7)	-16.4 (-15.8)	-11.2 (-11.6)
dZ (m)	694.6 (681.5)	683.9 (737.7)	523 (555.6)	291.5 (381)
dT (K)	7.0 (6.5)	6.1 (7.1)	6.0 (5.2)	5.0 (3.5)
Inv (K/100m)	1.8 (0.9)	0.9 (0.9)	1.5 (0.8)	2.0 (0.9)

Chapter 5. Conclusion

The primary goal of this work was to characterize trends and variability in observed surface-based temperature inversions at four stations in Alaska and elucidate any discernable connections to large-scale climate variability. A secondary goal of this work was to evaluate how well GCM and dynamically downscaled model data capture vertical temperature profiles and inversion characteristics during the 20th century. In addition, expected changes in inversions characteristics are explored using model output from a dynamically downscaled middle-of-the-road future scenario (A1B).

The existence of temperature inversions in the Arctic has been recognized for over a century and in that time, research has been performed on various aspects of the atmospheric phenomenon. Radiational cooling of the boundary layer is the physical driver leading to the formation of deep inversions in Alaska. Radiosonde observations show that inversions in the continental climate of Interior Alaska are strong, semi-permanent, and have important implications for degrading air quality, by trapping pollutants in the boundary layer. In contrast, inversions in the coastal regions of Alaska are shallow, transient, and can easily degrade due to the effect of coastal winds. Additionally, coastal regions tend to have a higher frequency of elevated inversions. In Alaska the magnitude of inversion parameters (depth, temperature difference, and strength) vary geographically.

Trends and variability in observed surface-based temperature inversions in Alaska are important under a changing climate. Inversion parameters such as surface temperature, inversion depth, inversion temperature difference, and inversion strength were analyzed from 1957-2008 to determine overall trends, variability, and relationships to other parameters during winter months (November-March). Surface temperature has positive trends in Fairbanks, McGrath, Anchorage, and Barrow, and show similar patterns of interannual variability at all four stations during December and January (Tables 3.1 and

3.2). Time series analysis of wintertime inversions indicates that when surface temperatures are warm (cold), inversion depths are shallow (deep) and inversion temperature differences are small (large) (Fig. 3.7). This relationship implies that recent warming of surface temperatures in Alaska could create shallower inversions, which has implications for regional air quality (Table 3.1). Strong, stable inversions trap pollutants in the lowest layer of the atmosphere causing threats to human safety and health. Additionally, growing populations in the Arctic could exacerbate these air quality issues.

Inversion depth and temperature difference in December and January from 1957-2008 have decreasing trends at all four stations which is consistent with increasing surface temperatures across Alaska. The strength of surface-based inversions over the period of record is decreasing in the coastal regions of Anchorage and Barrow, but increasing in the Interior stations at Fairbanks and McGrath. In this study, inversion strength was defined as inversion temperature difference over depth (dT/dz). Since each parameter (dT and dz) is decreasing, one would expect inversion strength to remain relatively constant at each station. However, if inversion depth decreases at a faster rate than temperature difference, the strength of inversions will increase as seen in the Interior. Concurrently, inversion strength on the coasts has decreased because the inversion temperature difference is decreasing at a faster rate than depth.

Interannual variability of inversion parameters over Alaska is often a result of synoptic-scale flow patterns. For example, cold anomalies last longer and are more frequent in the Interior than warm anomalies. According to Papineau (2001), strong inversions over the Interior limit the response of temperature to changes in synoptic-scale flow. Therefore, warm anomalies in this region are caused by synoptic-scale patterns while cold anomalies are a result of local conditions such as radiative cooling of the boundary layer and orographic blocking by the Alaska and Brooks Ranges. In addition to the effect of synoptic flow, however, trends and variability in inversions observed in Alaska appear to be linked to large-scale multidecadal variability. The PDO is positively correlated to

surface temperatures and negatively correlated to inversion depth. In other words, in the positive (negative) phase of the PDO when warm (cold) waters are present off the western coast of North America, surface temperatures in Alaska are warm (cold) and inversions are shallow (deep). Additionally, the PDO is positively correlated with the strength and frequency of storms entering Alaska (Dos Santos Mesquita 2008). Increased influx of storms in the positive phase of the PDO would create increased surface temperatures in Alaska as well as winds that mechanically degrade surface temperature inversions. Therefore, the correlation between increased storm activity and the PDO is a mechanism that affects surface temperatures during winter months in Alaska.

Multiple model simulations are investigated to determine whether varied model resolutions or techniques such as downscaling increases a model's ability to capture regional phenomena like inversions. The first model simulation analyzed was MM5 downscaled from NCEP Reanalysis data for the period of 1994-2004. Simulations were used in an attempt to determine model biases in the Polar MM5. Vertical profiles in December and January at each station showed that MM5 forced with NCEP was fairly accurate with respect to capturing overall profiles. However, MM5 downscaled from NCEP seemed to slightly overestimate inversion parameters at most stations (Table 4.2). Simulated vertical temperature profiles exhibit a cold bias at the surface, which subsequently translates into a sharp temperature increase in the lower 100 meters in Fairbanks, McGrath, and Anchorage that is not evident in observed profiles (Figs. 4.3-4.10). The interannual variability of simulated inversion parameters follows observed parameters well over the analysis period and in general captures trends well.

MM5 downscaled from a 20th century simulation of CCSM3 for model years 1979-1991 was compared to observed vertical temperature profiles (1957-2008) and GCM profiles (1979-1999) for December and January. The frequency of inversions in December and January is drastically overestimated in both the CCSM3 and MM5 downscaled from CCSM3 simulations. This finding could imply that model simulations fail to capture

inversion variability or that large-scale forcing in the model is weaker than observed. Observed profiles can be fairly complex in structure and are sometimes elevated above the first 100 meters. Since elevated inversions were not considered in this study, the overall frequency of inversions is reduced. Additionally, downscaled profiles slightly overestimate surface temperature at all stations except Anchorage, and underestimate inversion depth and temperature difference at all stations except Barrow (Tables 4.4 – 4.7). Similar to MM5 downscaled from NCEP, many MM5 profiles downscaled from CCSM3 exhibit a sharp increase in temperature with height in the first 100 meters. This pattern is a daily feature and is therefore evident in the overall average monthly profile. GCM simulated profiles fail to capture inversion profiles at each station and inadequately resolve vertical structure. Therefore, dynamically downscaled simulations do a better job at capturing overall average inversion profiles, and drastically improve the fine structure of the vertical temperature profile.

CCSM3 21st century projections of surface-based temperature inversions in 2010-2019, 2050-2059, and 2090-2099 were carried out using the middle-of-the-road A1B scenario. At all four stations, model projections in each subsequent decade indicate surface and column warming in December and January (Figs. 4.14-4.17). However, the change in temperature from 2010-2019 to 2050-2059 in January is comparably larger than the change in December. This large change in temperature is evident at all stations in January. Additionally, as surface temperatures warm in the future, the model predicts shallower inversions with smaller temperature differences, which is similar to the regime observed in RAOB data.

Overall, dynamical downscaling increased the quality of simulated data with respect to observations. But further analysis is needed in order to understand the mechanisms behind the modeled biases in surface based temperature characteristics in Alaska.

References

- AMS, 2000: *AMS Glossary of Meteorology*, 2nd ed. American Meteorological Society, Boston, MA, <http://amsglossary.allenpress.com/glossary/browse>.
- Andreas, E.L. and B. Murphy, 1986: Bulk transfer coefficients for heat and momentum over leads and polynyas. *J. Phys. Oceanogr.*, **16**, 1875-1883.
- Barrie, L.A., J.W. Bottenheim, R.C. Schnell, R.C. Crutzen, and R.A. Rasmussen, 1988: Ozone destruction and photochemical reactions at polar sunrise in the lower Arctic atmosphere. *Nature*, **334**, 138-141.
- Bengtsson, L.M. Botzett and M. Esch, 1996: Will greenhouse gas-induced warming over the next 50 years lead to higher frequency and greater intensity of hurricanes? *Tellus*, **48A**, 57-73.
- Bhatt U.S., J. Zhang, W.V. Tangborn, and C.S. Lingle, L. Phillips, 2007. Examining Glacier Mass Balances with a Hierarchical Modeling Approach, *Computing in Science and Engineering*, **9**, 61-67.
- Bilello, M.A., 1966: Survey of Arctic and Subarctic temperature inversions. Hanover, N.H.: U.S. Army Cold Regions Research & Engineering Laboratory, TR 161, 1-36.
- Bowling, S.A. Air Pollution in Fairbanks. *Alaska Science Forum*. (June 19, 1979) Retrieved on January 22, 2006. (<http://www.gi.alaska.edu/ScienceForum/ASF0/046.html>)
- Bowling, S., 1986: Climatology of high latitude air pollution as illustrated by Fairbanks and Anchorage, Alaska. *Journal of Climate and Applied Meteorology*, **25**, 22-34.
- Bradley, R.S. and F.T. Keimig, 1992: Climatology of Surface-Based Inversions in the North American Arctic. *J. of Geophys. Res.*, **97**, D14, 15699-15712.
- Bridgman, H.A., R.C. Schnell, J.D. Kahl, G.A. Herbert, and E. Joranger, 1989: A major haze even near Point Barrow, Alaska: Analysis of probable source regions and transport pathways. *Atmos. Environ.*, **23**, 2537-2549.
- Brooks, C.E.P., 1931: The vertical temperature gradient in the Arctic. *Meteorology Magazine*, **66**, 267-268.
- Chapman, W.L., and J.E. Walsh, 2007: Simulations of Arctic Temperature and Pressure by Global Coupled Models. *J. Climate*, **20**, 609-632.

Chun-Fung Lo, J., Z.L. Yang, and R.A. Pielke, 2008: Assessment of three dynamical climate downscaling methods using the Weather Research and Forecasting (WRF) model. *J. Geophys. Res.*, **113**, 1-16.

Collins, W. D., C.M. Bitz, M.L. Blackmon, G.B. Bonan, C.S. Bretherton, J.A. Carton, P. Chang, S.C. Doney, J.J. Hack, T.B. Henderson, J.T. Kiehl, W.G. Large, and D.S. McKenna, 2006: The Community Climate System Model Version 3 (CCSM3). *J. Climate*, **19**, 2122-2143.

Dos Santos Mesquita, M., N.G. Kvamst, A. Sorteberg, and D.E. Atkinson, 2008: Climatological properties of summertime extra-tropical storm tracks in the Northern Hemisphere. *Tellus*, DOI: 10.1111/j.1600-0870.2008.00305.x.

Durre, I., R.S. Vose, and D.B. Wuertz, 2006: Overview of the Integrated Global Radiosonde Archive. *J. Climate*, **19**, 53-68.

Hartmann, B. and G. Wendler, 2005a: Climatology of the Winter Surface Temperature Inversion in Fairbanks, Alaska. *8th Conference on Polar Meteorology and Oceanography*, JP2.26, 1-7.

Hartmann, B. and G. Wendler, 2005b: The Significance of the 1976 Pacific Climate Shift in the Climatology of Alaska. *J. Climate*, **18**, 4824-4839.

Holty, J.G., 1973: Air quality in a subarctic community, Fairbanks, Alaska. *Arctic*, **26**, 292-301.

Huovila, S. and A. Tuominen, 1989: Effect of radiosonde lag errors on upper-air climatological data. WMO Instruments and Observing Methods Rep. 35, WMO/TD No. **303**, 291-297.

Kadyrov, E.N. and A.S. Viazankin, 1999: Characteristics of the Low-Level Temperature Inversion at the North Slope of Alaska on the Base of Microwave Remote Sensing Data. *Ninth ARM Science Team Meeting Proceedings*, 1-7.

Kahl, J.D., 1990: Characteristics of the Low-Level Temperature Inversion Along the Alaskan Arctic Coast. *Int. J. Climatol.*, **10**, 537-548.

Kahl, J.D., M.C. Serreze, and R.C. Schnell, 1992: Tropospheric Low-Level Temperature Inversions in the Canadian Arctic. *Atmosphere-Ocean*, **30**, 511-529.

Kalnay, E., M. Kanamitsu, R. Kistler, W. Collins, D. Deaven, L. Gandin, M. Iredell, S. Saha, G. White, J. Woollen, Y. Zhu, M. Chelliah, W. Ebisuzaki, W. Higgins, J. Janowiak, K.C. Mo, C. Ropelewski, J. Wang, A. Leetmaa, R. Reynolds, R. Jenne, and D. Joseph, 1996: The NCEP/NCAR 40-Year Reanalysis Project. *Bull. Amer. Met. Soc.*, **77**, 437-471.

Kantha, L.H. and C.A. Clayson, 1994: An improved mixed layer model for geophysical applications. *J. Geophys. Res.*, **99**, 25235-25266.

Kerski, J., *GPS, Map, and Compass*. United States Geological Survey (USGS), Department of the Interior. 2005. 15 June 2008.
< <http://rmmcweb.cr.usgs.gov/outreach/gps.html>>

Kistler, R., E. Kalnay, W. Collins, S. Saha, G. White, J. Woollen, M. Chelliah, W. Ebisuzaki, M. Kanamitsu, V. Kousky, H. van den Dool, R. Jenne, and M. Fiorino, 2001: The NCEP–NCAR 50-Year Reanalysis. *Bull. Amer. Meteor. Soc.*, **82**, 247-267.

Leung, L.R., L.O. Mearns, F. Giorgi, and R. Wilby, 2003: Workshop on regional climate research: Needs and opportunities. *Bull. Amer. Met. Soc.*, **84**, 89-95.

Leung, L.R., Y. Kuo, and J. Tribbia, 2006: Research needs and directions of regional climate modeling using WRF and CCSM3. *Bull. Amer. Met. Soc.*, **87**, 1747-1751.

Li, Z., U.S. Bhatt, and N. Mölders, 2008: Impact of doubled CO₂ on the interaction between the global and regional water cycles in four study regions. *Climate Dynamics*, 10.1007/s00382-007-0283-4, 255-275.

Magee, N., J. Curtis, and G. Wendler, 1999: The Urban Heat Island Effect at Fairbanks, Alaska. *Theor. Appl. Climatol.*, **64**, 39-47.

Mahesh, A., V.P. Walden, and S.G. Warren, 1997: Radiosonde Temperature Measurements in Strong Inversions: Correction for Thermal Lag Based on an Experiment at the South Pole. *J. Atmos. and Oceanic Tech.*, **14**, 45-53.

Mantua, N.J., S.R. Hare, Y. Zhang, J.M. Wallace, and R.C. Francis, 1997: A Pacific decadal climate oscillation with impacts on salmon. *Bull. Amer. Met. Soc.*, **78**, 1069-1079.

Maxwell, J.B., 1982: *The Climate of Canadian Arctic Islands and Adjacent Waters*, **2**, pp 589, Atmospheric Environment Service, Downsview, Ontario, Canada.

Minobe, S. 1997: A 50-70 year climatic oscillation over the North Pacific and North America. *Geophys. Res. Lett.*, **24**, 683-686.

Mölders, N., and M.A. Olson, 2004: Impact of Urban Effects on Precipitation in High Latitudes. *J. Hydromet.*, **5**, Issue 3, 409-429.

Narapusetty, B. and N. Mölders, 2005: Evaluation of snow depth and soil temperatures predicted by the Hydro-Thermodynamic Soil-Vegetation Scheme (HTSVS) coupled with

the PennState/NCAR Mesoscale Meteorological Model (MM5). *J. Appl. Meteor.* **44**, 1827-1843.

Nonattainment Status for Each County by Year. U.S. EPA, (2006). Retrieved on January 22, 2006. <<http://www.epa.gov/oar/oaqps/greenbk/anay.html>>

Oltmans, S.J., R.C. Schnell, P.J. Sheridan, R.E. Peterson, S.M. Li, J.W. Winchester, P.P. Tans, W.T. Sturges, J.D. Kahl, and L.A. Barrie, 1989: Seasonal surface ozone and filterable bromine relationship in the high Arctic. *Atmos. Environ.*, **23**, 2431-2441.

Overland, J.E., 1985: Atmospheric boundary layer structure and drag coefficients over sea ice. *J. Geophys. Res.*, **90**, 9029-9049.

Overland, J.E., and P.S. Guest, 1991: Control of minimum snow and air temperatures over Arctic sea ice during winter. *J. Geophys. Res.*, **96**, 4651-4662.

Overland, J.E., and K.L. Davidson, 1992: Geostrophic drag coefficients over sea ice. *Tellus*, **44A**, 54-66.

Papineau, J.M., 2001: Wintertime temperature anomalies in Alaska correlated with ENSO and PDO. *Int. J. Climatology*, **21**, 1577-1592.

Rozell, N., 2002: Alaska's Urban Air Quality Has Come a Long Way. *Alaska Science Forum*, <http://www.gi.alaska.edu/ScienceForum/ASF15/1583.html>

Schmidli, J., C.M. Goodess, C. Frei, M.R. Haylock, Y. Hundecha, J. Ribalaygua, and T. Schmith, 2005: Statistical and Dynamical Downscaling of Precipitation: An Evaluation and Comparison of Scenarios for the European Alps. *J. Geophys. Res.*

Serreze, M.C., J.D. Kahl, and R.C. Schnell, 1992: Low-Level Temperature Inversions of the Eurasian Arctic and Comparisons with Soviet Drifting Station Data. *J. Climate*, **5**, 615-629.

Shulski, M. and G. Wendler, 2007: *The Climate of Alaska*. University of Alaska Press, 35-54.

Solomon, S., D. Qin, M. Manning, Z. Chen and others (eds), 2007: *Climate Change 2007: the physical science basis. Contribution of Working Group I to the Fourth Assessment Report of the Intergovernmental Panel on Climate Change*. Cambridge University Press, Cambridge.

Spak, S., T. Holloway, B. Lynn, and R. Goldberg, 2007: A comparison of statistical and dynamical downscaling for surface temperature in North America. *J. Geophys. Res.*, **112**, D08101, doi:10.1029/2005JD006712.

- Sverdrup, H.U., 1933: The Norwegian North Polar Expedition with the “Maud”, 1918-1925: Scientific Results. Bergen, 527 pp.
- Thompson, D.W.J., and J.M. Wallace, 1998: The Arctic Oscillation signature in the wintertime geopotential height and temperature fields. *Geophys. Res. Lett.*, **25**, 1297-1300.
- Trenberth, K.E., 1990: Recent observed interdecadal climate changes in the northern hemisphere. *Bull. Amer. Met. Soc.*, **71**, 988-993.
- Trenberth, K.E., and J.W. Hurrell, 1994: Decadal atmosphere-ocean variations in the Pacific. *Climate Dynamics* **9**, 303.
- U.S. Census Bureau, 2006: *American Community Survey*. Retrieved on January 22, 2006 (<http://www.census.gov/>)
- Wendler, G., 1975: Relation between CO concentration and meteorological conditions in a subarctic community. *Journal de Recherches Atmospheriques*, **9**, 135-142.
- Wendler, G. and K. Jayaweera, 1972: Some measurements on the development of the surface inversion in Central Alaska during winter. *Pure and Applied Geophysics*, **99**, 209-221.
- Wendler, G. and P. Nicpon, 1975: Low-Level Temperature Inversions in Fairbanks, Central Alaska. *Mon. Wea. Rev.*, **103**, 34-44.
- Wexler, H., 1936: Cooling in the Lower Atmosphere and the Structure of Polar Continental Air. *Mon. Wea. Rev.*, **64**, 122-136.
- Wigley, T.M.L., 2004: Input Needs for Downscaling of Climate Data. *California Energy Commission*, Discussion Paper, 1-23.
- Willmott, C.J. and K. Matsuura, 2000: Terrestrial air temperature and precipitation: Monthly and annual climatologies. [Available online at <http://climate.geog.udel.edu/~climate>]
- Zhang, J., U.S. Bhatt, W. V. Tangborn, and C.S. Lingle, 2007a: Response of glaciers in northwestern North America to future climate change: an atmosphere/glacier hierarchical modeling approach. *Annals of Glaciology*, **46**, 283-290.
- Zhang, J., U.S. Bhatt, W.V. Tangborn, and C.S. Lingle, 2007b: Climate downscaling for estimating glacier mass balances in northwestern North America: Validation with a USGS benchmark glacier. *Geophys. Res. Lett.*, **34**, L21505.

Zhang, Y., J.M. Wallace, and D.S. Battisti, 1997: ENSO-like interdecadal variability: 1900-93. *J. Climate*, **10**, 1004-1020.

Zhang X., J.E. Walsh, J. Zhang, U.S. Bhatt, and M. Ikeda, 2004: Climatology and Interannual Variability of Arctic Cyclone Activity, 1948 – 2002, *J. Climate*, **17**, 2300-2317.

Zhang, X. and J. Zhang, 2001: Heat and freshwater budgets and pathways in the Arctic Mediterranean in a coupled ocean/sea-ice model, *J. Oceanography*, **57**, 207-237.

Appendix A. Evaluating Fairbanks Radiosonde Data for the Urban Heat Island Effect (UHIE)

In order to determine the effect urbanization has had on wintertime surface temperatures in Fairbanks over time, an urban heat island analysis was performed comparing Fairbanks to nearby McGrath. Typically, a heat island develops in an area of weak winds and is caused mainly by land surface modification. Small changes in surface temperatures can have a notable effect on the strength of surface-based inversions. Therefore, when calculating inversion parameters over 1957-2008 a concern arose since Fairbanks has developed substantially over this period. Tests were conducted to determine whether corrections must be made to account for the UHIE in Fairbanks.

McGrath was chosen for comparison with Fairbanks since these two cities have similar orography, seasonal range of temperatures, and length of instrumental record. Also, McGrath has not had substantial development over this period, like Fairbanks. Since Fairbanks and McGrath are both controlled by the National Weather Service, it is expected that the observational practices and instrumentation differences are the same.

Analysis of surface temperature trends in McGrath and Fairbanks showed Fairbanks had no departure from recorded values in McGrath at a magnitude which would affect surface-based inversions (Fig. A.1).

Inversion depth and inversion temperature difference were also analyzed to determine whether any noticeable difference in trends was evident at the two stations (Fig. A.2). It was concluded that there is no discernable difference between trends of inversion parameters in Fairbanks and those in McGrath. Therefore, no adjustment was deemed necessary for the UHIE in Fairbanks.

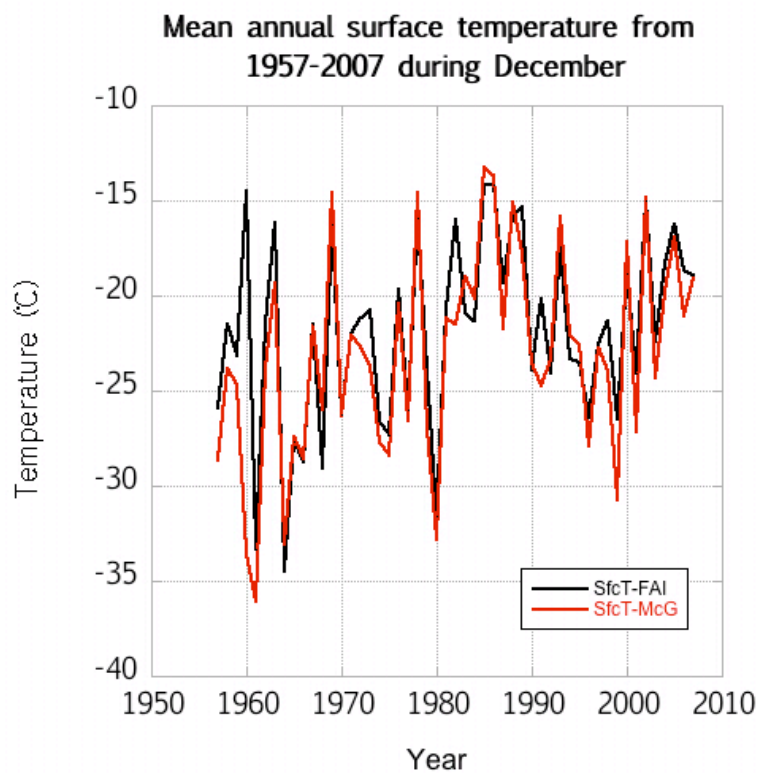


Figure A.1. Surface temperature time series in McGrath and Fairbanks. Surface temperatures in McGrath and Fairbanks from 1957-2007 in December as recorded by RAOB data.

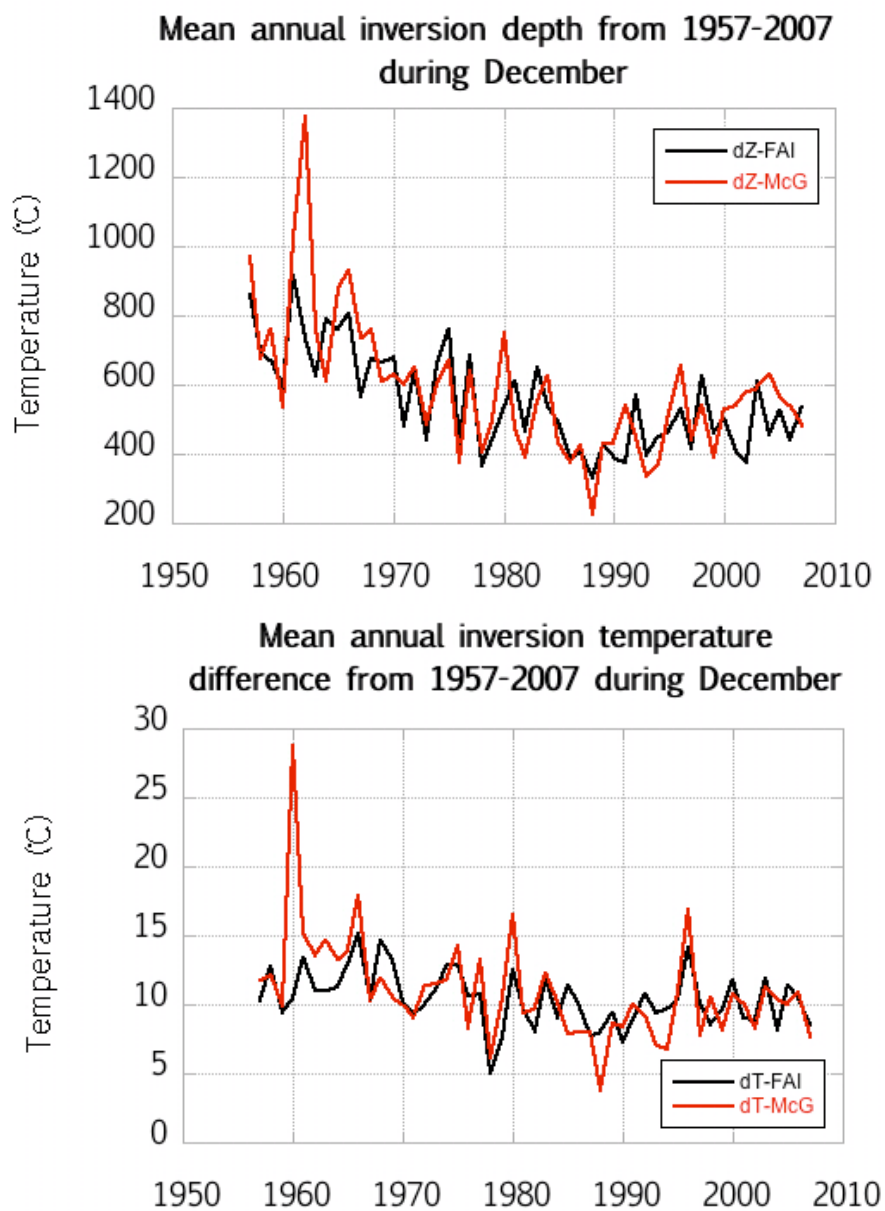


Figure A.2. Urban heat island analysis of inversion parameters. Time series of inversion depth and temperature difference are shown for Fairbanks and McGrath from 1957-2007 in December.

Appendix B. Relationship Between Cloud Cover and Surface-based Inversions

At high latitudes during the wintertime, clouds act as insulators that keep heat close to the surface. Due to their radiational effects, increased cloud cover generally weakens inversions. Therefore, it is important to establish a relationship between cloud cover and inversion strength. Increased cloud cover weakens inversions and warms surface temperatures which is consistent with increased synoptic activity during winter months in Fairbanks.

Cloud cover displays a large seasonal cycle in Fairbanks, Alaska with a low of 57% sky cover in February and March to 79% sky cover in October (Fig. B.1). Fairbanks is characterized by low cloudiness in February and March and above 75% cloud cover in August-October. November through January typically have between 65-70% cloud cover.

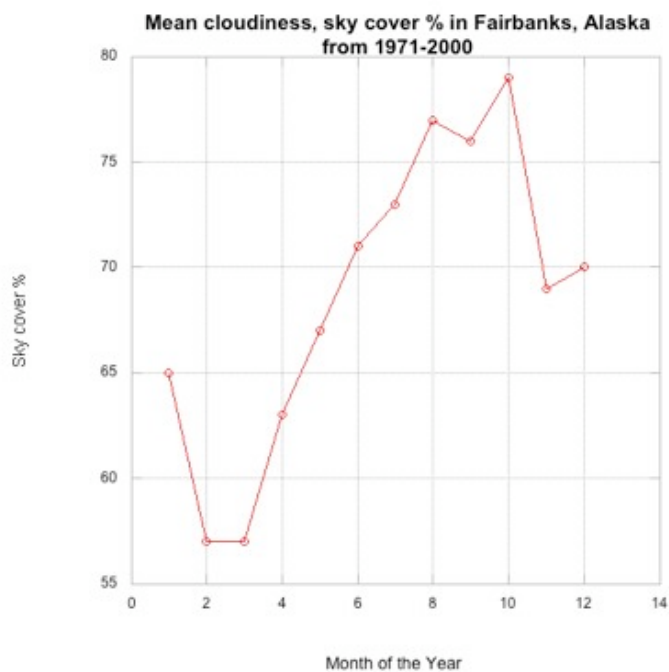


Figure B.1. Cloud cover climatology. Mean cloudiness calculated from data from 1971-2000 in Fairbanks, shown as a percentage of sky covered.

Cloud cover in January and February were examined for their relationship with inversions. Hourly cloud cover data was averaged for the three measurements around 0 and 12 Greenwich Mean Time (GMT) so that values of cloud cover were representative of the time in which RAOB soundings were measured. Cloud cover at 0 and 12 GMT \pm 1 hour was averaged and the time series for 1957-1996 is shown (Fig. B.2). Figure B.2 also shows the inverse relationship between cloud cover and inversion strength. Inversion strength and cloud cover are negatively correlated at -0.23 in January, and -0.41 in February. Therefore, when cloud cover is high (low) inversion strength is weakened (strengthened). But since the correlations are generally weak, an in-depth analysis using all stations was not performed.

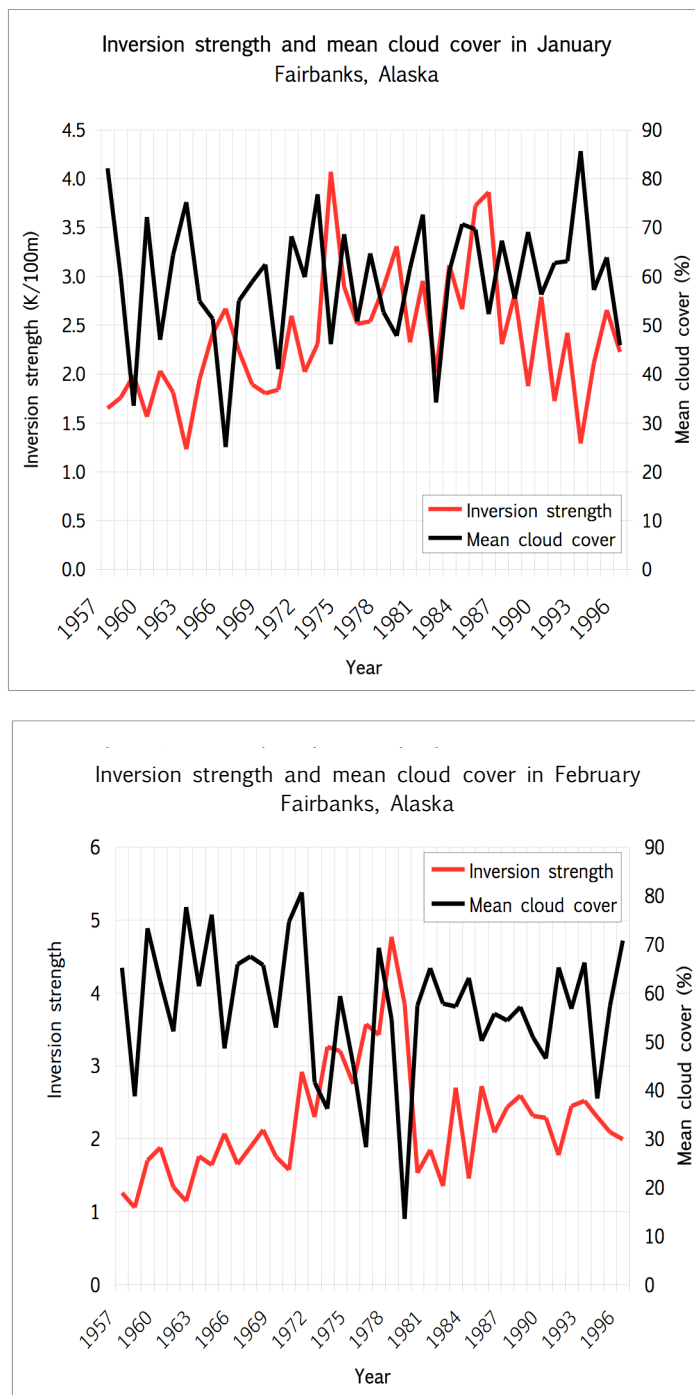


Figure B.2. Cloud cover and inversion strength (dT/dz) in Fairbanks. Inversion strength and cloud cover have an inverse relationship from 1957-1996 during January and February.